

Mathematical modeling of the transmission dynamics
of malaria in South Sudan

Abdulaziz Y.A. Mukhtar

Supervisor: Dr. J.B. Munyakazi

Co-Supervisor: Dr. R Ouifki

The logo of the University of the Western Cape, featuring a classical building facade with columns and a pediment.
UNIVERSITY *of the*
WESTERN CAPE

A Thesis submitted in partial fulfillment of the requirements for the degree of

Doctor of Philosophy

University of the Western Cape,

Department of Mathematics and Applied Mathematics, South Africa.

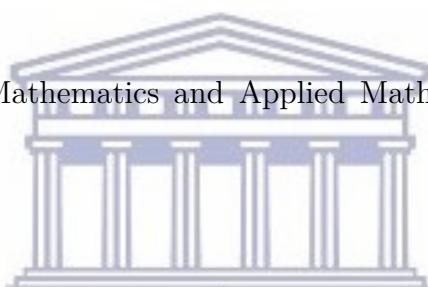
August 9, 2019

Abstract

Mathematical modeling of the transmission dynamics of malaria in South Sudan

Abdulaziz Y.A. Mukhtar

PhD thesis, Department of Mathematics and Applied Mathematics, University of the Western Cape.



Malaria is a common infection in tropical areas, transmitted between humans through female anopheles mosquito bites as it seeks blood meal to carry out egg production. The infection forms a direct threat to the lives of many people in South Sudan. Reports show that malaria caused a large proportion of morbidity and mortality in the fledgling nation, accounting for 20% to 40% morbidity and 20% to 25% mortality, with the majority of the affected people being children and pregnant mothers. In this thesis, we construct and analyze mathematical models for malaria transmission in South Sudan context incorporating national malaria control strategic plan. In addition, we investigate important factors such as climatic conditions and population mobility that may drive malaria in South Sudan. Furthermore, we study a stochastic version of the deterministic model by introducing a white noise. The models have also been parameterized in a Bayesian framework using Bayesian Markov Chain Monte Carlo (MCMC). The mathematical analysis for this study has included equilibria, stability and a sensitivity index on the basic reproduc-

tion number \mathcal{R}_0 . The threshold \mathcal{R}_0 is also used to provide a numerical basis for further refinement and prediction of the impact of climate variability on malaria transmission intensity over the study region. One of the stimulating contributions to this study was to validate our model with field data using Bayesian inferences and implement parameter estimation to increase realism of the model predications to the disease course. The results of the study pointed to the importance of incorporating detailed mosquito bionomics with climate-dependence into models for predicting the risk for malaria. The model predictions confirm that migration of a large number of people (for example in the case of an armed conflict) and their circulation can favor malaria transmission significantly compared to a lower migration scenario. It was also found that the disease persists in the low transmission areas when there is human inflow although the intervention coverage reaches 77%. The basic reproduction number \mathcal{R}_0 obtained from the numerical simulation confirms a substantial increase of incidence cases if no form of intervention occurs in the community. The study suggests that an effective use of LLINs can reduce malaria transmission in South Sudan. The thesis concluded that malaria sensitivity to human mobility is high and has implications on malaria control in South Sudan. Therefore, efforts to ameliorate health, monitor migrants and collect disaggregated data on malaria must be strengthened. We hope that the results of this study may be used to inform decision-making toward efficient malaria control in South Sudan.

Key words

Mathematical modeling of the transmission dynamics of malaria in South Sudan

Malaria

Compartmental model

Climate

Human mobility

LLINs

Differential equations

Bayesian framework

Maximum likelihood

Basic reproduction number

Stability



UNIVERSITY *of the*
WESTERN CAPE

Declaration

I declare that *Mathematical modeling of the transmission dynamics of malaria in South Sudan* is my own work, that it has not been submitted before for any degree or examination in any other university, and that all the sources I have used or quoted have been indicated and acknowledged by complete references.



Abdulaziz Y. A. Mukhtar

August 9, 2019

UNIVERSITY *of the*
WESTERN CAPE

Signed:

Acknowledgements

In the name of Allah, the most Beneficent, the most Merciful. Praise be to Allah for his guidance throughout the starting point and finishing of this dissertation.

I would like to express my profound gratitude to my supervisor, Dr Justin B. Mundayakazi for the guidance and his unwavering support toward this Ph.D study. His advice, motivation, enthusiasm, and friendship were priceless on both academic and personal levels for which I am very grateful. I am truly indebted to him.

In a special way, I want to thank Dr Rachid Ouifki for his support and the vital comments that he provided throughout this study. I wish to thank him for all the time spent discussing with me various aspects of my research and introducing me to South African Centre for Epidemiological Modelling and Analysis (SACEMA) and to Prof Robert Snow. I wish to extend my sincere thanks to Prof Robert Snow for the valuable discussions in the initial stages of this work and for providing part of the materials I used. I also thank Dr Thomas Ujjiga for availing the data used in this research.

I would like to acknowledge the financial support I received from the DST (Department of Science and Technology in South Africa)-NRF (National Research Foundation) Centre of Excellence of Mathematical and Statistical Sciences (CoE-MaSS) and SACEMA (South African Center of Epidemiology and Mathematical Analysis).

I am grateful to my parents for their prayers, caring and support. Special thanks to my dearest wife Safa Abdelsalam for her love, prayers and endless support to complete this work. I also express my thanks to my sisters, brothers, and in-laws for their support and valuable prayers. Last but not least, I would like to thank the Department of Mathematics and Applied Mathematics for the support it provided throughout this study. I am also

grateful to my friends in the Department of Mathematics and Applied Mathematics and beyond for their support and encouragement. Thank all you very much.



UNIVERSITY *of the*
WESTERN CAPE

Contents

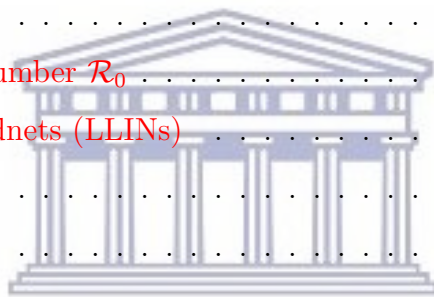
Abstract	ii
Keywords	iii
Declaration	iv
Acknowledgements	v
List of Acronyms	x
List of Notations	xi
List of Tables	xi
List of Figures	xiii
Publications	1
1 General Introduction	2
1.1 Life cycle of human malaria parasite	3
1.2 Malaria control/elimination	4
1.3 Motivation of the study in South Sudan	5
1.4 Rationale and Statement of the Research Problem	7
1.5 Literature review	8
1.6 Aim and Objectives	13
1.6.1 Objectives	13



1.6.2	Hypotheses	14
1.7	Research outline	15
2	Mathematical Preliminaries	17
2.1	Basic Reproduction Number R_0	20
2.2	Stochastic differential equation theory	23
2.3	Statistical approaches	24
3	South Sudan profile and data	27
3.1	Climatic patterns	29
3.2	Public Health System	30
3.3	Malaria epidemiology	33
3.4	Malaria control	35
3.5	Migrant pattern	39
4	Pressure-testing some mathematical models of malaria transmission	42
4.1	Introduction	42
4.2	Compartmental Models	44
4.2.1	An SIR Model	45
4.2.2	An SEIR Deterministic Model	47
4.2.3	An SEIAR deterministic model	50
4.2.4	An individual-based simulation model	52
4.2.5	Data fitting	55
4.3	Discussion and conclusion	58
5	Assessing the role of climate factors on malaria transmission dynamics	66
5.1	Introduction	67
5.2	Spatial trends	71
5.3	Method	73
5.3.1	Model formulation	73
5.3.2	Model fitting	80



5.4	Model analysis	82
5.5	Result and Discussion	91
5.6	Conclusion	96
6	Modelling the effect of bednet coverage on malaria transmission	97
6.1	Introduction	98
6.2	Study area and demography	101
6.3	Method	102
6.3.1	Human model formulation	104
6.3.2	Mosquitoes model formulation	105
6.3.3	Model fitting	106
6.4	Basic reproductive number \mathcal{R}_0	109
6.5	Intervention with bednets (LLINs)	114
6.6	Results	118
6.7	Conclusion	120
7	Assessing the role of human mobility on malaria transmission	123
7.1	Introduction	124
7.2	Model formulation	127
7.3	Model well-posedness	132
7.4	Basic Reproductive Number	135
7.5	Model fitting	141
7.6	Concluding remarks	145
8	Conclusion	149
	Bibliography	154



UNIVERSITY of the
WESTERN CAPE

List of Acronyms

RSS: Republic of South Sudan

SDE: Stochastic Differential Equation

DDT : Dichloro-Diphenyl-Trichloroethan

IRS: Indoor Residual Spraying

LLINs: Long-Lasting Insecticidal Nets

ACT: Artemisinin-Based Combination Therapy

MoH: Ministry of Health

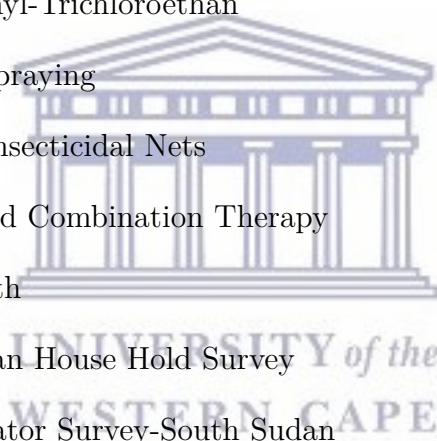
SHHS: The South Sudan House Hold Survey

MIS-SS: Malaria Indicator Survey-South Sudan

WHO: World Health Organization

USAID: United State Agency for International Development

UNICEF: United Nation International Children's Emergency Fund



List of Notations

\mathbb{E}^Q : the expectation under Q

$\frac{d\mathbb{P}^{(L)}}{d\mathbb{P}}$: the Radon-Nikodym derivative of $\mathbb{P}^{(L)}$ with respect to \mathbb{P}

σ : Volatility

Q : a martingale measure equivalent to the market measure

\mathbb{P} : a probability measure, usually the market measure

$(\Omega, \mathcal{F}, \mathbb{P})$: Probability triple

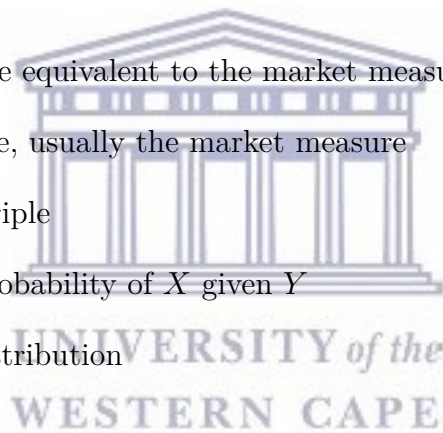
$P[X|Y]$: Conditional probability of X given Y

N : Standard normal distribution

$\{\mathcal{F}_n\}_{n \geq 0}, \{\mathcal{F}_t\}_{t \geq 0}$: Filtration

$\mathbb{E}[X/\mathcal{F}], \mathbb{E}[X_{n+1}/X_n]$: Conditional expectation

W : Brownian motion or Wiener process



List of Tables

3.1	Socio-economic and demographic data	28
3.2	Public health facilities managed by State	32
3.3	MIS 2009, Malaria incidence by States 2009-2012	34
3.4	Source [123] Malaria Parasites species percentage by region	35
3.5	Percentage of households with an insecticide treated net	38
3.6	South Sudan Refugees and IDPs by State [130]	39
4.1	Model Variables	46
4.2	Model parameters	49
4.3	Model Parameters: Description and value	52
4.4	Model Parameters: Description and value	55
5.1	Parameters for Anopheles Gambiae Model	77
5.2	Parameters for the human transmission model	83
5.3	Calculation of the expected value of basic reproduction number	93
6.1	Model Parameters: Description and value	107
6.2	Intervention Parameters	117
7.1	Model Variables	130
7.2	Model parameters	131
7.3	Model parameters estimated during the fitting process	146

List of Figures

1.1	Source: [19], malaria life cycle	3
1.2	Source: [124], South Sudan map by State	6
3.1	Source: [75], South Sudan Health Districts	31
4.1	State diagram for the SIR model	45
4.2	State diagram for the SEIR model	47
4.3	Flow diagram for the SEIAR model	50
4.4	Flow diagram for Human and Mosquito infection model	53
4.5	Model (4.2.1) fits to data and trajectory	56
4.6	Model (4.2.2) fits to data and trajectory	57
4.7	Model 4.2.3 fits to data and trajectory	59
4.8	Model (4.2.4-4.2.5) fits to data and trajectory	60
4.9	Predictions of malaria generated by model (4.2.1)	61
4.10	Predictions of malaria generated by the model (4.2.2)	62
4.11	Predictions of malaria generated by the model (4.2.3)	63
4.12	Predictions of malaria generated by the model (4.2.4)- (4.2.5)	64
4.13	Predicted numbers of symptomatic cases with effect of intervention	65
5.1	Weekly malaria reported cases of 2015	69
5.2	States map and climate pattern	72
5.3	Flow diagram for Human and Mosquito infection model	74
5.4	Simulation of model parameters function	78

5.5	Illustration of the model fitting and the trajectory simulation	81
5.6	Illustration of the model fitting and the trajectory simulation	82
5.7	Sensitivity index of \mathcal{R}_0 with respect to χ and V	87
5.8	Sensitivity index of \mathcal{R}_0 with respect to R and T	87
5.9	Simulation of the model	94
6.1	Reported weekly malaria cases between 2011 and 2015	99
6.2	Population density of South Sudan 2009	102
6.3	South Sudan selected state analysis map.	102
6.4	Flow diagram for Human and Mosquito infection model	103
6.5	Parameters estimation by fitting model to weekly malaria cases of CES	108
6.6	Parameters estimation by fitting model to weekly malaria cases of WBGZ	109
6.7	Parameters estimation by fitting model to weekly malaria cases of WRP	110
6.8	Model validation by fitting to malaria cases on weekly basis between 2011-2015	111
6.9	Sensitivity index of \mathcal{R}_0 with respect to χ for different values of V	119
6.10	Sensitivity index of \mathcal{R}_0 with respect to V for different values of χ	119
6.11	Prediction of malaria infections	120
6.12	Prediction of basic reproduction number	121
7.1	Source: [120], IDPs camp and movement patterns	125
7.2	Model flow diagram	128
7.3	Illustration of the model fitting	142
7.4	Simulation trajectory for the fitted model patch 1	143
7.5	Simulation trajectory for the fitted model patch 2	144
7.6	Simulation trajectory for the fitted model patch 3	144
7.7	Projected cases of malaria	147
7.8	Projection of Basic reproduction number	148

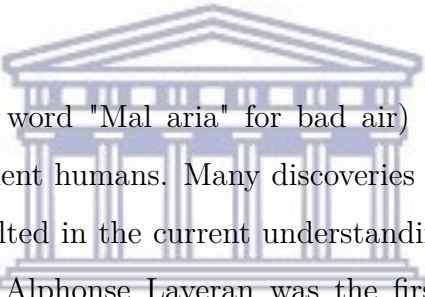
List of Publications

Part of this thesis has already been published/submitted in the form of the following research papers:

1. Mukhtar, A. Y., Munyaikazi, J. B., Ouifki, R., & Clark, A. E. (2018). Modelling the effect of bednet coverage on malaria transmission in South Sudan. *PloS One*, **13** (2018). DOI: 10.1371/journal.pone.0198280.
2. Mukhtar, Abdulaziz YA, Justin B. Munyaikazi, and Rachid Ouifki. Assessing the role of climate factors on malaria transmission dynamics in South Sudan. *Mathematical Biosciences*, **310** (2019) 13-23. DOI: 10.1016/j.mbs.2019.01.002.
3. Abdulaziz Mukhtar, Justin Munyaikazi, Rachid Ouifki. Assessing the role of human mobility on malaria transmission in South Sudan. Submitted for publication.

Chapter 1

General Introduction



Malaria (derived from Italian word "Mal aria" for bad air) is undoubtedly one of the ancient diseases that still torment humans. Many discoveries have led to continuous scientific studies which have resulted in the current understanding of the disease. In 1880, the French physician Charles Alphonse Laveran was the first to discover the malaria parasites followed with William MacCallum discovery on the sexual reproduction of a malaria-like parasite with a related haematozoan and *Haemoproteus columbae*, in birds in 1897 [32]. In the same year of MacCallum discovery, Ronald Ross, a British officer, was the first to prove that malaria parasites could be transmitted from infected patients to mosquitoes. Then year later a team of Italian scientists (Giovanni Grassi, Amico Bignami and Giuseppe Bastienelli) demonstrated conclusively that human malaria parasites were transmitted by *Anopheles Claviger* mosquitoes. Thus by 1890 it was known that malaria was caused by a protozoan parasite, and there were three species with specific periodicities namely, *Plasmodium Vivax*, *Plasmodium Falciparum* and *Plasmodium Malariae*. Moreover, in 1922 John Stephens who worked in West Africa recognized a fourth species described as *Plasmodium Ovale*, then later clinicians in South-East Asia have considered *Plasmodium knowlesi* malaria as the fifth human malaria parasite [5, 10]. These backgrounds of discoveries were an important step towards the development of new approaches for assessing and preventing transmission in nature.

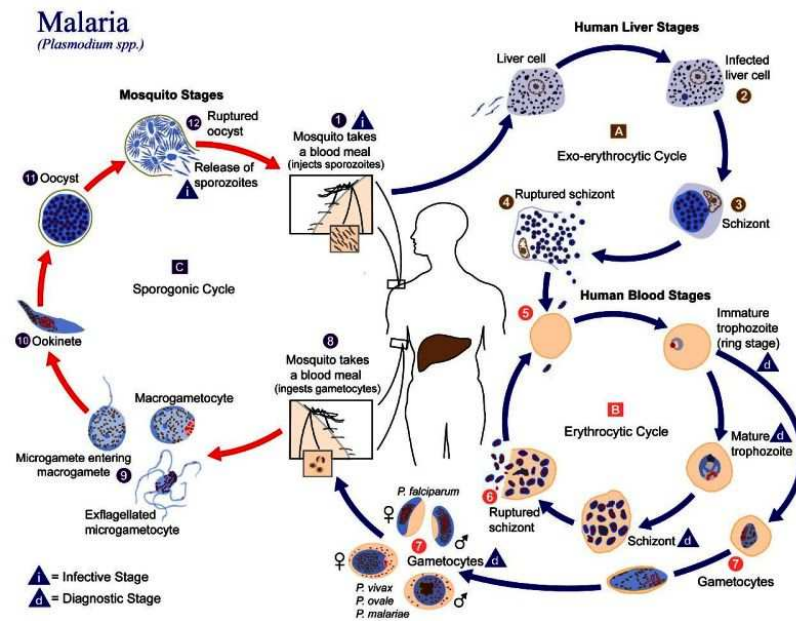


Figure 1.1: Source: [19], malaria life cycle

1.1 Life cycle of human malaria parasite

Malaria parasites, in order to survive successfully need to complete their life cycle in two alternative hosts of evolutionarily distant species (i.e. human and mosquito) illustrated in Figure 1.1 . Malaria transmission intensity varies geographically according to vector species of Anopheles mosquitoes. In tropical countries, the Plasmodium Falciparum is the most virulent parasite species that causes a large burden of disease. There are many species of Anopheles mosquito, each with its favorite aquatic habitats [32].

The life cycle starts when the infected female Anopheles mosquito bites a person and inoculates sporozoites which are injected with the saliva into the bloodstream. Within few minutes they invade the liver cells and multiply for 7-10 days forming thousands of merozoites [19]. Thereafter, the merozoites burst out of the liver and invade the Red Blood Cells (RBCs). Again they develop through ring forms to trophozoites and finally to multi-segmented schizonts. The infected RBCs (erythrocytes) rupture after about 12-16 days for falciparum (The exo-erythrocytic cycle). This reproduction can lead to the

thousands of cells infected with parasites in the host bloodstream causing clinical signs and perhaps a complications of malaria [31].

Therefore, the parasites multiplication in the mosquito is known as the sporogonic cycle, the gametocytes are ingested by an anopheles mosquito from humans. The male and female gametes generate zygotes and developed to oocysts. The oocysts grow, rupture, and release sporozoites, which make their way to the mosquito's salivary glands. Inoculation of the sporozoites into a new human host perpetuates the malaria life cycle [5]. Hence, the parasite is identified by slow evolution either in the Anopheles mosquito (15 days) and in human (15 days in the liver, 72 hours in the blood). Human infection cycle begins again when the mosquito takes a blood meal, injecting the sporozoites from salivary glands into the human bloodstream [31].

1.2 Malaria control/elimination

In about a century ago the discovery of the parasite life cycle was the first exertion of rationale malaria control. Subsequently, a Global Malaria Eradication Program (GMEP) campaign was a major success in the 1950s and 1960s, particularly in North America, Europe, and Australia. Nevertheless, the campaign was discontinued fourteen years later when it was recognized that eradication could not be achieved [92], and there were many burden countries in Africa lacking the technical assistance, funding, and infrastructure [127]. The first African malaria conference held in Kampala, Uganda (Garki proj) endorsed that malaria should be controlled by the modern methods such as Dichloro-Diphenyl-Trichloroethane (DDT) whatever the degree of endemicity [37]. Another approach was introduced during the 1950s by Ross-Macdonald's mathematical model to support a global eradication, which highlighted the significant superiority in increasing vector mortality [74, 110, 114].

Over the decades later, the Millennium Development Goals have renewed attention and resources to the global fight against malaria. The 60 years following Ross's identification of the vectors of malaria, important new tools such as Artemisinin drugs, insecticide-

treated bednets and indoor residual spraying with insecticides have been added to the malaria control arsenal [6, 81]. Many countries and international organizations continuously support the eradication process of this fatal disease by significantly increased bednet coverage with great impact.

The year 2015 was the final year for targets set by the World Health Assembly and Roll Back Malaria to reduce all suspected malaria cases and to mitigate almost to zero percent malaria deaths [140]. Hence, significant progress has been made globally as a result of increased coverage based on both Artemisinin-based Combination Therapy (ACT) and vector control through Long-Lasting Insecticidal Nets (LLINs) as well as an Indoor Residual Spraying (IRS) of insecticides. It is therefore estimated that between 2000 and 2015, malaria intervention saved over 6.2 million lives. Additionally it was found that about 5.9 million of the saved lives were under the age of five. The disease has been virtually eliminated in most parts of the world. Regrettably, millions of lives are still threatened by extreme malaria endemic in Africa, with about 90% of malaria related deaths occurring in Sub-Saharan Africa [49]. The death percentages could have been reduced in this region if there were sufficient distribution coverage of vector control interventions. Studies revealed that approximately 300 million people in sub-Saharan Africa are still lacking access to protective insecticide-treated nets [139].

1.3 Motivation of the study in South Sudan

Malaria remains a major problem globally as far as public health is concerned, causing human high morbidity and mortality in Africa especially. A report by WHO [140] estimated the number of cases of malaria worldwide in 2013 to 219 million people (range 124-283 million) with 584 000 (range 367 000-755 000) of malaria-related deaths. Over 80% of all malaria episodes and 90% of all malaria deaths occur in Sub-Saharan Africa [140]. In South Sudan alone, the number of malaria incidences has gradually increased from 71 948 in 2008 to 1 198 357 in 2012 and with the deaths of an estimated 44,000 people per year, while the mortality rate of children under the age of five is estimated

Chapter 1: General Introduction

to 250 per 1,000 live births [21]. The country has the highest rate of malaria burden in sub-Saharan Africa and its entire population is considered to be at risk of contracting the disease. Moreover, parasite prevalence rate in children under 5 years is in the range of 30%-40% and deaths are especially common amongst children under the age of five years and pregnant women. The levels of transmission are perennial with seasonal variations in rural areas and the peak malaria incidence occurs towards the end of the rainy season.

South Sudan is a landlocked country in east-central Africa which shares borders with six countries and comprises ten States (before the recent division) in three regions illustrated in Figure 1.2: Greater Equatoria region includes Eastern Equatoria, Western Equatoria and Central Equatoria; Greater Bahr el Ghazal region includes Western Bahr el Ghazal, Northern Bahr el Ghazal, Warrap and Lakes and Greater Upper Nile region includes Unity, Upper Nile and Jonglei. In South Sudan, malaria transmission rates can



Figure 1.2: Source: [124], South Sudan map by State

differ depending on local factors such as environmental and climatic (e.g massive flooding), movement of populations with little immunity into areas of high transmission and

types of mosquito species (Anopheles Gambiae, A. Arabiensis and Anopheles Funestus) in the area. The causative period of parasite occurs for 5 to 6 months of the year in the northern part of the country and for 7 to 8 months of the year in the southern part.

The infrastructures of the country are very poor and the public health system is not well constructed and remains totally devastated due to a number of reasons such as the legacy of long period of violence and instability. In addition 80% of healthcare system which is available is still provided and ran by international NGOs [106].

As a consequence of the situation explained above, the malaria infection constitutes 20% – 40% of all out-patient visits and 30% of all hospital admissions and it is a major cause of deaths in South Sudan [88]. During gestation period, malaria might lead to serious maternal health problems such as, abortions, stillbirths, miscarriages, anemia, and a low birth weight born babies.

1.4 Rationale and Statement of the Research Problem

Over years South Sudan has been exposed to the brunt of chronic warfare and probably has one of the highest malaria burden in the world where the entire population is at risk. The situation of the country is aggravated by an increase in the number of population due to refugees, returnees, and also about 131,990 internal conflict-related displacements in 2013 [22]. This situation has created a major stumbling block to malaria control. Also, there was no clear evidence of malaria reduction in all reports. Moreover access to diagnosis and treatment remains an obstacle due to long distances to health facilities, lack of functional microscopes, stock-outs of Rapid Diagnosis Test (RDTs) and anti-malaria treatment. The only key operational vector available is the distribution of LLINs that control intervention with limited use of IRS. Countrywide LLINs mass campaigns has been piloted with the target coverage of 80% and only about 4.7 million LLINs have been delivered to the population who are in need [106]. Despite this, the number of infected cases and deaths increased in all age groups. Malaria Indicator Survey-South Sudan (MIS-

SS) in 2009 indicates that the proportion of structures protected through IRS is about 2.1% of the population at risk.

The South Sudan House Hold Survey (SHHS) provides comprehensive surveys based on representative household sample estimates of a range of health and demographic indicators. These surveys conducted in the period from 2006 to 2010 indicate the proportion of 11.6% – 34.2% of households ITN ownership. However, only 27.4% of children less than 5 years of age slept under an LLINs [22].

Government of South Sudan has limited funding and inadequate support for malaria control with high degree of donor dependency, mainly provided by the Global Fund, UNICEF, WHO, USAID with contributions from the World Bank, Department for International Development (DFID) and Malaria Consortium. Generally, malaria parasite propagation still very high and that requires consistent and expansively scaled-up coverage of effective tools of control [35]. Control with existing tools is quite challenging due to ecological diversity of malaria transmission in Africa with wide range of epidemiological settings [119]. Dynamic mathematical models of this disease with a particular emphasis on South Sudan are uncommon. Also, no mathematical study has been conducted previously in South Sudan to establish the effects of multi intervention on the malaria epidemic. The research aims to explore the prediction of malaria prevalence, using model scenario based on intervention and local factors incorporating real data of MIS-SS between 2010 to 2015.

1.5 Literature review

Mathematical modeling has become an important tool in understanding the mechanisms of disease transmission and in decision making processes regarding intervention programs for controlling diseases. Over the years several mathematical models have been developed to gain insight into transmission dynamics of malaria, starting from the basic malaria model of Ross [110] and Macdonald [74]. Subsequently, these models have been extended by researchers considering different factors related to malaria transmission dynamics and

control.

Age structure

Forouzannia and Gumel [41] designed a new deterministic model of age-structured and rigorously analyses the transmission dynamics of malaria in a community. The result of numerical simulations indicates that the cumulative number of new cases of infection and mortality due to malaria increase with increasing average lifespan and birth rate of mosquitoes.

Filipe et al. [40] explored a model of age-structured of malaria transmission that acquired immunity and acts in three different ways: reducing likelihood that an infected person develops a symptomatic disease, speeding the clearance of parasites, and increasing tolerance to subpatent infections. Their results show that the first two mechanisms together leads to patterns of malaria by age group that is consistent with those observed in different malaria endemic environments in Africa. Their model also suggests that immunity to symptomatic disease has shorter memory, develops faster if there are higher levels of infection in the population, and increases with age. On the other hand, their model suggests that immunity that helps to clear infection lasts longer (20 years or more), develops later in life, and does not depend on the amount of transmission in the population.

Ngonghala et al. [90] described a dynamic model for malaria spread between human and mosquito and explore the impact of ITNs on malaria infection and control. The function used to model personal protection through ITN captures the decrease in effectiveness due to physical decay and human behavior, as well as mosquito biting behavior as a function of time. In their compartmental model, the human population is divided into four classes: susceptible, exposed, infectious, and immune humans (partial immunity) and mosquito population into susceptible, exposed and infectious mosquitoes. Lastly they perform uncertainty and sensitivity analyses to identify and rank parameters that play a critical role in malaria transmission and control.

Mwanga et al. [83] proposed a deterministic model for the transmission of the malaria, including in particular asymptomatic carriers and two age classes in the human population. Their model demonstrates four possible control strategies to be used namely

long-lasting treated mosquito nets, indoor residual spraying, screening and treatment of symptomatic and asymptomatic individuals. The results show that by use of optimal control the disease can be brought to a stable disease free equilibrium when all four controls are used.

Immunity

Dietz et al. [36] developed a mathematical model of malaria for comparing the expected parasitological effects of alternative control measures. They considered three aspects of immunity that are acquired at different rates: loss of infectivity, increase in recovery, and decrease in detectability. They also described both the temporal changes of the *P. Falciparum* infection rate and the immunity level of the population as a function of the dynamics and characteristics of the vector populations.

Okell et al. [94] developed a mathematical model of malaria transmission in human and mosquito population by introducing artemisinin-based combination therapy (ACT) and alternative first-line treatment in six regions of Tanzania with different level of malaria transmission. In their study, they found that ACT may reduce malaria transmissions in low transmission area if were widely used as effective as the widespread use of the insecticide-treated bednet. Their model also shows that in the area with high transmission the use of long-acting treatment with or without artemisinin component might be a good method to reduce the transmission. The finding suggests that properties of antimalarial drugs need to be taken into a consideration together with the level of transmission in the areas in order to achieve highest impact on malaria transmission.

Yang [143] presented malaria transmission model by taking into account different levels of acquired immunity among human and most importantly temperature-dependent parameters related to vector mosquitoes. Model analysis was carried out by means of basic reproduction number R_0 and also derived an expression for an endemic equilibrium that is biologically relevant only when $R_0 > 1$.

Climate change

Parham and Michael [104] in their effort, investigated a simple model that permitted valuable and novel insights by considering the simultaneous effects of rainfall and temper-

ature on mosquito population dynamics, malaria invasion and the impact of seasonality on transmission. On their result identified a temperature window of around 32 °C-33°C where endemic transmission is optimized. Another key result on their finding is that by influencing vector abundance, changes in rainfall patterns in particular strongly govern malaria endemicity, invasion, and extinction. Martens et al. [79] used a rules-based modelling approach to examine how climate change might affect global malaria transmission. Their model consists of several linked systems: the climate system, the malaria system (divided into a human subsystem and a mosquito subsystem), and the impact system. They used temperature and precipitation as the main climate factors that have a bearing on the malarial transmission potential of the mosquito population.

Hoshen and Morse [58] formulated dynamic mathematical malaria model comprising both the weather-dependent within-vector stages and the weather-independent within host stages. Lindsay and Birley [71] presented a simple mathematical model to investigate the effects of temperature on the ability of *Anopheles Maculipennis* to transmit *Plasmodium Vivax* malaria.

Chitnis et al. [23] proposed a malaria model by evaluating the sensitivity indices of the reproductive number, and the endemic equilibrium to model parameters at the baseline values. In their study point out that, the reproductive number and the equilibrium proportions of infectious humans are both most sensitive to the mosquito biting rate in areas of low transmission, while, in areas of high transmission the equilibrium proportion of infectious humans is also most sensitive to the human recovery rate. According to their study, controlling the rate of mosquito bites and the human recovery rate is a successful control strategy.

Case of optimization

Okosun and Makinde [97] investigated the possible impact of optimal treatment and control of drug resistance on the transmission of malaria disease by introducing a class of drug resistant individuals into the population. Theoretically, they carried out the stability properties of the model and determine conditions on the parameters for the existence of equilibrium solutions.

Rafikov et al. [108] proposed a mathematical continuous model that considers the generation overlapping and variable environment factors by using optimal control problem strategies. Their model considers interactions between wild and transgenic mosquito populations in a variable environment.

Jia [60] formulated and examined a mathematical model for malaria transmission that includes incubation periods for both infected human hosts and mosquitoes. Briët and Benny [16] considered using stochastic individual based models to run the dynamic simulation of malaria on the OpenMalaria platform. They tried to determine optimal LLIN distribution rates by examining the malaria transmission and disease dynamics in scenarios with sustained LLINs and CM interventions. They examined also the effects of abruptly halting LLIN distribution. Their result concluded that in the long-term, LLIN repeated distributions might sustainably reduce transmission and disease burden in all settings. In addition, they note that progress towards malaria control and elimination requires coverage of effective intervention such as insecticide-treated nets (ITNs), IRS, Intermittent Preventive Treatment (IPT), diagnostic testing and appropriate treatment. The scaling up of these interventions coverage is based on evidence on the effectiveness of programme.

Griffin et al. [51] Constructed individual-based simulation model for Plasmodium Falciparum transmission in an African context incorporating the effect of the switch to artemisinin-combination therapy (ACT) and increasing coverage of LLINs. Their findings explored the possibility of available control measures to reduce parasite prevalence to a low level as laid out in the control phase of the global elimination framework.

White MT et al. [136] made significant contribution to the literature by conducting a systematic review of the published works on the costs of all malaria control interventions using electronic database. Result of the study identified 78% of fifty-five studies of the costs and forty three studies of the cost-effectiveness of malaria interventions in Sub-Saharan Africa. Economies of scale were observed in the implementation of ITNs, IRS and IPT, with lower unit costs reported in their studies with population level benefit, the median incremental cost effectiveness ratio per disability adjusted life year averted was

provided to inform rational resource allocation by donors and domestic health budgets.

Smith et al.[115] used mathematical models to establish rationally defined endpoints, timelines and criteria for monitoring and evaluation of ITN programs. The model predicts that over the period of 5-10 year endemic control will be stabilized and it is also possible to transform malaria in the short to medium-term through high levels of ITN ownership.

Stuckey et. al [126] introduced OpenMalaria stochastic simulation modeling to simulate the impact of case management and malaria control interventions (singly and/or in combination of interventions) in western Kenya compared to the corresponding simulated outputs of a case without interventions. Their results indicate that increased coverage of vector control intervention has a huge impact compared to adding an IST intervention to the current implementation strategy.

The epidemiology of malaria has moved beyond the parasite and the risk factors associated with its transmission to more insights into disease behaviour. These extensive studies of malaria models integrating various factors confirm that they are significantly relevant in understanding the occurrence of the disease in the studied regions and assessing the impact of these factors on the course of the epidemic. Hence, in this study, we apply mathematical models that incorporate various factors to draw insight into further understanding of malaria in South Sudan as the first step as its particularly important for epidemiologist in developing effective intervention strategies.

1.6 Aim and Objectives

The aim of this thesis to understand the course of the malaria epidemics in South Sudan by paying attention to the different factors that sustain the epidemics through the means of deterministic and stochastic models.

1.6.1 Objectives

The specific objectives are to:

- To review literature on the malaria in South Sudan and on the factors that promote its spread
- To validate mathematical models using Bayesian approach and illustrate the malaria dynamics and projection by means of numerical simulations
- To investigate the impact of possible types of interventions available that may curb the spread of malaria. The coverages of these combined interventions will be targeted, rather than of "one size fits all" type.
- To establish stability analysis of the models in terms of the basic reproduction number and other invariants.

1.6.2 Hypotheses

The study intends to examine the hypotheses that emerge from the following factors:

- **Climate:** Malaria transmission is seasonal across the country, with peaks towards the end of the rainy season from September to November due to freshwater pools serving as mosquito breeding sites. Based on the foregoing and established studies, the heterogeneity of malaria in South Sudan can be explained by the varied agro-climatic conditions that exist between the regions. Therefore, I intend to explore the potential links between climate and malaria infection in South Sudan's three climatically distinct regions (Chapter 5).
- **Intervention coverage:** According to ongoing studies, a gradual increase in malaria burden across the country can be attributed to the constant decline in LLIN coverage from 2009. I intend to assess LLINs ownership and use by predicting parasite prevalence at State level based on the coverage given by Malaria Indicator Survey between 2009 -2013 using a deterministic model ideally to support metrics for pre-elimination and recommend a scaling-up entry point of LLIN distribution that targets households in areas at risk of malaria (Chapter 6).

- Human movement: In recent years (since independence), South Sudan has experienced a huge human mobility which includes returnees; refugee from Sudan; and mass population displacements. On the other hand, incidence of malaria across many areas of the country (since 2013) is gradually increasing and the chance of a second consecutive season marked by extremely high numbers of malaria cases and preventable death is imminent. Against this backdrop, I assume that the large mobility and constant displacement from conflict-affected areas to safety areas may have significantly influenced the malaria trend observed after 2013 onward. Hence, I emphasize on the role of population movement in the prevalence of malaria parasite using stochastic model (Chapter 7).

1.7 Research outline

Chapter 1 presents the historical background of malaria discoveries and the parasite cycle. It discusses malaria eradication programs and their implication in addressing the ultimate public health challenges worldwide. It describes the rationale of the study, research problems and an overview of mathematical models of malaria. The objectives and hypotheses of the study are laid out and the introductory chapter is concluded with the structure of the thesis.

Chapter 2 provides definitions of some terminologies, theorems and basic reproductive numbers that will be useful in the subsequent chapters. Chapter 3 introduces the overall profiles of South Sudan including population distribution and urbanization, population migration (internal displaced persons, Refugees), topography and climate, health system and malaria epidemiology. It also provides an overview of malaria control and the broad evolution of policies and strategies. Chapter 4 presents pressure tests on four different nested mathematical models of malaria. Tests include assumptions and results. Chapter 5 presents a mathematical model for malaria transmission examining the impact of climate variability as a first step to a further understanding malaria in the whole South Sudan.

In Chapter 6 a compartmental model of malaria is developed to provide some assistance

Chapter 1: General Introduction

in defining the specific needs of malaria interventions in different parts of the country. Chapter 7 further extends the model in Chapter 6 by incorporating stochasticity on human compartments of the model. The movement of human population is captured to provide further insights into the development of effective intervention strategies. We conclude and summarize the main results in Chapter 8.



UNIVERSITY *of the*
WESTERN CAPE

Chapter 2

Mathematical Preliminaries

Consider the following n dimensional first order ordinary differential equation (ODE):

$$\frac{dX}{dt} = F(X), \quad (2.0.1)$$

$$X(0) = X_0, \quad (2.0.2)$$

where $X \in \mathbb{R}^n$ and $F : \mathbb{R}^n \rightarrow \mathbb{R}^n$ is bounded in the neighborhood of the initial condition.

Now to prove that there is a unique solution to the initial value problem (2.0.1 - 2.0.2), we have the following the theorem.

Theorem 2.1 (See Birkhoff and Rota [15]) Let E be an open subset of \mathbb{R}^n containing X_0 and assume that $F \in C^1(E)$ ($C^1 \Rightarrow$ Lipschitz) Every continuously differentiable function is locally Lipschitz), there exists an $a > 0$ such that the initial value problem of the system (2.0.1) has a unique solution $X(t)$ on the interval $[-a, a]$

By Considering the n dimensional initial value autonomous system (2.0.1). An *equilibrium solution* X^* (steady-state solution, fixed point, or critical point) of the differential system is a constant solution X following algebraic equation

The characteristic equation at X^* is given by:

$$P(\lambda) := \det(\lambda I - J(X^*)) = 0 \quad (2.0.3)$$

Chapter 2: Mathematical Preliminaries

The stability of X^* is determined by the roots of (2.0.3).

In particular,

- a. If all the roots of (2.0.3) have negative real parts, then X^* is locally asymptotically stable.
- b. If at least one root of (2.0.3) has a positive real part, then X^* is unstable.

In order to derive sufficient conditions for the global stability and asymptotic stability of such a rest point, we will apply the so called direct method of Lyapunov and Routh-Hurwitz Criteria. Routh-Hurwitz Criteria is an important Criteria that gives necessary and sufficient conditions for all of the roots of the characteristic equation to lie in the left half of the complex plane are known as the Routh-Hurwitz Criteria. The Routh-Hurwitz Criteria are used in the next chapters to determine local stability of an equilibrium point for nonlinear systems of differential equations. We state the Routh-Hurwitz Criteria in the next theorem.

Theorem 2.2 (see Allen [4]) **Routh-Hurwitz Criteria.** *Given the polynomial*

$$P(\lambda) = \lambda^n + a_1\lambda^{n-1} + \dots + a_{n-1}\lambda + a_n,$$

where the coefficients a_i are reals constants, $i = 1; \dots; n$, define the n Hurwitz matrices using the coefficients a_i of the characteristic polynomial:

$$H_1 = (a_1), \quad H_2 = \begin{pmatrix} a_1 & 1 \\ a_3 & a_2 \end{pmatrix}, \quad H_3 = \begin{pmatrix} a_1 & 1 & 0 \\ a_3 & a_2 & a_1 \\ a_5 & a_4 & a_3 \end{pmatrix},$$

and

$$H_n = \begin{pmatrix} a_1 & 1 & 0 & 0 & \dots & 0 \\ a_3 & a_2 & a_1 & 1 & \dots & 0 \\ a_5 & a_4 & a_3 & a_2 & \dots & 0 \\ \vdots & \vdots & \vdots & \vdots & \dots & \vdots \\ 0 & 0 & 0 & 0 & \dots & a_n \end{pmatrix}$$

where $a_j = 0$ if $j > n$. All of the roots of the polynomial $p(\lambda)$ are negative or have negative

Chapter 2: Mathematical Preliminaries

real part if the determinants of all Hurwitz matrices are positive:

$$\det(H_j) > 0, \quad j = 1, 2, \dots, n.$$

When $n = 2$ Routh-Hurwitz Criteria simplify to $\det(H_1) = a_1 > 0$ and

$$\det(H_2) = \det \begin{pmatrix} a_1 & 1 \\ 0 & a_2 \end{pmatrix} = a_1 a_2 > 0$$

or $a_1 > 0$ and $a_2 > 0$. For polynomial of degree $n = 2, 3, 4$ and 5 , we summarize the Routh-Hurwitz Criteria below

Routh-Hurwitz Criteria for $n = 2, 3, 4$, and 5

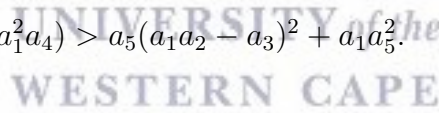
$$n = 2 : a_1 > 0 \text{ and } a_2 > 0.$$

$$n = 3 : a_1 > 0, a_3 > 0 \text{ and } a_1 a_2 > a_3.$$

$$n = 4 : a_1 > 0 \text{ and } a_2 > 0, a_4 > 0 \text{ and } a_1 a_2 a_3 > a_3^2 + a_1^2 a_4.$$

$$n = 5 : a_i > 0 \quad i = 1, 2, 3, 4, 5, a_1 a_2 a_3 > a_3^2 + a_1^2 a_4 \text{ and}$$

$$(a_1 a_4 - a_5)(a_1 a_2 a_3 - a_3^2 - a_1^2 a_4) > a_5 (a_1 a_2 - a_3)^2 + a_1 a_5^2.$$



Definition 2.3 (see Allen [4]). Let U be an open subset of \mathbb{R}^2 containing the origin. A real-valued $C^1(U)$ function, $V : U \rightarrow \mathbb{R}$, $[(x, y) \in U, V(x, y) \in \mathbb{R}]$ is said to be positive definite on the set U if the following two conditions hold.

(i) $V(0, 0) = 0$

(ii) $V(x, y) > 0$ for all $(x, y) \in U$ with $(x, y) \neq 0$.

The function V is said to be negative definite if $-V$ is positive definite.

Definition 2.4 (see Jordan and Smith [62]). $V(X)$ is said to be *positive (negative) definite* in a neighbourhood U of the origin if $V(X) > 0$ ($V(X) < 0$) for all $X \neq 0$ in U , and $V(0) = 0$. $V(X)$ is *positive (negative) semidefinite* in a neighbourhood U of the origin if $V(X) \geq 0$ ($V(X) \leq 0$) for all $X \neq 0$ in U , and $V(0) = 0$.

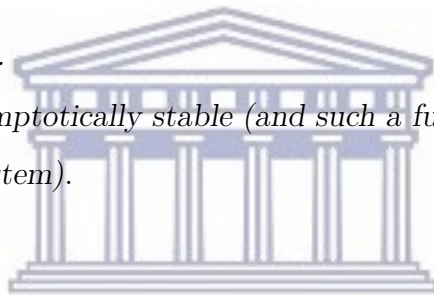
Theorem 2.5 (see Jordan and Smith [62]). Let $X^*(t) = 0, t \geq t_0$, be the zero solution of the regular system $\dot{X} = X(t)$, where $X(0) = 0$. Then $X(t)$ is uniformly stable for $t \geq t_0$ if there exists $V(X)$ with the following properties in some neighborhood of $X = 0$:

- (i) If $V(X)$ and its partial derivatives are continuous;
- (ii) If $V(X)$ is positive definite;
- (iii) If $\dot{V}(X)$ is negative semi-definite.

Theorem 2.6. Suppose that all the conditions of the Theorem (2.5) apply, except that condition (iii) is replaced by

- (iii)' \dot{V} is negative definite.

Then the zero solution is asymptotically stable (and such a function V is called a strong Lyapunov function for the system).



UNIVERSITY of the
WESTERN CAPE

2.1 Basic Reproduction Number R_0

The basic reproduction number, denoted by R_0 , plays a vital role in understanding the propagation of the relevant epidemic. It is defined as the average number of secondary infections that occur when one infective individual is introduced into a completely susceptible host population. Basic reproduction number, R_0 ; is determined by the method of next generation matrix in Watmough and Van den Driessche [132]. For simple cases, when there is only a single infected compartment, the value for R_0 is simply the product of the infection rates and the duration of the infection.

We consider the following system of equations for the disease transmission model (epidemic model)

$$\dot{x}_i = f_i(x) = \mathcal{F}_i(x) - \mathcal{V}_i(x), i = 1, \dots, n, \quad (2.1.4)$$

where

$$f(x) = \begin{pmatrix} f_1(x) \\ \vdots \\ \vdots \\ \vdots \\ f_n(x) \end{pmatrix}, \text{ and } x = \begin{pmatrix} x_1 \\ \vdots \\ \vdots \\ \vdots \\ x_n \end{pmatrix}$$

models the rate of change of x_i (where $x_i \geq 0$, is the number of individuals in each compartment i) with

$$\mathcal{V}_i = \mathcal{V}_i^- - \mathcal{V}_i^+$$

and

- $\mathcal{V}_i(x)$ is the rate of appearance of new infections in compartment i ,
- $\mathcal{V}_i^-(x)$ is the rate of transfer out of the i^{th} compartment,
- $\mathcal{V}_i^+(x)$ is the rate of transfer into the i^{th} compartment,

and each of these functions is assumed to be continuously differentiable at least twice.

Also,

$$\mathcal{X}_s = \{x \geq 0 | x_i = 0; i = 1, \dots, m\}$$

\mathcal{X}_s represents the set of all disease-free state. We assume that, these functions satisfy the assumptions ($\mathcal{H}_1, \dots, \mathcal{H}_5$) as described below:

\mathcal{H}_1 If $x_i \geq 0$, then $\mathcal{V}_i(x), \mathcal{V}_i^-(x), \mathcal{V}_i^+(x) \geq 0$ for $i=1, \dots, n$.

\mathcal{H}_2 If $x_i = 0$, then $\mathcal{V}_i^-(x) = 0$ and in particular, $\mathcal{V}_i^+(x) = 0$, if $X \in \mathcal{X}_s$ for $i = 1, \dots, m$ this implies that there can be no transfer of individuals out of an empty compartment by any means. These two assumptions imply that if $x_i = 0$, then $f_i(x) \geq 0$. Therefore the equation (2.1.4) is positively invariant; that is if the initial conditions are positive, then so are the solutions.

\mathcal{H}_3 $\mathcal{F}_i = 0$ if $i > m$ holding for the fact that the rate at which infection occurs (incidence of infection) in an uninfected compartment is zero.

\mathcal{H}_4 $\mathcal{F}_i = 0$ and $\mathcal{V}_i^+(x) = 0$ if $x \in \mathcal{X}_s$, $i = 1, \dots, m$. This condition is to guard against the disease-free subspace being altered and the assumption \mathcal{H}_4 implies that if a population is free of disease then it remains free with no room for immigration of infectious into the diseases free compartment.

\mathcal{H}_5 If $\mathcal{F}(x)$ is set to zero, then all eigenvalues of $Df(x_0)$ have negative real parts.

The following lemma [132] assures that, under conditions $(\mathcal{H}_1, \dots, \mathcal{H}_5)$ the Jacobian, $Df(x_0)$ can be partitioned into a matrix of new infection and that of transfer of individuals in and out of a compartment.

Lemma 2.7. If x_0 is a Disease-Free Equilibrium (DFE) of (2.1.4) and $\mathcal{F}_i(x)$ satisfies the assumptions (\mathcal{H}_1) through (\mathcal{H}_5) , then the derivatives $DF(x_0)$ and $DV(x_0)$ are partitioned as

$$DF(x_0) = \begin{pmatrix} F & 0 \\ 0 & 0 \end{pmatrix}, \text{ and } DV(x_0) = \begin{pmatrix} V & 0 \\ J_3 & J_4 \end{pmatrix}$$

, where F and V are the $m \times m$ matrices defined by

$$F = [\frac{\partial \mathcal{F}_i}{\partial x_j}(x_0)], \text{ and } V = [\frac{\partial \mathcal{V}_i}{\partial x_j}(x_0)], \text{ where } 1 \leq i, j \leq m$$

Further, F is non-negative, V is a non-singular M -matrix and all the eigenvalues of Jacobian matrix J_4 have positive real parts. Thus the matrix V^{-1} is non-negative, and so is FV^{-1} .

If an infected individual is introduced into a compartment k of a disease free population, then the (j, k) entry of V^{-1} can be interpreted as the average length of time this individual spends in compartment j during its lifetime and the (i, j) entry of F can be interpreted as the rate at which infected individuals in compartment j produce new infections in compartment i .

The FV^{-1} matrix is called the next generation matrix for the model [132]. The (i, k) entry of the next generation matrix is the expected number of new infections in compartment i produced by the infected individual originally placed into compartment k . The basic

reproduction number, R_0 , is to

$$R_0 = \rho(FV^{-1})$$

where $\rho(FV^{-1})$ denotes the spectral radius of the FV^{-1} . R_0 is a threshold parameter for the stability of the DFE.

2.2 Stochastic differential equation theory

A stochastic process is called a diffusion or a random process if it satisfies the Markov property and if its paths X_t are continuous functions [98].

Definition 2.8 (Ito diffusion). An Ito diffusion is a time homogeneous stochastic process $X_t : [t_0, \infty) \times \Omega \rightarrow \mathbb{R}^n$ which is the solution of the following stochastic differential equation

$$dX_t = f(t, x)dt + g(t, x)dB_t \text{ with } X_{t_0} = x, t \geq 0 \quad (2.2.5)$$

where f is the continuous deterministic component or drift coefficient, g is the continuous random component or diffusion coefficient [65], defined by $f : \mathbb{R}^n \times [t_0, +\infty) \rightarrow \mathbb{R}^n$ and $g : \mathbb{R}^n \times [t_0, +\infty) \rightarrow \mathbb{R}^{n \times m}$, and B_t is an m -dimensional Brownian motion. For our case study we need only the one-dimensional with Brownian motion $m = 1$ and $n = 4$.

Theorem 2.9 (Ito's theorem). Let X_t be an Ito process and $f, g \in C^{1 \times 2}([0, \infty) \times \mathbb{R}^n)$. Then

$$Y_t = g(t, X_t)$$

is again Ito process, and

$$dg(t, X_t) = \frac{\partial g}{\partial t}(t, X_t)dt + \frac{\partial g}{\partial x}(t, X_t)dX_t + \frac{1}{2}\frac{\partial^2 g}{\partial x^2}(t, X_t)(dX_t)^2 \quad (2.2.6)$$

with $X_{t_0} = x, t \geq 0$ holds with $(dt)^2 = dt dB = 0$ and $(dB)^2 = dt$.

Definition 2.10. Let X_t be an Ito diffusion. Then the infinitesimal generator Δ is defined by

$$\Delta z(x) = \lim_{t \rightarrow 0} \frac{E^x[z(X_t)] - z(x)}{t}$$

Now we apply Ito's theorem 2.9 and define a function $z \in C_0^2(\mathbb{R})$ in order to find a relation between the generator Δ and the coefficients f and g . We have

$$z(X_t) = z(X_0) + \int_0^t (f(X_s) \frac{\partial z}{\partial x}(X_s) + \frac{1}{2} g^2(X_s) \frac{\partial^2 z}{\partial x^2}(X_s)) ds \quad (2.2.7)$$

$$+ \int_0^t (g(X_s) \frac{\partial z}{\partial x}(X_s)) dB_s \quad (2.2.8)$$

Setting up the expectation one gets the following equation by using the martingale property of the Ito integral.

$$E[z(X_t)] = z(X_0) + E\left[\int_0^t (f(X_s) \frac{\partial z}{\partial x}(X_s) + \frac{1}{2} g^2(X_s) \frac{\partial^2 z}{\partial x^2}(X_s)) ds\right]. \quad (2.2.9)$$

A complete proof can be found in [98] of Øksendal.

2.3 Statistical approaches

In general, there are few techniques that can be used for parameter estimation, namely least-squares estimation (LSE), maximum likelihood estimation (MLE) and Bayesian estimation. For linearly parametrized systems, the least squares method generally gives the optimal estimate of parameters, however, it has no basis for testing hypotheses or constructing confidence intervals. In the use of maximum likelihood approach a nonlinear mathematical model that confronts a data can be influenced by the exact relationship between the parameters or by the complexity of the model [117]. The Bayesian estimation of distribution parameters is given as the mean of the posterior distribution which are based on the likelihood, combined with a prior probability distribution. The Bayesian framework, in particular, Markov chain Monte Carlo (MCMC) approaches have demonstrated to be a powerful inference tool for complex systems to data analysis which provides a clear advantage over MLE [48, 53, 117]. In addition, the MCMC method is to be used in the process of parameter estimation in the dynamics of nonlinearly model, ability to generate statistical samples from a high dimensional targeted distribution and convenience for statistical analysis of results [48].

Chapter 2: Mathematical Preliminaries

In order to estimate the unknown parameters θ using a Bayesian approach in nonlinear ODEs given by the following equation as a representation of a biological system:

$$\frac{dx}{dt} = F(\theta, x(t), t), x(t_0) = x_0, \quad (2.3.10)$$

$y(t) = G(x(t)) + \epsilon(t)$, where $x \in R^n$ denotes the system's state variables, x_0 is the initial state, θ represent all the parameters that describe dynamic reactions and assume positive values, $y \in R^n$ represents a sample (observed) data subject to a Gaussian white noise $\epsilon(t) \sim N(0, \sigma^2)$, $F(\cdot)$ is a set of nonlinear functions describing the dynamical property of the biological systems, and $G(\cdot)$ represents a measurement function such as, Binomial, Poisson, etc. With parameter values θ , $p(\theta)$ is the prior and the "evidence," $p(y)$ is the probability of the data according to the model.

If Y_1, Y_2, \dots, Y_n denote the random variables associated with a sample of size n , the notation $L(y_1, y_2, \dots, y_n | \theta)$ denote the likelihood of the sample.

Using the likelihood of the data and the prior on θ , it follows that the join likelihood of Y_1, Y_2, \dots, Y_n is

$$f(y_1, y_2, \dots, y_n) = L(y_1, y_2, \dots, y_n | \theta) \times p(\theta)$$

and that the marginal density or mass function of Y_1, Y_2, \dots, Y_n is

$$m(y_1, y_2, \dots, y_n) = \int_{-\infty}^{\infty} L(y_1, y_2, \dots, y_n | \theta) \times p(\theta) d\theta.$$

Then we have Bayes's rule (the posterior density of $\theta | y_1, y_2, \dots, y_n$) as follows:

$$p(\theta | y_1, y_2, \dots, y_n) = \frac{L(y_1, y_2, \dots, y_n | \theta) \times p(\theta)}{\int_{-\infty}^{\infty} L(y_1, y_2, \dots, y_n | \theta) \times p(\theta) d\theta}$$

So to obtain estimates for parameters conditional on the data, we consider that the data represent Poisson samples with expectation $p * I$, where p is the reporting proportion. Hence the basic of all regression models for count data is the Poisson regression model [102] expressed as

$$y_i \sim pois(\lambda_i)$$

Chapter 2: Mathematical Preliminaries

where

$$\lambda_i = \exp(x_i^T \theta)$$

, $x_i = [1, x_{i1}, x_{i2}, \dots, x_{ip}]^T$ is the covariate vector for sample i

θ = vector of parameter estimates

Assuming an equal dispersion

$$E[y_i|x_i] = \text{var}[y_i|x_i] = \exp(x_i^T \theta)$$



UNIVERSITY *of the*
WESTERN CAPE

Chapter 3

South Sudan profile and data

During the past 50 years Southern Sudan was the most violent and marginalized region in Sudan. The region has been destructively affected by two civil conflicts. One broke out immediately after Sudan independence in 1955 and ended by the Addis Ababa Agreement of 1972. The second war began 1983 and ended by the Comprehensive Peace Agreement (CPA) in Naivasha-Kenya 2005 [50, 111]. In 2011 after enduring two decades of civil war, the people of Autonomous Regions have voted on break away from Sudan and declare an independent country under the name Republic of South Sudan. However, the political violence in the fragile country does not end with independence but takes on new forms. In the run-up to December 2013, a political difference within the ruling party triggered violence in Juba County, which later spread to the rest of the country's counties. Civilians throughout the country were targeted based on their location and ethnicity, and with hundreds of thousands fleeing their pre-crisis homes for safety [121].

The bearings of these two wars have led to a substantial population displacement. More than four million have fled their home to major Towns and mainly into Khartoum as Internally Displaced People (IDPs). There were also up to one million refugees, living mainly in camps and cities in Kenya, Uganda, Central Africa Republic, Ethiopia, Egypt and other neighboring countries [50]. Up to 1.9 million people have been killed throughout the 20 year conflict by violence, disease and starvation [111]. Most of these IDPs have returned to Southern Sudan during the referendum period. However, less than two years

Chapter 3: South Sudan malaria profile and data

Table 3.1: Socio-economic and demographic data

Indicators	Value	Period	source
Population (last census)	8.260 million	2008	Census
Population (projection)	11.296 million	2013	WHO
Population density	13 km square	2012	WHO
Urban composition	18 %	2011	WHO
Population growth rate	4.12 %	2014	WHO
Total fertility rate	5.9	2013	WHO
Crude birth rate	37.68 birth/ 1,000	2013	[124]
Crude death rate	8.42 death/1000	2013	WHO
Infant mortality rate	68.16 death/1000	2014	WHO
Maternal mortality rate	2,054 death/1000	2006	
Net migration rate	11.9/1000	2014	WHO
Life expectancy at birth	55 years	2012	Census
Health life expectancy at birth	48 years	2012	Census

after independence two million individuals have been displaced, including over 500,000 refugees, and an estimated 1.5 million internally displaced persons for the recent on-going conflict. The war has had a major impact on the operation of the basic health system, schools, and water and sanitation supply throughout the country. The mortality of children under the age of five years is counted one of the highest in the world [133], which are exposed to deadly epidemics diseases such as measles, diphtheria, whooping cough, tetanus, and malaria.

The vast majority of the population is rural and the standard of living in the household largely dependent on subsistence farming at 80.7%. Over 7.9% lived mainly on salaries, 6.1% on business, 1.5% on property income and 3.8% on remittances and aid. Among the female-headed households, 81.8% live mainly on subsistence farming, partly as a result of young men migrating to urban zones in search of employment. Rural to urban migration has also deprived households of productive labor. The pre-independence national census

estimated population at 8.2 million people in 2008, with 42% of the population aged under 15 years, 19% group of the median age and only 5% population aged over 60 years [120]. The present estimate may be as high as 11 million due to natural population growth rates and returnees. According to 2008 census, over 368,436 people live in the capital city of Juba, with the crude population density of 20 persons per km² but this is highly variable across the country. The birth and death rates were estimated to 406.2 births and 125 deaths per 1000 people in 2013 (Table 3.1).

The country's fertility rate is 5.9 births per women in [120]. The household average size is 7.5 in 2008 and one-third of households have a chronically ill family member. Country has the highest rate of maternal mortality in the world, at 2,054 per 100,000 live births. The Census reported life expectancy at birth for both sexes increased by 7 year(s) over the period of 2000-2012, while the World Health Report (WHR) regional average of life expectancy increased by 7 year(s) in the same period.

3.1 Climatic patterns

The country covers approximately 640,000 square kilometers (km²), and lies between 250 to 300 east longitude and 40 to 120 north latitude [122]. The proximity to the equator and the running of the white Nile throughout the country are major contributors to the diversity of the country's landscape which consists of tropical rainforest. South Sudan is one of the world's largest wetlands and its climate varies but is essentially tropical where terrain includes tropical forests, swamps, grassy savannas and the sudd is a large swampy, comprising more than 15% of the total area. The country has an average annual high temperature of 33.7° C and a low temperature of 21.6° C. The total average annual rainfall is 953.7 mm (37.54 inches) and to a certain extent the south and west region receives between 1,000–1,500mm while the north and southeastern regions receive between 500–750mm[109]. In a large part of South Sudan people depend on the rainfall for basic agriculture and many of them are nomadic, traveling with their herds of sheep and cows. Along the White Nile, there is well-irrigated farms growing cash crops.

Therefore, agriculture is the main source of income for more than 85% of the population.

Climate change plays a key role in malaria infection as warmer temperature enhance physiological processes of parasites, similarly in mosquito activity such as biting rate, growth and reproduction. Hence, prevalence of malaria depends on temperature. For instance, a small climate variation would, therefore, affect the lifespan and patterns of mosquitoes and also provide transiently suitable conditions for unstable transmission within populations and then demography. In addition, the sensitivity of tropical climates, where there is sufficient rainfall and subsequent stagnant waters provide an enabling environment for mosquito breeding. More rainfall might increase the abundance of mosquito larvae and this eventually leads to more vectors to spread the disease [1].

The country has a tropical climate with a bimodal rainfall pattern and two seasons (wet and dry). Rains normally commences in March-June with a break in late June and restart in July-December. Average temperatures range between 27-30° Celsius in January to February and 30-35° Celsius from December to March [124]. Though, rain seasons continue to mid-December and are usually a period for crop production, people are very vulnerable to mosquitoes biting. Thus, this period coincides with the malaria transmission period of up to 8 months occurring in some areas of agriculture schemes areas, while the urban cities may have another transmission during winter (December- February) due to broken water pipes and stagnant waters.

3.2 Public Health System

The health system has collapsed gradually in the Republic of South Sudan during a long civil war and about 80% of primary health care was delivered by Non-Governmental Organizations (NGOs) and Faith-Based Organizations (FBOs). Within the Comprehensive Peace Agreement (CPA), the Ministry of Health (MoH) recommenced responsibility for rebuilding and transforming the public health system. In the route with a decentralized management structure, the Ministry of Health (MoH) and the State Ministry of Health (SMoH) are in advocating for the health sector policy, partner coordination, and health

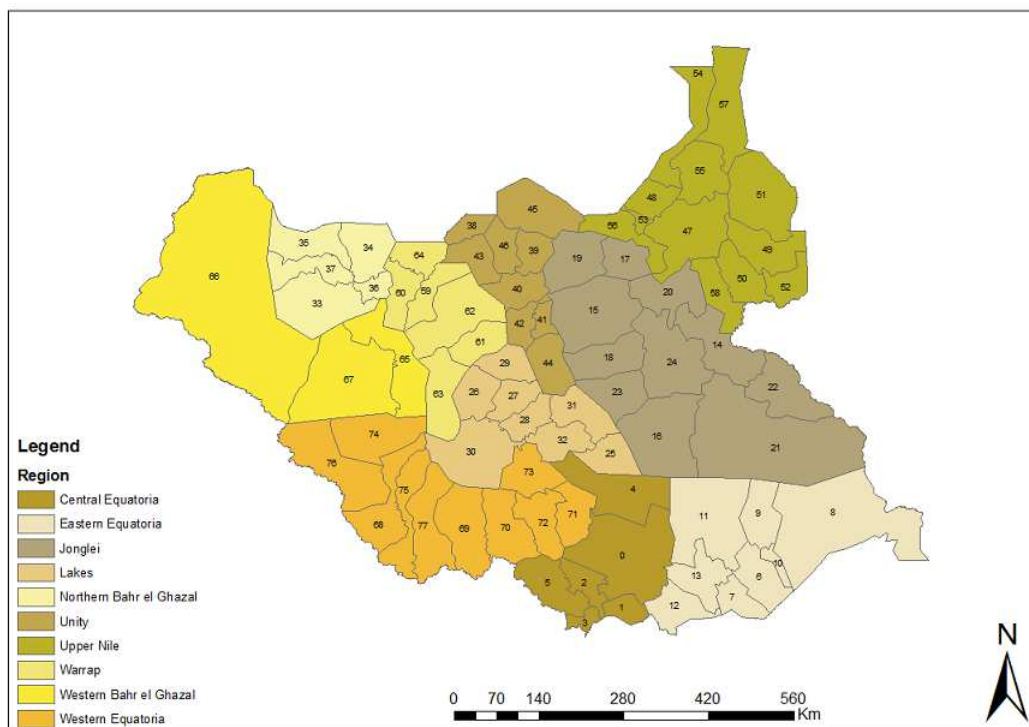


Figure 3.1: Source: [75], South Sudan Health Districts

financing [57]. It provides stewardship and guidance to the sector, manages the Tertiary (Teaching) Hospitals and executes a supportive role to the State Ministries of Health (SMoH). In the 10 States of South Sudan, leadership is provided by the State Ministry of Health for the health service delivery and management to State Hospitals, and County Hospitals [122] as well as County Health Departments (CHD) (Table 3.2). At the County level the health structure is divided into the 79 CHD to oversee the delivery of primary health care services in 270 primary health care centers and 1377 primary health care units across their respective County (see facilities map 3.1).

Nevertheless almost all the facilities are now either run privately or by Non-Governmental Organizations (NGOs) with largest support from World Health Organizations (WHO). At the national level there are over 110 health partners who contribute in the Health Cluster. Here are the most effective NGOs/agencies working hand to hand with Government of South Sudan (GoSS) to provide health services: UNICEF, International Medical

Chapter 3: South Sudan malaria profile and data

Table 3.2: Public health facilities managed by State

States	County #	Hospitals	Primary health care	Health provider
Central Equatorial	6	3 county hospitals, 4 state hospitals and 4 other	32 centers and 160 units	26 health facilities by NGOs and the rest by GoSS
Eastern Equatoria		Kapoeta Hospital	46 centers and 165 units	Almost all health facilities are run by NGOs (UNICEF)
Jonglei	11	3 county hospitals and 1 state	44 centers and 176 units	25 health facilities run by NGOs and the rest by GoSS
Lakes	8	5 county hospitals and 1 state	20 centers and 88 units	Almost all health facilities are run by NGOs
Northern Bahr El Ghazal	4	1 state hospital, 2 military clinic and 1 police clinic	11 centers and 72 units	Almost all by NGOs (Save the Children, CONCERN, FR, MSF, PPF)
Unity	9	State hospital	25 centers and 10 units	Almost all health facilities are run by NGOs
Upper Nile	13	7 county hospitals, 1 state hospital	61 centers and 124 units	Almost all health facilities are run by NGOs
Warrap		5 county hospitals	23 centers and 89 units	3 hospital and all PHCCs in the States are run by an NGOs
Western Bahr el Ghazal	3	5 hospitals	3 centers and 7 units	The health facilities available are either run privately or by NGOs

Corps (IMC), MSF France International, Catholic Relief Services (CRS), Sudanese Red Crescent Society (SRCS), Danish Red Cross (DRC); Deimzubeir, Boro Madina, German Leprosy Relief Association (GLRA) , WHO, WFP, GOAL, ADRA, World Vision, IRD, Oxfam GB, PACT, Tear Fund, ICRC, Save The Children USA, MSF Holland, White Nile Petroleum Company (WNPOC), CARE, ACF, Greater Nile Petroleum Operating Company (GNPOC) , World Relief, World Relief, CCM, ADARA.

3.3 Malaria epidemiology

Malaria history in South Sudan is not a new phenomenon. However transmission is perennial due to multitude of local factors such as environmental/climate (e.g rain pattern, favorable temperature), movement of populations with little immunity into areas of high transmission, socio-economical instability, war related improper housing/ camps and unaffordable preventive means. The burden of disease attributable to malaria varies substantially between different regions of the country which depend on amount of rain and air temperature. It is important to obtain information on the endemicity levels by region or county so that malaria control interventions and treatment can be targeted accordantly. But is not the case in south Sudan, where relevant data on the microepidemiology of parasitemia, morbidity, mortality are limited.

The household cluster sample surveys carried out in 2005 with a total of 2,797 households in 150 different locations. The result shows that malaria prevalence was 24.5% among children under age of five and 9.9% among pregnant women [106]. About 64% of children and 46% of pregnant women were affected by anemia. Only 2% of households were covered by indoor residual spraying (IRS) [47]. Dating back in 1960s the latest comprehensive malariametic survey was conducted and demonstrated percentage of *Plasmodium falciparum* distribution per region which oscillated around 83.6% in Greater Equatoria, 56.8% in Greater Bahr el Ghazal and 86.1% in Greater Upper Nile. According to Malaria indicator survey of 2009, the parasite prevalence ranged from less than 1% in mid northern area to more than 40% in the greater Equatoria region with an average

Chapter 3: South Sudan malaria profile and data

prevalence rate of 14.2% among children fewer than five years of age.

Table 3.3: MIS 2009, Malaria incidence by States 2009-2012

	2009	2010	2011	2012
CES	128494	201632	241099	236878
EES	8113	44454	122169	95291
JNG	10948	23433	30779	80178
LAKES	17308	45594	89133	87460
NBGZ	18330	24701	99280	71469
UNITY	17698	36508	46350	81805
UNS	14800	23625	23458	174291
WBGZ	19955	16207	107910	94824
WES	23894	85682	134348	159639
WRP	28107	48574	103605	116522

In the year 2005, the disease burden goes higher as it goes South, and prevalence could be in some counties as higher as 75%-100%. This can be attributed to climate is being more favorable to the disease in the South than it is in the North. Or, it could be explained by the high consideration of refugee camps in the South. These are speculations.

Malaria situation in South Sudan is hard to quantify due to patchy reporting and the lack of updated information confirming the epidemiology and distribution of parasite species. Estimates of morbidity and mortality therefore contrast enormously. In 2009 it was estimated that 85 per 100, 000 population of mortality are related to malaria and cases were more than 500 per 1000 population and roughly the number of incidences has gradually increased from 71 948 in 2008 to 1 198 357 in 2012 [35] (see Table 3.3).

The three species of Anopheles that are abundant in South Sudan and have high rates of transmission of malaria, are Anopheles Funestus, Anopheles Gambiae, and Anopheles Arabiensis. The Anopheles Gambiae is the main malaria vector. Plasmodium Falciparum is the predominant species, which is responsible for up to 90% of malaria infections and Plasmodium Vivax accounts for 5% (see Table 3.3). Beside Plasmodium Malariae may

Table 3.4: Source [123] Malaria Parasites species percentage by region

	P. Falciparum	P. Vivax	P. Malariae	Mixed species
Rural	94.5	4.8	0.8	6.5
Urban	93.7	6.3	0	4.7
Upper Nile	100	0	0	0
Bahr El Ghazal	100	0	0	3.5
Equatoria	92.4	6.8	0.9	7.9
Total	94.4	5	0.7	6.3

account for up 0.7% of infection [20, 123]. Consequently, malaria is endemic across the entire country with year-round transmission but peaking towards the end of the rainy season from September to December. Endemicity varies between meso-, hyper- and holoendemic [35].

3.4 Malaria control

It has been quite a journey from the WHO, which supported the beginnings in 1998 when the first health policy was launched in the South Sudan region before independent. Since the signing of the comprehensive peace agreement (CPA) in 2005, South Sudan has achieved major milestones in the fight against malaria. Subsequently the Malaria Task Force was established in 2003 with only a Programme Manager. Then a year later, National Malaria Control Programme (NMCP) was formed [21]. The NMCP has so far implemented a single Strategic Plan (July 2006-July 2011) with many malaria policies, guidelines and staff capacity have been developed at all levels. In 2007 the transitions to the Malaria Technical Working group akin to the country Roll Back Malaria (RBM) partnership. The fact of the matter is that malaria has a clear priority in the National Health Policy (2007-2011), included National Health Sector Strategic Plan and the Health Sector Development Plan (2012-2016) which are a key component of the Ministry

Chapter 3: South Sudan malaria profile and data

of Health basic package of health services.

During the past decade, the first-line treatment against uncomplicated Plasmodium Falciparum malaria was the Chloroquine (CQ) with Sulphadoxine-Pyrimethamine (SP) as the second line treatment [125]. A study in South Sudan has shown high parasite resistance to CQ and SP which ranges between 40% and 93% for CQ and from 15% to 69% for SP. An in vivo study was carried out on the efficacy of CQ, SP in Kajo Keji County, which provides important missing data. The study pointed out that none of these drugs could be used in monotherapy against Falciparum malaria. This suggests that even in combination with artemisinin, cure rates might not be efficient enough [125]. Plasmodium Falciparum resistance to chloroquine was detected in Lui (Mundri) of West Equatoria in 2002, with 91% of treatment failure. Another trial was carried out in Upper Nile State in 2001 to test for the efficacy of Amodiaquine (AQ), CQ and SP. Results revealed that CQ and AQ produced treatment failures of 11.5% and 5.6% respectively [122]. The low efficacy of CQ can be described by the regular use of the drug within and outside the official health system. However in Africa, SP preserved its efficacy until the late 1990s but since then its resistance has spread quickly [22]. SP was introduced in Sudan since the early 1970s. In 2002/2003 testing for CQ and SP in several sentinel sites reported an overall failure rate of CQ as 43.7% in the Northern Sudan and 80.2% in the Southern Sudan [106]. Nevertheless, recently the country has replaced its treatment policy to Artemisinin-based Combination Therapy (ACT) in order to avoid malaria aggravation induced morbidity and mortality. Although SP is still the drug of choice for Intermittent Presumptive Treatment (IPTp) for malaria in pregnancy [47].

With limited data, Dichloro-diphenyl-trichloroethan (DDT) was one of insecticide resistance identified for susceptibility of Anopheles species populations without any characterization to malaria vectors species [124]. A study in Juba County found that Anopheles species were tolerant to DDT and deltamethrin [125]. Moreover, in the late 70s and early 80s indoor residual spraying and larviciding was used to prevent malaria transmission in and around the major towns and municipalities. However, due to the collapse of infrastructure and public services as a result of civil Wars (1955-1972 and 1983-2005), these

Chapter 3: South Sudan malaria profile and data

interventions and treatments have ceased. After several decades without any vector control, programmatic control of the malaria vectors was relaunched in Sudan along with malaria case management in 2004 [57].

Since then considerable progress has been made in the country relative to first Malaria Strategic Plan (2006-2011). This formed the first framework within which malaria control would be implemented in South Sudan. The National Malaria Strategic Plan of 2014-2020 aimed at reducing by 80% reported malaria morbidity and deaths of 2013 levels and malaria parasite prevalence by 50% of the 2013 levels, by 2021 [124]. The strategy precisely targets at reducing mortality rate of children under-5 year of age mortality rate from 250 to 140 per1000 live births [124].

However, in South Sudan mosquito nets remain the most effective prevention available against malaria. Insecticide-treated bednets (ITNs) usage has long history in South Sudan, where they were first introduced through the Upper Nile Project in 1996. On the other hand ITNs distribution is hard to maintain in the post-conflict situation. Therefore, LLINs remain the main present strategy whereby pregnant women and children under 5 years of age are major targets particularly in the rural and remote areas.

Notably LLIN is one of the most effective preventive measures for malaria in South Sudan. In 2008, the successful mass distribution campaign of free LLINs was done in all States countrywide. With support from partners, over 9,335,035 LLINs were distributed over the review period although only 2,141,806 (53%) of these LLINs were deemed protective of the entire population by the end of 2013 [124]. Further intervention considered by NMCP since 2007 included, early diagnosis through diagnosis test (RDTs), with limited use of Indoor Residual Spraying (IRS) and Larviciding and intermittent preventive treatment (IPTp) [22]. People also use locally untreated bednet made out of cotton, called Aldamuria. Furthermore, the proportion of children below the age of 5 years sleeping under an ITN at night increased to at least 60%. Additionally, the proportion of households with at least one ITN increased to 70% and structures in targeted areas sprayed with quality IRS to at least 80%.

The mosquito bednets survey in 2009 provides information on the percentage of house-

Chapter 3: South Sudan malaria profile and data

holds with ITN and LLIN (Table 3.4). However, malaria control has recently been implemented through a combination of Case Management (CM) and LLINs, in Central Equatorial State and in some other States, although CM coverage may not be achieved in the near future. Ownership of mosquito net by Central Equatorial State count of 54%. The intervention was nearly as effective as expected, probably because of suboptimal LLIN coverage, retention, and utilization. Many of the targeted households were sleeping outdoors, without a bednet. Some used the distributed nets for fishing or fencing. Although the national guidelines for intervention distributions recommended that only bednet types that had been prequalified by the WHO to be distributed, not all of the distributed nets met this criterion [22]. Countrywide, LLINs mass campaigns were piloted with the target coverage of 80% and only about 4.7 million were delivered to the population who are in need. Despite this, the number of infected cases and deaths increased in all age groups. Malaria indicator survey in 2009 indicates that the proportion of structures protected through IRS is about 2.1% of the population at risk.

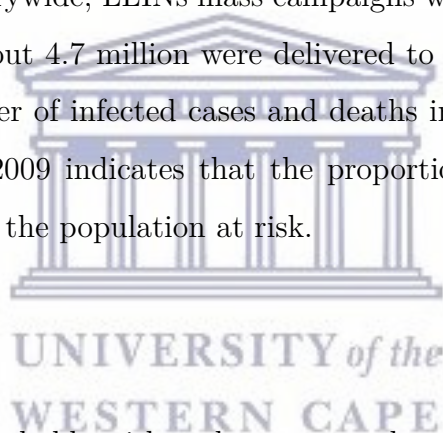


Table 3.5: Percentage of households with at least one and more than one mosquito net
South Sudan MIS 2009

Characterstic	Rural	Urban	Countrywide
PH have at least one ITN	52%	64.1%	54.2%
PH have more than one ITN	39.4%	51%	42%
PH have at least on LLIN	49%	69.9%	51%
PH have more than one LLIN	37.7%	49.5%	39.8%
Average number of Nets per houshold	1.9	1.6	1.7
Number of Bednets	3092	821	3913

3.5 Migrant pattern

In South Sudan, displacement is closely related to ethnic affiliation, which is often tied to ancestral homelands and traditional grazing areas. The country has an extremely mobile population, with many herders undertaking seasonal migration as a result of cattle grazing. Natural hazards, predominantly flooding, cause regular disaster-induced displacement, while more recent conflicts, as well as rural-to-urban migration have caused many people to live in a location that is different to their ancestral home [50, 121].

Table 3.6: South Sudan Refugees and IDPs by State [130]

State	Refugees	IDPs	Total	Percentage
Central Equatorial	17,665	63,400	81,055	5.3%
Eastern Equatoria		7600	7600	0.5%
Jonglei	2339	579,700	582039	38%
Lakes	0	133,800	133,800	8.7%
Northern Bahr El Ghazal	0	700	700	0.5
Unity	84,895	280,800	365,695	23.9%
Upper Nile	128,944	193,700	322,644	21.1%
warrap	0	8800	8800	0.6%
western equatoria	9,394	25	9419	0.6%
Western Bahr el Ghazal	0	12,600	12,600	0.8%

More than a million Southern Sudanese were living in Khartoum (North Sudan) and initially sought refuge after the invasion of Khartoum in 1956. Many people were able to return to their homes (southern region) to safe areas in the early 1980s, following the Addis Ababa agreement. Upon signing the comprehensive peace agreement in 2005, South Sudan has been receiving a steady stream of returnees (internal displacement and refugee) people who were displaced during the civil war and wishing to resettle in the newly independent country.

Since the outbreak of the fight and political upheavals in December 2013, some capri-

Chapter 3: South Sudan malaria profile and data

cious States of the world's youngest country are experiencing complex humanitarian emergency situations with ongoing armed and intercommunal violence. Access to displaced people is so difficult and refugees/IDPs have faced serious humanitarian concerns such as hunger, the destruction of markets, massive disruption to livelihoods caused by people fleeing from the conflict and water-borne diseases, in particular malaria. The UNHCR estimates to 1,660,141 individuals who remain internally displaced in 258 locations across the country (shown in Table 3.6 by State) and more than 505,298 individuals refugees to Sudan, Kenya, Ethiopia and Uganda [130].

According to a recent assessment, more than 35,000 South Sudanese people were forced to flee Maridi County. In addition, 196 houses were burnt and the town market entirely looted. Had it not been assumption responsibility taken by international donors and NGOs to support basic health services, the situation would have worsened. However, estimates one in five of South Sudan's 11 million people have fled their homes, often hiding in the bush without access to bednets, food, water or medical care. While the security situation has stabilised in some parts of the country, the situation remains fragile and there have been relatively few voluntary returnees from displacement sites. Some of these sites are located at Swamp areas which are highly attractive to mosquito breeding. There is increasing pressure to relocate IDPs from Protection of Civilian (PoC) sites, but most IDPs are reluctant to leave these sites until peace is restored throughout the country. Major displacement sites in six of the most conflict-affected States in South Sudan are Central Equatoria, Jonglei, Lakes, Unity, Western Bahr el Ghazal and Upper Nile, which are also home to the largest concentrations of internally displaced persons [130].

In week 29 of 2015, a total of 5,715 malaria cases were reported with the highest malaria incidence (cases per 10,000) being reported in Bentiu PoC (270), followed by UN House (216), Malakal (166) and Renk (117) and these are the top camps that count for the morbidity among IDPs and registered a proportionate morbidity of 28.9%, which represents an increase when compared to 18% in the corresponding week of 2014 [140] (for more details see Table ??). In August 2015 the Medecins Sans Frontieres (MSF) described malaria as skyrocket with 4,000 patients receiving treatment each week in Bentiu camp

Chapter 3: South Sudan malaria profile and data

and the vast majority of them were women and children, who have endured a difficult and dangerous journey to reach the camp [120]. Nevertheless, access to the most conflict affected settings remains a challenge affecting health service delivery. For instance in the bigger part of the Upper Nile areas, Unity, Jonglei , and Central Equatoria States where thousands are displaced, access to health facilities continues to be hampered by insecurity.




UNIVERSITY *of the*
WESTERN CAPE

Chapter 4

Pressure-testing some mathematical models of malaria transmission

4.1 Introduction



Over the last decade, the significance of the topic of mathematical modelling and real-world examples in all fields has increased enormously. In particular, compartmental models of mathematical epidemiology have become an important tool in understanding the mechanisms of disease transmission and in decision making processes regarding intervention programs for controlling the diseases in many countries. A large number of mathematical models in epidemiology have been developed to gain insight into transmission dynamics of malaria, starting from the basic malaria model of Ross [110] and Macdonald [74]. Subsequently these models have been extended by researchers considering different factors related to malaria transmission dynamics and control, such as latent period of infection in mosquitoes and humans, acquired immunity, the effect of climate change, the effect of age-structure on malaria spread and control [8, 9, 30, 66, 73, 86].

Aron [8] presented two different approaches to study the dynamics of acquired immunity to malaria. These approaches were exposure to infections to generate qualitatively different results. Chiyaka et al. [25] proposed a deterministic model with two latent periods in the non-constant hosts and vector populations for assessing the impact of per-

Chapter 4: Pressure-testing some mathematical models of malaria transmission

sonal protection, vaccination and treatment in curtailing the spread of malaria. Buonomo and Vargas [17] extended the vector-bias model of malaria transmission introduced by Chamchod and Britton [20] to incorporate both immigration and disease-induced death of humans. In their extended model, they examined for exhibit backward bifurcation by using the theory of center manifold. Moreover, nonlinear stability analysis by means of the Lyapunov theory and the LaSalle invariance principle has been performed. Esteva et al. [39] proposed a deterministic model for monitoring malaria transmission dynamic with impact of anti-malarial drug.

Okell et al. [94] developed a mathematical model of parasite transmission in human and mosquito population by introducing artemisinin-based combination therapy (ACT) and alternative first-line treatment in six regions of Tanzania with different level of malaria transmission. In their study, they found that in low transmission area ACT may reduce malaria transmissions if it is widely used effectively as well the widespread use of the insecticide-treated bednets. The model also shows that in the area with high transmission the use of long-acting treatment with or without artemisinin component might be a good method to reduce the transmission. Their findings suggested that properties of anti-malarial drugs need to be taken into consideration together with the level of transmission in the areas in order to achieve highest impact on malaria transmission.

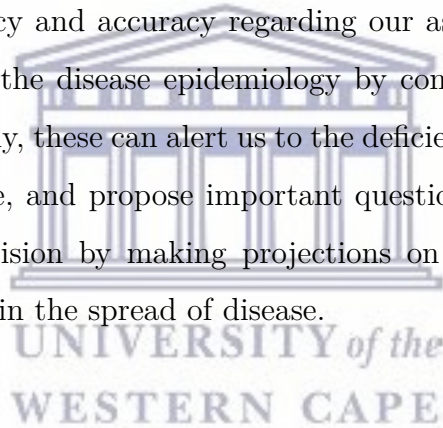
Smith et al. [114] review the historical development of a theory for mosquito-transmitted pathogens and the development of strategies for mosquito-borne disease prevention by Ross followed by Macdonald's seminal contributions and subsequently described Ross-Macdonald models as the best set of assumptions identified, including the concept of vectorial capacity, methods for measuring key components of transmission by mosquitoes, and a quantitative theory of vector control.

In all of these models, there are no ideal models that can be suitable for malaria disease whilst different structures may be used to model the same situation. However, the structure of the model involves identification of parameters that can strongly influence model outcomes and also model assumptions that when relaxed can strongly affect the results of the model. Moreover, the main reason for building a model in the first place

Chapter 4: Pressure-testing some mathematical models of malaria transmission

is to make novel predictions that stimulate subsequent rounds of disease dynamics. The rationale for testing models is significantly important by measuring model parameters directly from actual observation data which many of these models ignore.

In this chapter, we aim to pressure test four different structures of models. The models are validated using malaria incidence data of the highest transmission State (Central Equatoria) of South Sudan to estimate their parameters by fitting empirical observations. This can help understand the nature of the models and their trajectory behaviour differences that can be applied to make predictions on the course of malaria dynamics and to control its transmission. An important benefit derived from mathematical modelling is that it requires transparency and accuracy regarding our assumptions that enable us to test our understanding of the disease epidemiology by comparing model results and observed patterns. Importantly, these can alert us to the deficiencies of our current understanding of the disease course, and propose important questions to investigate. Models can also help to make a decision by making projections on important issues such as intervention-induced changes in the spread of disease.



4.2 Compartmental Models

We consider different compartmental models to test how they fit observation data and compare their outcome and prediction of the disease dynamics. The first model consists of a simple SIR-model (Susceptible - Infected - Recovered) for human and a simple SI (Susceptible - Infected) for mosquito with the assumption that at any time, drug therapy and intervention coverage can be incorporated into the model. The second model considered is a simple SEIR-model (extension of SIR models that include an exposed class) for human and a simple SEI for mosquito. Third model as an intermediate example based on a slight modification of a host-vector model presented by Filipe et al. [40]. The expression of the SEIAR Model for the human host which infected class of the model II is subdivided into two categories clinically infectious individuals I , asymptomatic infectious individuals A and SEI Model formulation for vector with the presence of drug therapy. The fourth

Chapter 4: Pressure-testing some mathematical models of malaria transmission

model is as more complex model, similar to that of Griffin et al. [51] which consists of six human distinct compartments and three mosquitoes incorporated with drug therapy.

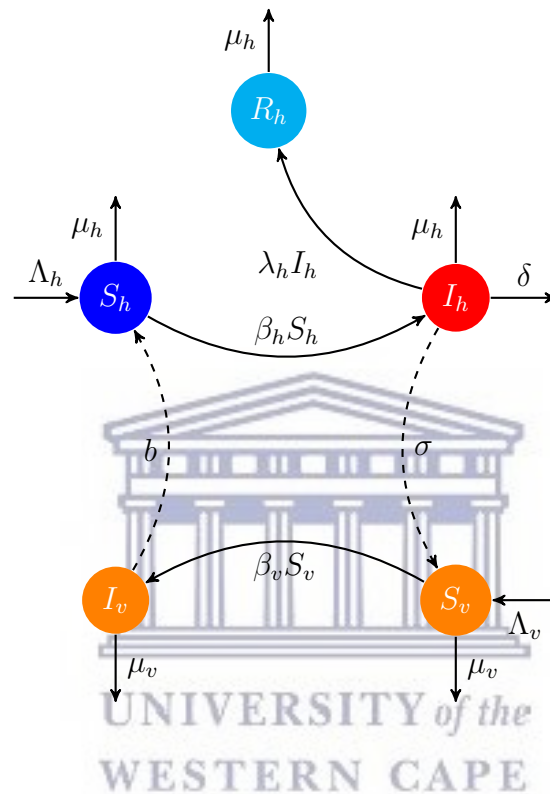


Figure 4.1: State diagram for the SIR model

4.2.1 An SIR Model

The simple compartmental model without an incubation period is based on a previous model of malaria transmission [110] with five compartments, for both human population and mosquito population at time t . The susceptible compartments for both humans and mosquitoes are recruited by birth at a rate of $\Lambda_h = \mu \times N_h$ and Λ_v respectively. The total human population N_h is divided into a proportion of the susceptible (S_h) that is assumed to be infected at a rate β_h then becomes infectious (I_h).

Some individuals from the I_h class recover from the disease and become part of the R_h class with lifelong immunity and individuals may not become susceptible again. The Mosquito population N_v consists of a two compartments, the susceptible (S_v) popula-

Chapter 4: Pressure-testing some mathematical models of malaria transmission

tion gets infected with rate β_v which then becomes infectious (I_v) and mosquitoes do not recover. The model [110] in which the classes have been formulated in a general SIR compartmental epidemic model with the attractiveness of infectious humans to mosquitoes, will now be pressed. The ordinary differential equations that describe the dynamics of malaria in the human and mosquito populations with initial value are as follows.

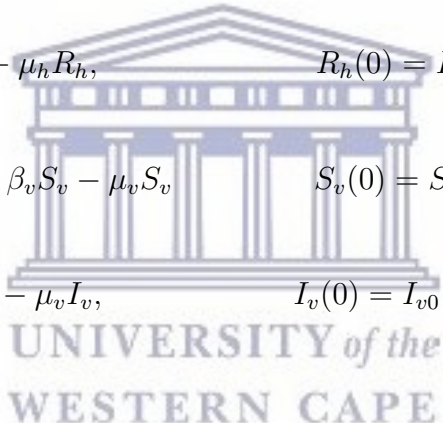
$$\left\{ \begin{array}{l} \frac{dS_h}{dt} = \Lambda_h - \beta_h S_h - \mu_h S_h, \quad S_h(0) = S_{h0} \geq 0 \\ \frac{dI_h}{dt} = \beta_h S_h - \lambda I_h - \delta I_h - \mu_h I_h, \quad I_h(0) = I_{h0} \geq 0 \\ \frac{dR_h}{dt} = \lambda I_h - \mu_h R_h, \quad R_h(0) = R_{h0} \geq 0 \\ \frac{dS_v}{dt} = \Lambda_v - \beta_v S_v - \mu_v S_v, \quad S_v(0) = S_{v0} \geq 0 \\ \frac{dI_v}{dt} = \beta_v S_v - \mu_v I_v, \quad I_v(0) = I_{v0} \geq 0 \end{array} \right. \quad (4.2.1)$$


Table 4.1: Model Variables

Symbols	Description
S_h	Susceptible individuals
I_h	Individuals with malaria symptoms
R_h	Recover individuals
S_v	Susceptible mosquitoes
I_v	Infectious mosquitoes

where

$$\beta_h = \frac{\epsilon b I_v}{N_h}$$

and

$$\beta_v = \frac{\epsilon \sigma I_h}{N_h}$$

Chapter 4: Pressure-testing some mathematical models of malaria transmission

represent the force of infection (the infectious rate) on humans and mosquitoes respectively. They controls the rate of spread which represents the probability b, σ of transmitting the disease between a susceptible human and an infectious mosquito and ϵ is the bite rate. The parameter $\lambda = \frac{1}{D}$ is the recovery rate determined by the average duration of infection D . Human either die naturally with the rate μ_h or due to the disease with probability δ . The parameter μ_v is the mosquito death rate.

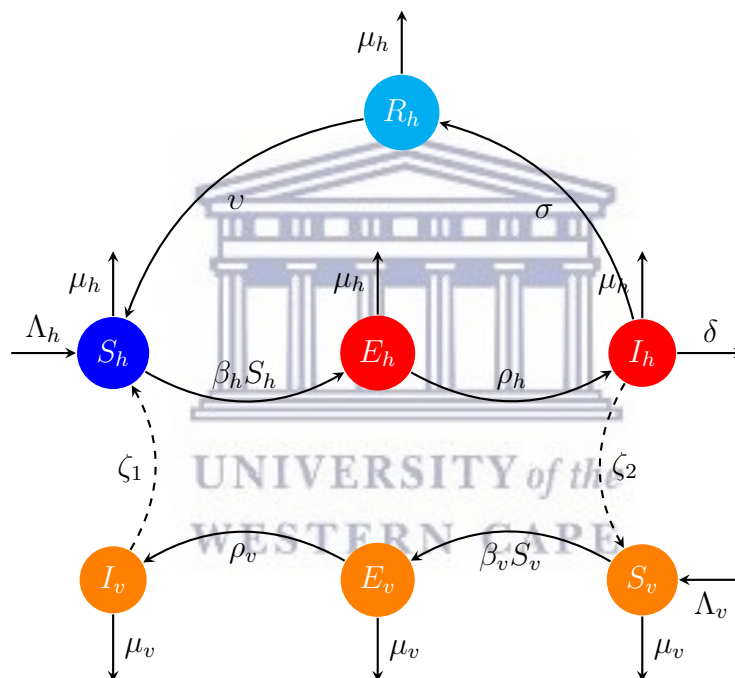


Figure 4.2: State diagram for the SEIR model

4.2.2 An SEIR Deterministic Model

In the case of an SEIRS model, we considered Buonomo and Vargas [17] extended the vector-bias model of malaria transmission introduced by Chamchod and Britton [20] to incorporate both immigration and disease-induced death of humans. The human population N_h is divided into four classes: Susceptible, S_h ; exposed E_h ; infectious, I_h ; and recovered (immune), R_h and the female mosquito population N_v into three classes: Sus-

Chapter 4: Pressure-testing some mathematical models of malaria transmission

ceptible, S_v ; exposed E_v and infectious, I_v . Such that $N_h = S_h + E_h + I_h + R_h$ and $N_v = S_v + E_v + I_v$. Individuals move from one class to the other as their status with respect to the disease evolves.

Susceptible, S_h class represent population size of individuals not yet infected with the malaria parasite at time t and assumes that all individuals are not necessarily at risk. The class size is enlarged by recruitment through birth and immigration at constant rate $\Lambda_h = \mu_h N_h$, and is decreased either through infection or reinfection to the infectious class or death at a rate μ_h .

Exposed class represent the fraction of population whose individuals are newly-infected, but are not capable of transmitting the infection to susceptible mosquitoes. During this stage, parasite abundance is very low for effective transmission to other susceptible hosts. The interaction between susceptible and exposed classes happen at the rate β_h when an infectious mosquito bites a susceptible human, with some finite probability ζ_1 that the parasite will be passed on to the human. Individuals become infected at a rate determined by the force of infection in the population, which is dependent of the ratio of vectors to humans, the biting rate per mosquito on humans and the proportion of infectious mosquitoes in the vector population. The biting rate is the average number of humans bitten by a mosquito per unit time. The force of infection β_h and β_v are given by

$$\beta_h = \frac{\zeta_1 \epsilon I_v}{N_h}$$

and

$$\beta_v = \frac{\zeta_2 \epsilon I_h}{N_h}$$

Infectious class, I_h represent the fraction of population which progresses from exposed class to infectious class at the rate ρ_h , then infected individuals move to join the immune class at rate σ due to treatment or natural immunity. While some individual leave the population through natural death rate μ_h or disease-induced death rate are δ . Recovered (immune), R_h represent populations who have recovered from the disease. We assumed that recovered human have no plasmodium parasites in their bodies and hence they can

Chapter 4: Pressure-testing some mathematical models of malaria transmission

not transmit the infection to mosquitoes. The model equations are given by:

$$\left\{ \begin{array}{l} \frac{dS_h}{dt} = \Lambda_h - \beta_h S_h - \mu_h S_h + v R_h, \\ \frac{dE_h}{dt} = \beta_h S_h - \rho_h E_h - \mu_h E_h, \\ \frac{dI_h}{dt} = \rho_h E_h - \sigma I_h - \delta I_h - \mu_h I_h, \\ \frac{dR_h}{dt} = \sigma I_h - (v + \mu_h) R_h, \\ \frac{dS_v}{dt} = \Lambda_v - \beta_v S_v - \mu_v S_v, \\ \frac{dE_v}{dt} = \beta_v S_v - \rho_v E_v - \mu_v E_v, \\ \frac{dI_v}{dt} = \rho_v E_v - \mu_v I_v, \end{array} \right. \quad (4.2.2)$$

with initial conditions $S_h(0), S_v(0) > 0, E_h(0), I_h(0), R_h(0), E_v(0), I_v(0) \geq 0 > 0$.

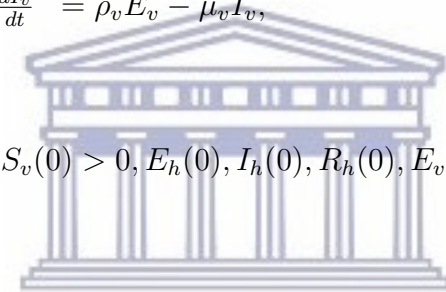


Table 4.2: Model parameters

Parameters	Description
ϵ	Infectious mosquito bites rate
ζ_1	Probability of infection
ζ_2	Onward infectivity from an asymptomatic infectious
Λ_h	Birth/ Migration rate of humans
Λ_v	Per ca-pita birth rate of mosquitoes
μ_h	Natural death rate of humans
μ_v	Daily mosquito mortality
ρ_h	Human infectious rate
ρ_v	Daily survival probability of mosquito infection
σ	Recovery rate
v	human Re-susceptibility rate

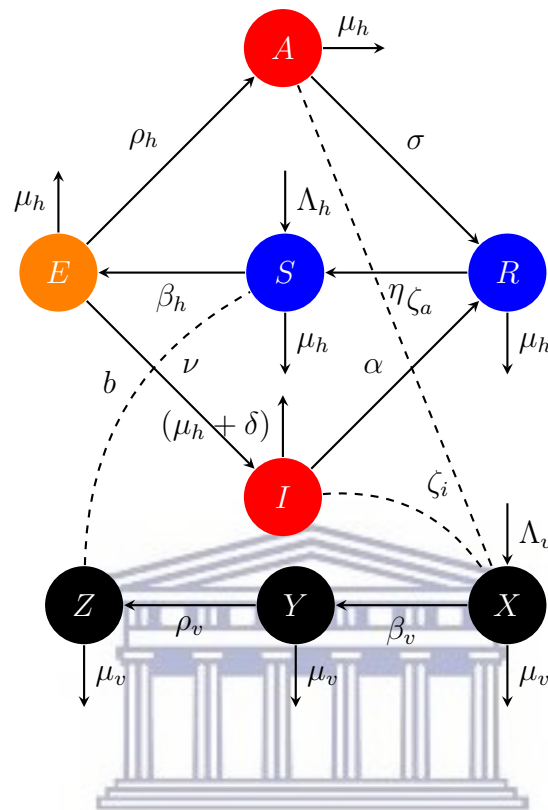


Figure 4.3: Flow diagram for the SEIAR model

4.2.3 An SEIAR deterministic model

We performed an analysis of the parasite transmission using a deterministic compartmental structure similar to that of Filipe et al [40]. Human population is represented by five classes (this model takes with treatment into account): Susceptible S , latent E , infected with the symptomatic disease (severe and clinical cases) I , asymptomatic patient infection A and recovery R . It's assumed that individuals become infected at rate β_h which depends on the biting rate ϵ , the prevalence of infection in the mosquito population Z and the probability of developing blood stage infection b . The following set of differential equations describes the transmission dynamics among the human population and the mosquito population in the presence of treatment:

Chapter 4: Pressure-testing some mathematical models of malaria transmission

$$\left\{ \begin{array}{l} \frac{dS}{dt} = \Lambda_h - \beta_h S + \eta R - \mu_h S \\ \frac{dE}{dt} = \beta_h S - \rho E - \nu E - \mu_h E \\ \frac{dI}{dt} = \nu E - \tau \pi I - (1 - \pi)\alpha I - \delta I - \mu_h I \\ \frac{dA}{dt} = \rho_h E - \sigma A - \mu_h A \\ \frac{dR}{dt} = \sigma A + \tau \pi I + (1 - \pi)\alpha I - \eta R - \mu_h R \\ \frac{dX}{dt} = \Lambda_v - \beta_v X - \mu_v X \\ \frac{dY}{dt} = \beta_v X - \mu_v Y - \rho_v Y \\ \frac{dZ}{dt} = \rho_v Y - \mu_v Z \end{array} \right. \quad (4.2.3)$$

with initial conditions $S(0), X(0) > 0, E(0), I(0), A(0), R(0), Y(0), Z(0) \geq 0$. For the treatment of symptomatic (clinical) infection, we assume that access to treatment happen at a rate of π and the duration of both drug recovery and the period of seeking treatment at a rate of τ while natural recovery period is at rate α . The model include births at rate Λ_h and deaths at rate μ_h which can sustain an epidemic or allow new introductions because new births provide more susceptible individuals. The transmission among mosquitoes is integrated dynamically and responds to changes in the prevalence of infected humans. Mosquitoes are recruited into a susceptible class X at a rate Λ_v and if they become infected they enter a latent class Y before becoming infectious Z . A constant death rate μ_v and population size is assumed. The transitions between these states are described by Λ_v , the rate at which mosquitoes become infectious once infected and ρ_v is the progression rate of mosquito. The force of infection for human β_h and that for mosquito β_v are given by

$$\beta_h = \frac{b\epsilon Z}{N_h}$$

and

$$\beta_v = \frac{\zeta_i \epsilon I + \zeta_a \epsilon A}{N_h},$$

where b is the probability of infection if bitten by an infectious mosquito with $0 < b \leq 1$, ζ_a is the onward infectivity from an asymptomatic infectious with $0 < \zeta_a \leq 1$, and ζ_i is the onward infectivity from a clinical infection with $0 < \zeta_i \leq 1$.

Chapter 4: Pressure-testing some mathematical models of malaria transmission

Table 4.3: Model Parameters: Description and value

Symbol	Description	Estimate & Ref
Λ_h	Birth rate of humans	Humans/Day Est
Λ_v	Per ca-pita birth rate of mosquitoes	0.13 [23]
μ_h	Natural death rate of humans	0.00006614 Est
ϵ	Mosquitoes biting rate	Derived from data
b	Probability of infection	Derived from data
ζ_a	Onward infectivity from an asymptomatic infectious	0.2 fixed [134]
ζ_i	Onward infectivity from a clinical infectious	Derived from data
ρ_h	Probability of asymptomatic infectious	0.0071 fixed [134]
ν	Probability of acquiring clinical disease	Derived from data
α	Clinical infection rate	Derived from data
σ	Asymptomatic infection rate	1/200 (1/180-1/250) fixed [52]
δ	Humans death rate due to malaria	0.0004 (0.00027-0.0005) fixed [26]
η	Human Re-susceptibility rate	Based on drug
μ_v	Daily mosquito mortality	Derived from data
ρ_v	Daily survival probability of mosquito infection	Derived from data

4.2.4 An individual-based simulation model

Here we introduce a slightly modified model of Griffin et al. [51] which is an individual-based simulation model for parasite transmission incorporating the effect of the switch to Artemisinin-Combination Therapy (ACT). The model found to explore the potential for available control measures to reduce parasite prevalence to a low level as laid out in the control phase of the global elimination framework.

The dynamics of the human host is described by six infectious states: susceptible (S), treated clinical disease (T), untreated clinical disease (D), asymptomatic patent infection (A), sub-patent infection (U) and protected by a period of prophylaxis from prior treatment (P). People move between these states with rates/probabilities described under

Chapter 4: Pressure-testing some mathematical models of malaria transmission

the assumption that on infection, individuals either progress to the clinical disease at a probability ϕ or develop patent asymptomatic infection at probability $(1 - \phi)$. For those of clinical disease progress at the probability rate of f_T of being treated successfully (T) and for those of fail treatment move to the class (D) at the probability rate $1 - f_T$ which is eventually becomes patently asymptomatic (A) with rate r_D . From patent asymptomatic infection, individual assumed to be moved to sup-patent stage (U) at a rate r_A . It is assumed that those who are treated enter the period of prophylactic protection (P) with rate r_T before return to susceptible class at a rate of r_P .

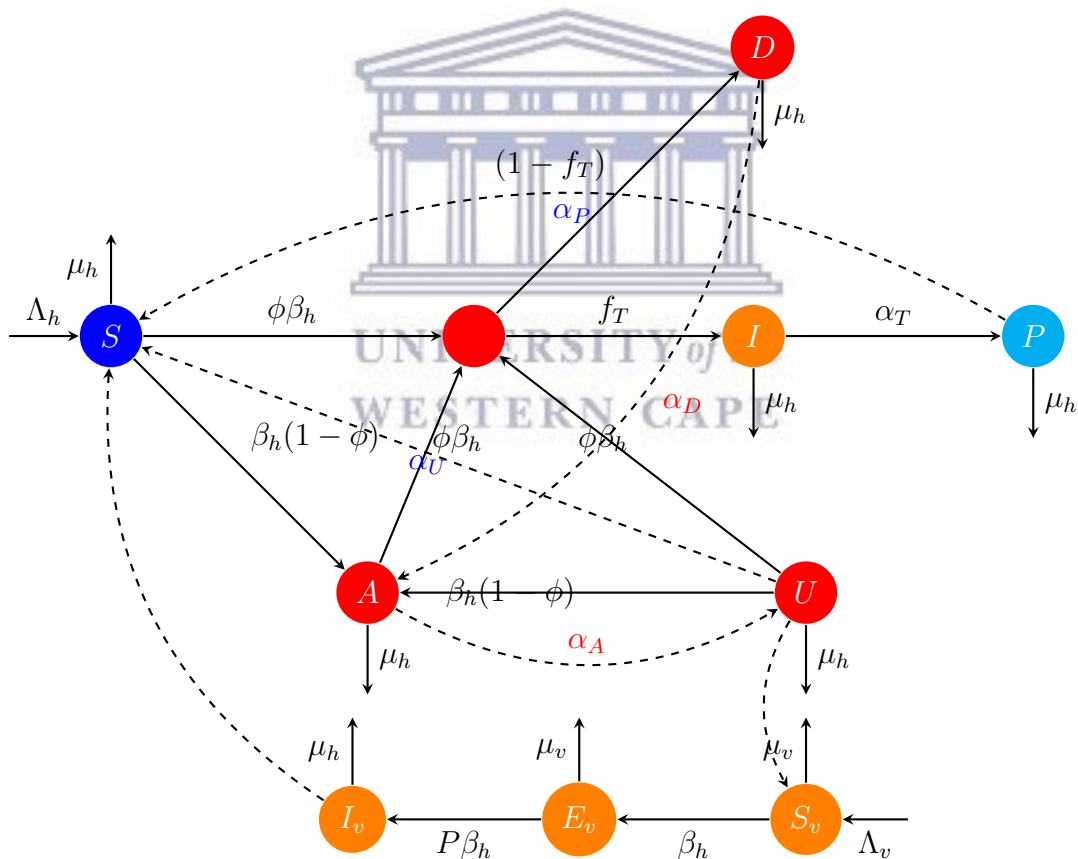
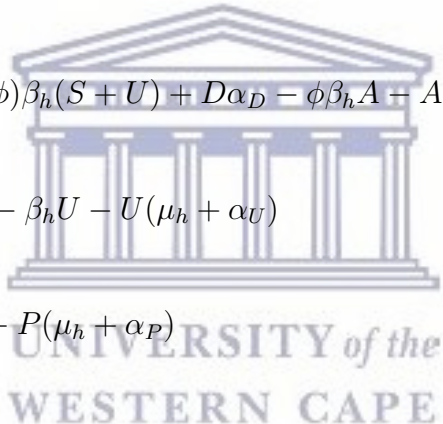


Figure 4.4: Flow diagram for Human and Mosquito infection model

In the deterministic form and without age dependence, the model can be written as

Chapter 4: Pressure-testing some mathematical models of malaria transmission

the following ordinary differential equation (ODE):

$$\left\{ \begin{array}{l}
 \frac{dS}{dt} = \Lambda_h - (\beta_h + \mu_h)S + P\alpha_P + U\alpha_U \\
 \frac{dI}{dt} = \phi f_T \beta_h (S + A + U) - I(\mu_h + \alpha_T) \\
 \frac{dD}{dt} = \phi(1 - f_T) \beta_h (S + A + U) - D(\mu_h + \alpha_D) \\
 \frac{dA}{dt} = (1 - \phi) \beta_h (S + U) + D\alpha_D - \phi \beta_h A - A(\mu_h + \alpha_A) \\
 \frac{dU}{dt} = A\alpha_A - \beta_h U - U(\mu_h + \alpha_U) \\
 \frac{dP}{dt} = I\alpha_T - P(\mu_h + \alpha_P)
 \end{array} \right. \quad (4.2.4)$$


where t represents time, f_T ratio of clinical cases receiving effective treatment and $\alpha_T, \alpha_D, \alpha_A, \alpha_U, \alpha_P$ symbolise human infection durations. We assumed people have a similar biting rate irrespective of their body size, in conjugation with Okell study assumption and hence ignore the age effect on the force of infection given by $\beta_h = \epsilon b I_v / N$, where ϵ is the Entomological Inoculation Rate (EIR) as measured for adults at time t and b is the probability of infection if bitten by an infectious mosquito. For the mosquito model, considered the *Anopheles Gambiae* as main species transmit *Plasmodium falciparum* in the country. Assumed a vector can be in one of three states, susceptible (S_m), latently infected (E_m) and infectious (I_m). The dynamics of infection in the mosquito is given by the set of differential equations:

$$\left\{ \begin{array}{l} \frac{dS_v}{dt} = \Lambda_v - \beta_v S_v - \mu_v S_v \\ \frac{dE_v}{dt} = \beta_v S_v - \lambda_v E_v - \mu_v E_v \\ \frac{dI_v}{dt} = \lambda_v - \mu_v I_v, \end{array} \right. \quad (4.2.5)$$

where λ_v is the probability that a mosquito survives the extrinsic incubation period (EIP), μ_v is the death rate, β_v is the force of infection acting on mosquito.

Table 4.4: Model Parameters: Description and value

Symbol	Description	Estimate & Ref
$1/\mu_h$	Human life expectancy, years	Estimated
$f\Gamma$	Proportion treated varied between sites	Estimated
α_A	Patent infection duration fixed days	Derived from data
α_I	Clinical disease duration (treated)	5 days (fixed) [51]
α_D	Clinical disease duration (untreated)	7 days (fixed) [51]
α_U	Subpatent infection duration fixed days	Derived from data
α_A	prophylaxis from treatment	Derived from data
ϕ	The probability of clinical disease	Derived from data

4.2.5 Data fitting

In this section, we fit the models presented in section (4.2) to data cases of malaria obtained from the National Malaria Indicator Survey (MIS) of South Sudan. There are a few statistical techniques that are usually used to undertake parameter estimation when building a statistical model. In particular, Bayesian arguments are the most novel statistical tools used to provides a general framework in which models can be successfully parametrized from data.

In this study we utilise Markov Chain Monte Carlo (MCMC) to obtain the posterior

Chapter 4: Pressure-testing some mathematical models of malaria transmission

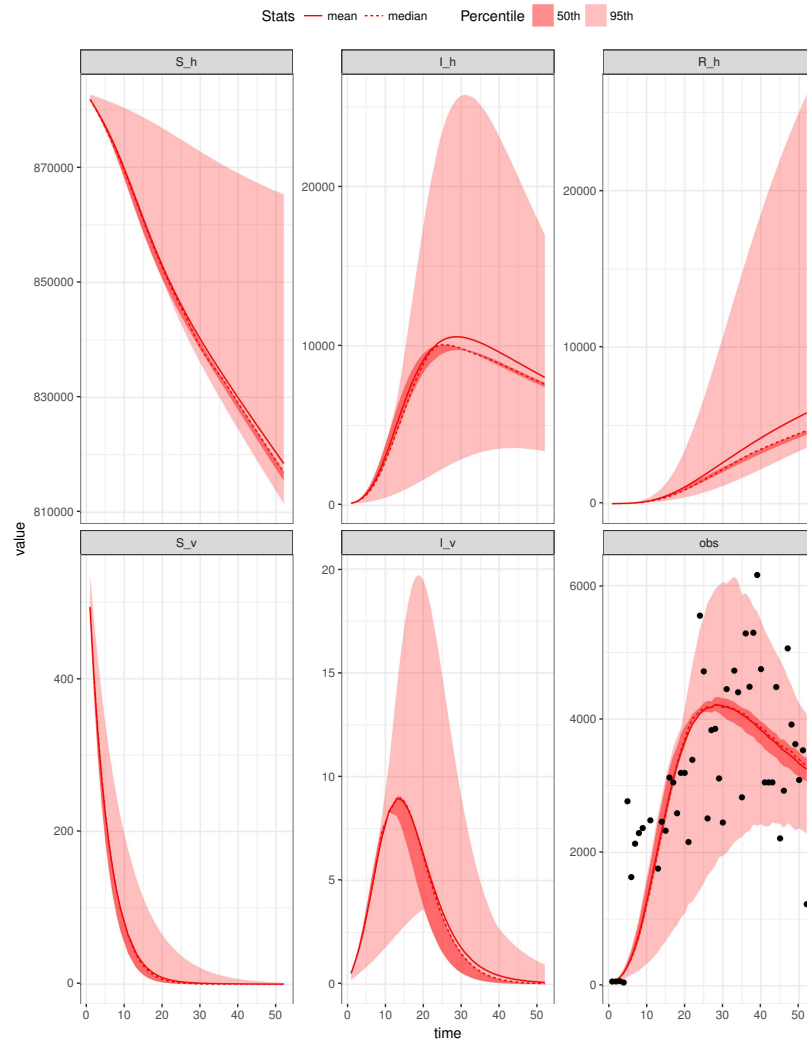


Figure 4.5: Model (4.2.1) fits to data and trajectory: For model fitting, black points show data used to estimate the model parameter values while the red line indicates the observation generated by the model with the confidence intervals of 50th and 95th. For simulation shows SIR-states trajectory for human and SI-states trajectory for mosquito.

samples of the parameters of the models. The models fitting was undertaken by using weekly malaria cases data of 2011 for Central Equatorial State on each model (shown in Figures 4.5- 4.8. 6. We consider stage variable (I) of all the models to track the daily number of new cases, assuming that these new cases are reported when they become symptomatic or infectious. We assume that weekly malaria data were reported according

Chapter 4: Pressure-testing some mathematical models of malaria transmission

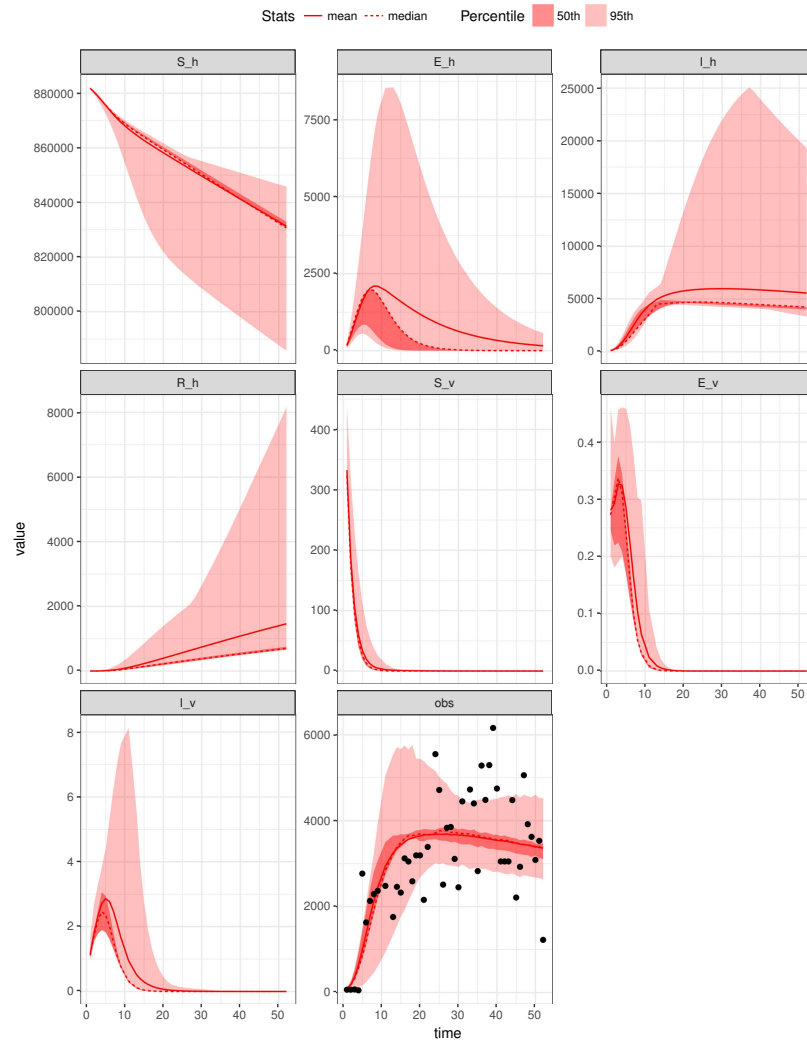


Figure 4.6: Model (4.2.2) fits to data and trajectory: For model fitting, black points show data used to estimate the model parameter values while the red line indicates the observation generated by the model with the confidence intervals of 50th and 95th. For simulation shows SEIR-states trajectory for human and SEI-states trajectory for mosquito.

to a Poisson process with reporting rate γ . Since the reporting rate is unknown we assume it to be no larger than 85%. Assume also that x_{ij} ($i = 1, \dots, n; j = 1, \dots, 3$) are the observed weekly malaria cases for State j during week i .

Dynamic models take as input the parameters controlling the spread of disease, producing predicted incidence of malaria cases as output. During the models fitting process,

Chapter 4: Pressure-testing some mathematical models of malaria transmission

we used uniform distributions to model the prior belief regarding the mosquito biting rate ϵ and the clinical duration of infections. Our models parameters $\epsilon, \mu, \alpha, \sigma, \rho, \nu, \pi, b = 0.7, \alpha_T, \alpha_A, \theta, \alpha_U, \alpha_D, \alpha_P, \mu_v, \beta_v, \sigma_a$ and σ_i were estimated or fixed (in agreement with previous studies) in setting. These parameters were assumed to be constant and were jointly estimated by utilizing fitR (version 0.1 [18]) to obtain posterior samples of 10000 iterations and a burn-in of 1000 iterations used for three chains. The credibility intervals produced in Figure 4.5 - 4.8 was a 95% confidence intervals with different accepting rate of each figure.

4.3 Discussion and conclusion

In this chapter, we have presented different models of epidemics, the structure of which can be determined by the biology of the causative factor and its effects on the host: (i) the SIR model, when immunity is permanent, (ii) the SEIR model which immunity is not permanent, (iii) the SEIAR model which represents clinical and subclinical infections and for infections that do not elicit a long-lasting immune response and (iv) the SIDAUP model that describes host-vector systems with life-long protection following for both clinical and subclinical infections.

In order to assess which of the predictions provided by the trustworthy model, it is essential to examine the results of different models, thus enabling us to test our understanding of the disease epidemiology by comparing observed patterns. This study describes the differential equations that govern the classic deterministic SIR, SEIR and SEIAR compartmental models to simulate an SIR/SEIR models. In this category of models, we assumed that individuals experience a different infectious duration, for instance with/without a long incubation (the “exposed” category) duration where the individual cannot yet transmit the parasite to others. We have presented and studied the dynamics of a various determinist models of malaria transmission between human and mosquito, we fitted these models to actual data and predicted the existence of Disease-Free Equilibrium (DFE) and Endemic Equilibrium (EE) of the model within the simulation trajectory

Chapter 4: Pressure-testing some mathematical models of malaria transmission

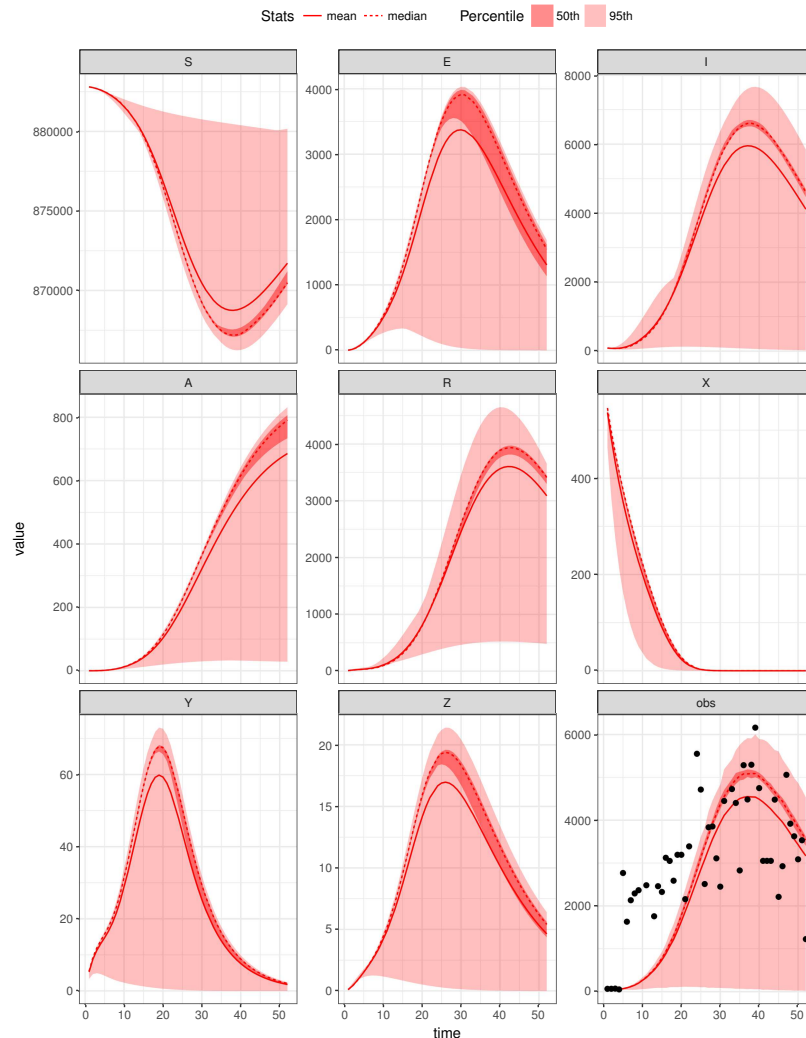


Figure 4.7: Model (4.2.3) fits to data and trajectory: For model fitting, black points show data used to estimate the model parameter values while the red line indicates the observation generated by the model with the confidence intervals of 50th and 95th. For simulations, shows SEIAR-state trajectory for human and SEI for mosquito trajectory.

Figure (4.5-4.8). Our study also shows that the transmission of the disease is strongly influenced by the model structure and uncertainty around the parameter's value. To account for the real-world complexity of malaria transmission, numerous parameters have been added to the first two simple models to increase its predictive power.

Chapter 4: Pressure-testing some mathematical models of malaria transmission

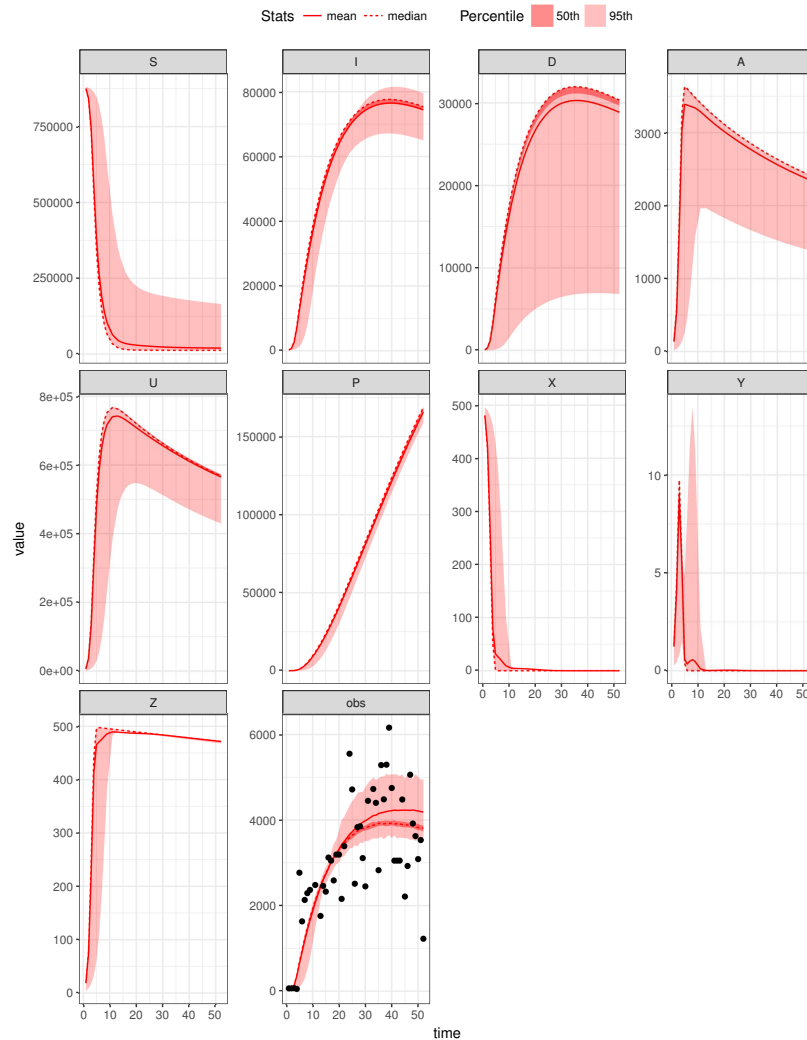


Figure 4.8: Model (4.2.4)- (4.2.5) fits to data and trajectory: For model fitting, black points show data used to estimate the model parameter values while the red line indicates the observation generated by the model with the confidence intervals of 50th and 95th. For simulations shows SIAUDP-state trajectory for human and SI for mosquito trajectory.

We observed that the simulations trajectory of each model acts differently Figure (4.9-4.12). In particular, the SEIR model consists of epidemic, extended peak and short tail compared to a single SIR pandemic, and it may have more than one peak due to latency. In Figure 4.13 we observe that the infection has died out or turned to zero so rapidly

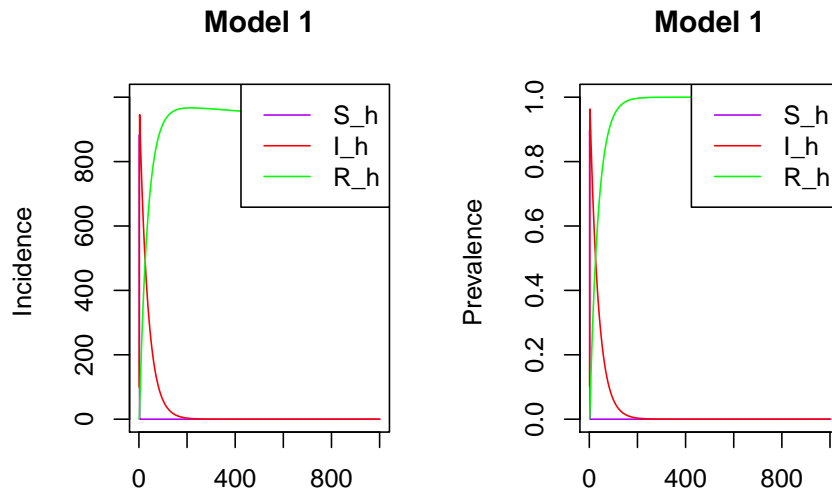


Figure 4.9: Distribution of disease incidence and prevalence generated by the model (4.2.1): Time responses of the state variables S_h , I_h , and R_h with initial conditions $S_h = 882$, $I_h = 10.00$, $R_h = 0$ against time. Where the parameters: $\epsilon = 80.5$, $\mu_h = 0.00006166$, $\lambda = 1/35$, $\delta = 0.0000027$, $\sigma = 0.00628$, $\mu_v = 0.132$, and $b = 0.7$. For this model Only the susceptible state exists. The human population of infective, and recovery classes approach zero and reaches disease-free equilibrium

in the case of the model (4.2.1) and (4.2.3) due to the impact of treatment, while in the case of model (4.2.2) the disease gradually decrease compared with model (4.2.4)- (4.2.5) where the infection in the steady stage (is much stable). This informs the significance of the structure of models to reveal the true underlying system traits.

From the analytical point of view, the ideal is to harness mathematical models that represent the population in specific environments as a system, that is changing over time. The behavior of the system can be modified by controlling one or more variables that can be manipulated (e.g., treatment) to achieve the desired outcomes. Based on ideal representation, a basic decision can be defined using the principles of optimal control. In the next chapters, we consider a more realistic model by incorporating the important

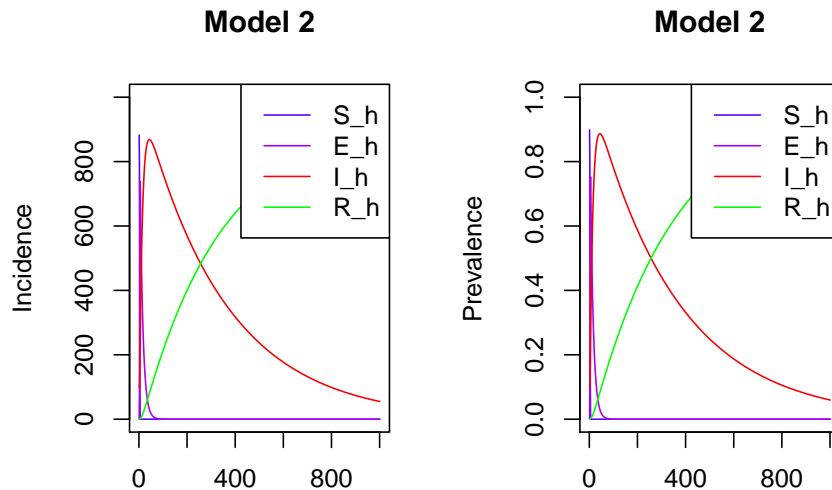
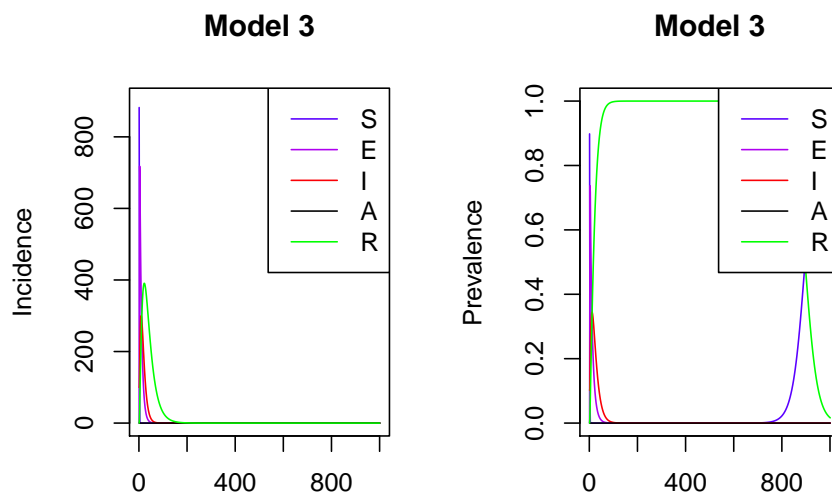


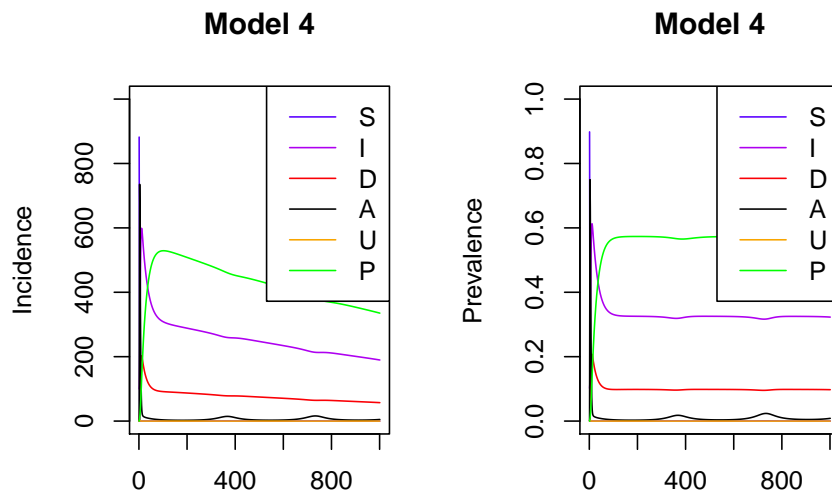
Figure 4.10: Distribution of disease incidence and prevalence generated by the model (4.2.2): Time responses of the state variables S_h , E_h , I_h , and R_h with initial conditions $S_h = 882$, $E_h = 0$, $I_h = 10.00$, $R_h = 0$ against time. Where the parameters: $\epsilon = 185.5$, $\mu_h = 0.00006166$, $\delta = 0.0000027$, $\sigma = 0.00628$, $\mu_v = 0.132$, and $b = 0.7$. $\rho_h = 1/12$, $\nu = 1/350$, $\rho_v = 0.08$. For this model all the distinct states coexist in the population and therefore approach endemic equilibrium

factors that may drive the malaria disease into a particular setting. In addition, we also take into account the degree of vulnerability of human populations in the model.



WESTERN CAPE

Figure 4.11: Distribution of disease incidence and prevalence generated by the model (4.2.3): Time responses of the state variables S , E , I , A , and R with initial conditions $S = 882$, $E = 0$, $I = 10.00$, $A = 0$, $R = 0$ against time. Where the parameters: $\epsilon = 125.5$, $\mu_h = 0.00006166$, $\delta = 0.0000027$, $\sigma = 1/200$, $\mu_v = 0.132$, $\nu = 1/10$, $\pi = 0.6$ $b = 0.7$. $\rho = 1/36$, $\tau = 1/9$, $\alpha = 1/8$, $\beta_v = 0.083$, $\zeta_a = 0.3$, and $\zeta_i = 0.62784$. For this model Only the uninfected state exists. The human population of Infective classes approach zero and reaches disease-free equilibrium



WESTERN CAPE

Figure 4.12: Distribution of disease incidence and prevalence generated by the model (4.2.4-4.2.5): Time responses of the state variables S , I , A , D , U , and P with initial conditions $S = 882$, $A = 0$, $I = 10.00$, $U = 0$, $D = 0$, $P = 0$ against time. Where the parameters: $\epsilon = 250$, $b = 0.75$, $\mu_h = 0.000514$, $\alpha_T = 0.03523$, $ft = 0.71$, $\alpha_A = 1/56$, $\theta = 0.04$, $\alpha_U = 1/200$, $\alpha_D = 1/21$, $\alpha_P = 1/50$, $\sigma_a = 0.0084$, $\sigma_i = 0.092$, $\mu_v = 0.0013$, $\lambda_v = 0.08$. For this model all the distinct states coexist in the population and therefore approach endemic equilibrium

Chapter 4: Pressure-testing some mathematical models of malaria transmission

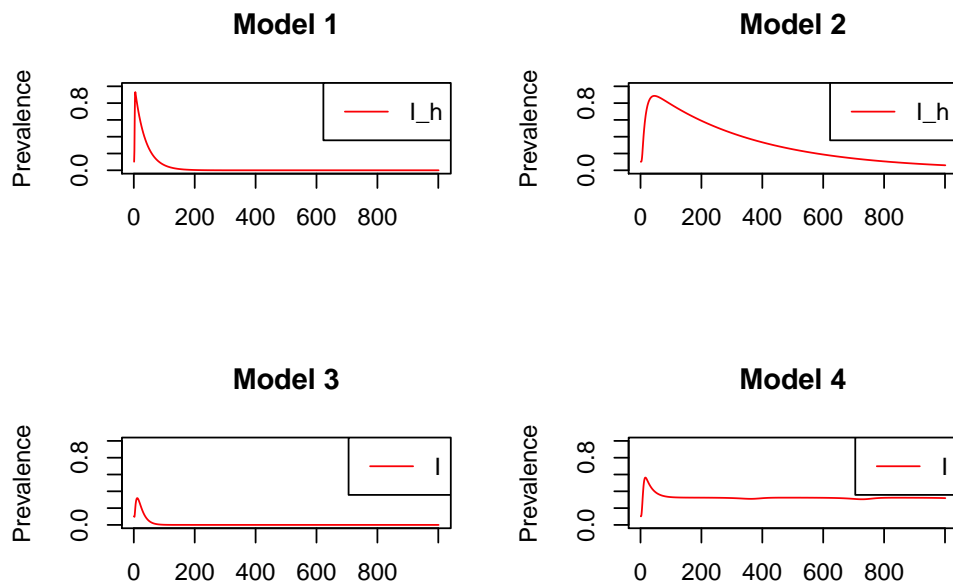
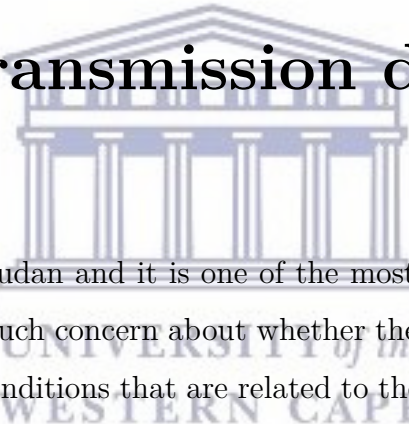


Figure 4.13: Predictions of the disease incidences with impact of Introducing intervention coverage with 80% Efficacy

Chapter 5

Assessing the role of climate factors on malaria transmission dynamics



Malaria is endemic in South Sudan and it is one of the most severe diseases in the war-torn nation. There has been much concern about whether the severity of its transmission might depend upon climatic conditions that are related to the reproduction of the single-cell parasite attaching to female mosquitoes, especially in high altitude areas. The country experiences two different climatic conditions; namely one tropical and the other hot and semi-arid. In this study, we aim to assess the potential impact of climatic conditions on malaria prevalence in these two climatically distinct regions of South Sudan. We develop and analyze a host-mosquito disease-based model that includes temperature and rainfall. The model has also been parametrized in a Bayesian framework using Bayesian Markov Chain Monte Carlo (MCMC). The mathematical analysis for this study has included equilibria, stability and a sensitivity index on the basic reproduction number \mathcal{R}_0 . The threshold \mathcal{R}_0 is also used to provide a numerical basis for further refinement and prediction of the impact of climate variability on malaria transmission intensity over the study region. The study highlights the impact of various temperature values on the population dynamics of the mosquito.

5.1 Introduction

Malaria is the most prevalent human mosquito-borne disease caused by a single-cell parasite that infects female *Anopheles* mosquitoes [11, 24]. This disease remains one of the biggest health threats facing humanity and is transmitted more robustly and incessantly in Sub-Saharan Africa than it is elsewhere. The Republic of South Sudan (RSS), the youngest country with civil unrest is one of the countries in Sub-Saharan Africa that is severely confronted by malaria. There have been approximately 1.54 million malaria episodes and almost 718 deaths reported in 2014, with 65% of those being children [49]. Moreover, malaria is endemic within the country [49]. However, little is known about local environmental conditions that may contribute to the severity of the disease during wet seasons. Improving our perception of host-parasite interactions in the war-torn nation is a priority in which mathematics can bring insight, especially regarding conjectures that attribute this gravity to climatic factors.

The malaria parasite depends upon the *Anopheles* mosquito to supplement its life cycle through a human intermediary. This relationship means that a climatic influence on mosquitoes' bionomics will trigger the trend towards malaria that is most likely to follow the climatic pattern, especially in the endemic zone. For this reason, an increase in mosquito density leads to a higher risk of malaria prevalence. For instance, Abiod and Ewing [1, 34] have recently revealed that climate fluctuations not only have a reproducible effect on the mosquito lifespan, but also impact positively on the development of sporogonic stages of the malarial parasite within the mosquito's body. Warmer temperature increases mosquito activity and more rainfall can lead to an abundance of mosquito larvae [11, 12, 59, 101]. Thus, the use of mean temperatures might be appropriate under certain conditions, which are generally found to have significant implications in determining the risk of malaria [14, 112].

Similar research [103, 129] has shown that mosquitoes are particularly active at dusk and dawn, while prolonged sun exposure can lead to their dehydration. Little is known about the survival of mosquito-borne diseases and malaria transmission during the winter,

Chapter 5: Modeling the effect of climate change on malaria transmission

however, it is often noted that mosquitoes tend to disappear in winter or when temperatures drop below 10°C . Nonetheless, the vertebrate host is the immediate source of winter infection in mosquitos, since the virus simply survives in the cold weather, waiting for warmer weather to reproduce. According to a study by [129] female mosquitoes spawn tumblers, which ultimately freeze in winter (or at temperatures below 10°C). The frozen eggs are saved until the temperature warms, when mosquito proliferation begins again, with disastrous effects on humans. These findings point to the effect of changes in ambient temperatures and precipitation levels on mosquito populations and thus stimulates interest in understanding the impact of these factors on mosquito-borne disease transmission.

In South Sudan malaria transmission is alleged to be perennial across the country, with peaks towards the end of the rainy season from September to November [35, 78], as freshwater pools become mosquito breeding sites. The country has two different climatic conditions, a hot semi-arid climate and a tropical climate. It is observed that malaria prevalence is significantly higher in the southern region (a tropical region, i.e., Central Equatorial State (CES)) than it is in northern region (a hot semi-arid region, i.e., Western Baher El Ghazal State (WBZ)) as is illustrated in Figure 5.1. The disease prevalence could be as high as 75% to 100% in some counties in the South. It is still uncertain, and a matter of discussion, whether and how the changes in transmission might occur. Understanding the dynamics of mosquito population is crucial for gaining insight into the abundance of mosquitoes, and thus design operational strategies for control. With this backdrop, we endeavor to understand the exact role that climate plays on the transmission of malaria in two different climatic zones of South Sudan through mathematical modelling. The CES and WBZ States are chosen (one from each climatic zone) due to the severity of malaria within their region. This is the first study designed for this purpose in CES and WBZ since the call for the implementation of the malaria control program.

A number of studies using mathematical models have established the direct role that climate variables, such as temperature and rainfall, play in the transmission dynamics of vector-borne diseases [11, 29, 34, 45, 58, 64, 71, 79, 101, 112, 143]. Yang [143] presented a malaria transmission model by taking into account different levels of acquired immu-

Chapter 5: Modeling the effect of climate change on malaria transmission

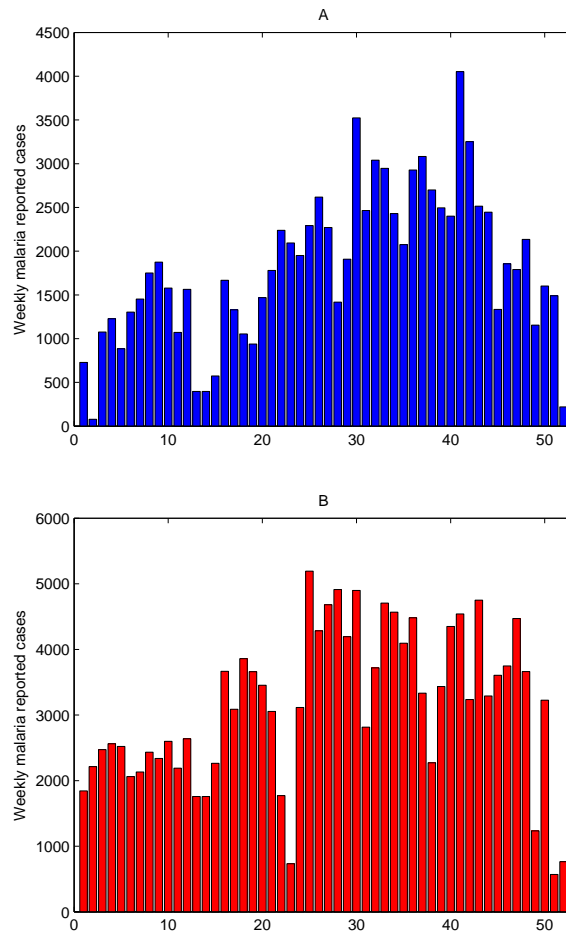


Figure 5.1: Weekly malaria reported cases of 2015 for (A) Western Baher el Ghazal State (in region 2) and (B) Central equatorial State (in region 1)

nity among humans and, most importantly, temperature-dependent parameters related to vector mosquitoes. A model analysis was carried out by means of the basic reproduction number R_0 . Additionally, an expression was derived for an endemic equilibrium that is biologically relevant only when $R_0 > 1$. Hoshen and Morse [58] formulated a dynamic malaria model comprising both the weather-dependent within-vector stages and the weather-independent within-host stages. Martens et al. [79] used rules-based modelling approach to examine how climate change might affect global malaria transmission. Their model consists of several linked systems: the climate system, the malaria system (divided into a human subsystem and a mosquito subsystem), and the impact system. Birley [71]

Chapter 5: Modeling the effect of climate change on malaria transmission

presented a simple mathematical model to investigate the effects of temperature on the ability of *Anopheles maculipennis* to transmit *Plasmodium vivax* malaria.

In recent decades also several contributions have been made in Africa concerning the distribution of mosquitoes affected by various environmental (climatic) factors such as temperature, humidity, rainfall and wind [1, 3, 33, 59, 63, 72, 104, 141, 142]. For instance, Parham et al. [104] developed an integrated modeling framework for assessing and predicting the simultaneous effects of rainfall and temperature on malaria dynamics. They illustrated the role that large-scale climate simulations and infectious disease systems may provide in predicting changes in the basic reproduction number across Tanzania. This offers powerful tools for understanding geographic shifts in incidence as climate changes. Yamana et al. [141] assessed the influence of climate change on malaria transmission in West Africa. Their simulation results stated that the changes in the pattern of rainfall play a significant role on malaria transmission compared to the potential impact of rising temperatures. They suggest that it will be necessary to integrate the changes in rainfall pattern in order to accurately project the environmental suitability for malaria transmission in future climates. Lunde et al. [72] formulated a realistic representation of *Anopheles Gambiae* s.s. and *Anopheles Arabiensis* in order to ameliorate the understanding of the dynamics of these vectors. Their study highlight how parameters can influence the success of these two species, as temperature, relative humidity and mosquito size are essential aspects in malaria transmission.

In spite of these studies, most modellers often ignore to validate their climate-based models with field data in order to carry out a quantitative assessment of the human component of the model. The aim of this chapter is to assess the impact of temperature and rainfall on the dynamics of mosquito population of a certain region of South Sudan and taking into consideration the climate-driven dynamics model. In addition, we further consider the importance of evaluating the numerical values of the model parameters with real data in order to allow for a computational simulation of dynamics that provides accurate prediction of the reaction.

Without accurate predictions, calculations of the basic reproduction number which ex-

plains the capability of a disease to persist in a population, will be subject to a significant error. This may help in a better understanding of the regulations of the biological system of the disease that can help decision-makers in developing efficient intervention strategies to tackle the disease. Therefore, the model framework is designed to accommodate human-mosquito population dynamics and to estimate its parameters using the Bayesian approach. Bayesian approaches, in particular Markov Chain Monte Carlo (MCMC) turn out to be a powerful inference tool for complex systems raised in behavioral science and computational biology [48, 144]. The input data required to validate our model are malaria incidence cases at state level in each region for a given period of time. The climate data are obtained from [122] and Regional Meteorological Service [42].

5.2 Spatial trends

According to Köppen and Geiger, South Sudan has two different climates [106]:

(i) A tropical savanna climate which is characterized by a rainy season of high humidity followed by a dry season with mild temperatures ranging from an average minimum of 20°C to a maximum of 38°C [106], (ii) A hot semi-arid climate characterized by a more moderate summer temperature regime, with daily mean temperatures of around 19°C. The study is conducted in two climatically distinct regions: Equatorial region and Baher El Ghazal region. A map of the study area is provided in Figure 5.2. The seasonal changes in these environments drive a strong vectorial capacity that sustains high levels of transmission. Our study domain is determined by longitude and latitude, which is interpolated to the spatial resolution data. These two distinct regions are described as:

Region (1): The Southern Part of the country is characterized by an equatorial (tropical) climate, forested, with comparatively lower refugee migration flows, but with some seasonal migration related to agricultural work. This region is divided into 241 counties and mostly comprised of greenbelt, hills and mountains. Average rainfall is between 901 and 1800 mm annually, with the longest rainy season lasting from 7–8 months, as can be seen in Figure 5.2(right). Humid conditions and a relatively warm climate make this

Chapter 5: Modeling the effect of climate change on malaria transmission

region conducive to the reproduction of mosquitoes. Our study focuses on the Central Equatorial State (CES) as a representative of this region.

Region (2): The northern part of the country is divided into 128 counties and has a climate that is classified as hot and semi-arid. The landscape features western and eastern flood plains that slope gently towards the rivers. Annual average rainfall ranges from between 400 to 600 mm and the duration of the rainy season is from 5–6 months (see Figure 5.2(right)). Our study focuses on the Western Baher El-Ghazal State (WBGZ) as a representative of this region.

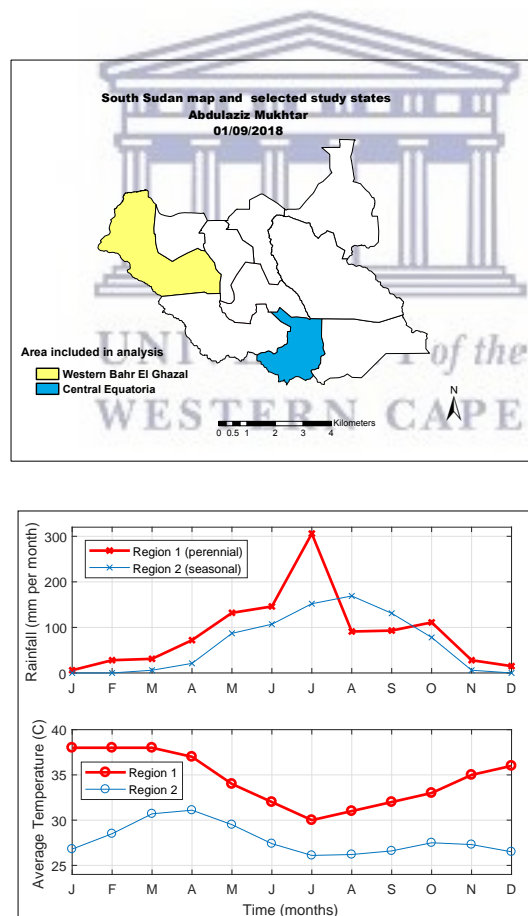


Figure 5.2: South Sudan States Map (left) and Average rainfall and Temperature for CES & WBGZ (right)

5.3 Method

We begin with the formulation of a classical epidemiological model that considers human and mosquito populations. The model structure is similar to that of [87] that includes a realistic, climate-based model for capturing the simultaneous effects of rainfall and temperature on malaria transmission. The human component is utilized to fit the model to the actual observed data via a Bayesian approach in order to predict future samples with available observational data. Both components of the model are used simultaneously to estimate mosquito bite rate that is assumed to be influenced by LLINs intervention coverage and not climate-dependent. We hence end this section by applying a Bayesian approach to estimate the posterior distribution of parameters given actual-settings data.

5.3.1 Model formulation

Based on the foregoing and established studies, we presume the heterogeneity of malaria in South Sudan can be explained by the varied agro-climatic conditions that exist between the regions. Consequently, we slightly extend the model in [87] by using a deterministic compartmental structure for the endemic malaria disease incorporating the climate factor that leads to understanding the impact of temperature and rainfall. This compartmental model captures the situations including intervention coverage and allows to calibrate parameters against the real observed data. The human components of the model is presented to capture the relationship between effective treatment and parasitic prevalence. The total mosquito population N_M is divided into aquatic mosquitoes (egg, larva and pupa) stage denoted by M and adult mosquitoes N_V . The adult mosquitoes is subdivided into susceptible mosquitoes S_v , mosquitoes exposed to malaria parasite E_v and infectious mosquitoes I_V . In model formulation, we assume all variables represented in each compartments are differentiable with respect to time and all parameters are non-negative. As illustrated in the flow diagram (Figure 5.3.1) the total population of humans and mosquitoes at time t will be:

$$N_H(t) = S_H(t) + E_H(t) + I_H(t) + R_H(t);$$

Chapter 5: Modeling the effect of climate change on malaria transmission

and

$$N_M(t) = M(t) + N_V(t)$$

respectively.

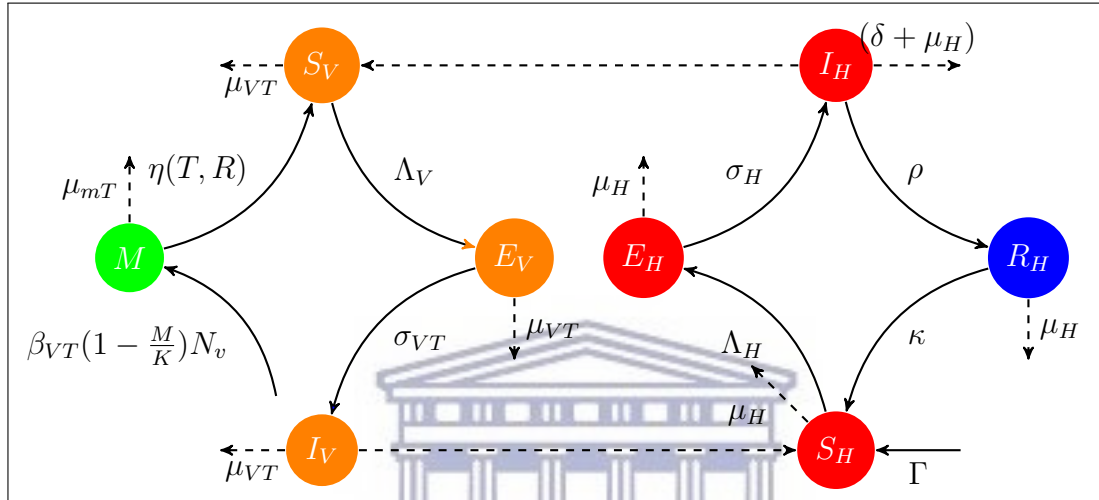


Figure 5.3: Flow diagram for Human and Mosquito infection model

The susceptible compartment is recruited by birth into the community at a rate Γ and increased with recovery rate κ when individuals lose their immunity. We presume susceptible individuals (S) acquire malaria and become infected at a rate Λ_H when they are bitten by infectious mosquitoes (entomological inoculation rate; EIR). After bites from infectious mosquitoes, individuals move to the exposed humans compartment. The exposed human population remains exposed for a fixed number of days as the parasites still in the asexual stages in their bodies before moving to infected humans with probability σ_H . On infection, they develop clinical infection in which they have gametocytes in their bloodstream. Those that are developing disease either die (naturally or due to the disease with probability δ) or successfully recovered (naturally or with treatment) with rate ρ and subsequently enter a period of prophylaxis (recovery state R). Upon treatment intervention, the rate ρ is determined by the proportion of treatment access π , duration of drug recovery period ν and treatment seeking period τ , hence is given by $\rho = (1 - \pi)/\gamma + \pi/(\nu + \tau)$, where γ is natural recovery period. Those who are recovered

Chapter 5: Modeling the effect of climate change on malaria transmission

either lose their immunity and return to susceptible class or naturally die. The deterministic model for the human dynamics is as follows

$$\begin{cases} \frac{dS_H}{dt} = \kappa R_H - \Lambda_H S_H - S_H \mu_H + \Gamma, \\ \frac{dE_H}{dt} = \Lambda_H S_H - (\mu_H + \sigma_H) E_H, \\ \frac{dI_H}{dt} = \sigma_H E_H - (\mu_H + \delta + \rho) I_H, \\ \frac{dR_H}{dt} = \rho I_H - (\mu_H + \kappa) R_H, \end{cases} \quad (5.3.1)$$

where t represents time and the force of infection Λ_H is assumed to vary by degree of exposure to mosquito due to geographic variation, governed by the function

$$\Lambda_H = \frac{\epsilon \beta_{HV} I_V}{N_H},$$

where $\epsilon = (1 - V_\chi)\epsilon$ is mosquito biting rate that is assumed to be influenced by LLINs intervention coverage, β_{HV} is the probability of infection if bitten by an infectious mosquito.

We consider *Anopheles Gambiae* mosquitoes which is the main anopheles species that transmits *Plasmodium Falciparum* in South Sudan to be included in the model. We model a life cycle of mosquito in a compartmental formulation [70], starting with aquatic mosquitoes stages, eggs, larvae and pupae grouped into a single compartment M and further subdivide adult mosquito into three compartments. When Adult mosquitoes lay eggs at rate β_{VT} which is temperature dependent, the aquatic (immature) mosquitoes population is then produced at the temperature and rainfall-dependent rate $\beta_{VT}(1 - M/K)$ [87, 105], by the usage of the carrying capacity parameter K for limitation of the immature mosquito population that depend on habitat availability. The immature mosquito population develop into adult mosquitoes at the birth rate $\eta(T, R)$ which is dependent on temperature- and rainfall and also decreases by natural death rate $\mu_i(T)$. Figure 5.4 illustrates the effect of climate on these parameters of immature mosquitoes.

Thereafter, adult mosquito population is subdivided into three compartments: susceptible S_V , latent infected E_V and infectious I_V . Susceptible female mosquitoes emerge

Chapter 5: Modeling the effect of climate change on malaria transmission

from the last immature stage at the birth rate adapted from [87, 105] as

$$\eta(T, R) = \frac{\varpi(T)p_i(R)p_2(T)}{\tau_{EA}(T)},$$

where $\varpi(T)$ is the total number of eggs laid per adult per oviposition which is temperature dependent, and $p_i(R)$ is the daily survival probability of immature in stage i given rainfall R (where $i = 1, 2$, and 3 corresponds to eggs, larvae, and pupae respectively). It is assumed that survival probability of eggs and pupae are independent of temperature [33, 105] and $p_2(T) = \exp(-(0.00554T - 0.06737))$ is daily survival probability of the temperature dependent larvae. The total development time of immature mosquito, denoted by $\tau_{EA}(T)$ is given by $1/(-0.00094T^2 + 0.049T - 0.552)$.

In addition, the extreme levels of rainfall may decrease the immature mosquitoes by flushing out larvae and breeding sites [11]. Thus, assumed that a quadratic relationship between Rainfall R and the daily survival probabilities of immature mosquitoes $p_i(R)$ is defined by [105] as $p_i(R) = \frac{4*P_i^*}{R_L^2}R(R_L - R)$, where R_L is the rainfall limit beyond which breeding site get flushed out and no immature mosquitoes survive and P_i^* is the maximum daily survival probability of each stage i .

Adult mosquitoes seeking host for meal might die at a temperature-dependent rate μ_{VT} . Survivors seeking meal acquire malaria at a rate Λ_V which depends on the infectiousness of the human population, since study mainly performed on human host.

$$\Lambda_V = \frac{\epsilon(\beta_{VH}I_H + R_H\xi)}{N_H}$$

where β_{VH} and ξ are probability of infection from infectious and recovery humans to susceptible mosquitoes respectively.

When the mosquito bites an infectious human, the parasite (in the form of gametocytes) enters the survivors mosquito, and subsequently process to the infectious compartment I_V through a latent period E_V . The mosquitoes become infectious at rate σ_{VT} to humans and remain infectious for life (until they die). The population dynamics and infection process of anopheles Gambiae mosquitoes are given by the following set of ordinary differential equations.

Chapter 5: Modeling the effect of climate change on malaria transmission

$$\begin{cases} \frac{dM}{dt} = \beta_{VT} \left(1 - \frac{M}{K}\right) (N_V) - \mu_i M - \eta(T, R) M, \\ \frac{dS_V}{dt} = \eta(T, R) M - \Lambda_V S_V - S_V \mu_{VT}, \\ \frac{dE_V}{dt} = \Lambda_V S_V - (\mu_{VT} + \sigma_{VT}) E_V, \\ \frac{dI_V}{dt} = \sigma_{VT} E_V - I_V \mu_{VT}, \end{cases} \quad (5.3.2)$$

Table 5.1: Parameters for Anopheles Gambiae Model

Description	Estimate and function form	Ref
Per capita egg deposition rate, β_{VT}	$-0.153 T^2 + 8.61 T - 97.7$	[100]
Immature mosquito death rate, $\mu_i(T)$	$1.0257 - 0.094 T - 0.0025 T^2$	[87]
Adult mosquito death rate, μ_{VT}	$-\ln(0.522 - 0.000828 T^2 + 0.0367 T)$	[82]
Adult mosquito birth rate, $\eta(T, R)$	$\frac{\varpi(T)p_1(R)p_2(R)p_3(R)}{\tau_{EA}(T)}$	[82]
The lifetime number of eggs laid, $\varpi(T)$	β_{VT}/μ_{VT}	[82]
Daily survival probabilities of eggs, $p_1(R)$	$\frac{4*0.93}{R_L^2} R(R_L - R)$	[105]
Daily survival probabilities of larva, $p_2(R)$	$\frac{4*0.25}{R_L^2} R(R_L - R)$	[105]
Daily survival probabilities of pupae, $p_3(R)$	$\frac{4*0.75}{R_L^2} R(R_L - R)$	[105]
Daily survival probabilities of larva, $p_2(T)$	$e^{-(0.00554 T - 0.06737)}$	[105]
Rainfall beyond which no immature stages survive, R_L	50	[87]
Duration of immature development, $\tau_{EA}(T)$	$1/(-0.00094 T^2 + 0.049 T - 0.552)$	[82]
Progression rate of mosquitoes, σ_{VT}	$e^{1/(-4.41+1.31 T-0.03 T^2)}$	[33]
Carrying capacity of larvae K	1000000	[87]

We note that the model describes a population and therefore it is very important to prove that all the state variables $S_H(t); E_H(t); I_H(t); R_H(t); M(t); S_V(t); E_V(t)$ and $I_V(t)$ are non-negative at all times. For the biological benefit System (5.3.1) and (5.3.2) will be analyzed in a suitable feasible region \mathfrak{R} defined by.

$$\mathfrak{R} = \left\{ (S_H; E_H; I_H; R_H) \in \mathbb{R}_+^4 \mid 0 \leq N_H(t) \leq \frac{\Gamma}{\mu_H}, (M; S_V; E_V; I_V) \in \mathbb{R}_+^4 \mid 0 \leq N_V(t) \leq \frac{\eta M}{\mu_{VT}} \right\}.$$

Chapter 5: Modeling the effect of climate change on malaria transmission

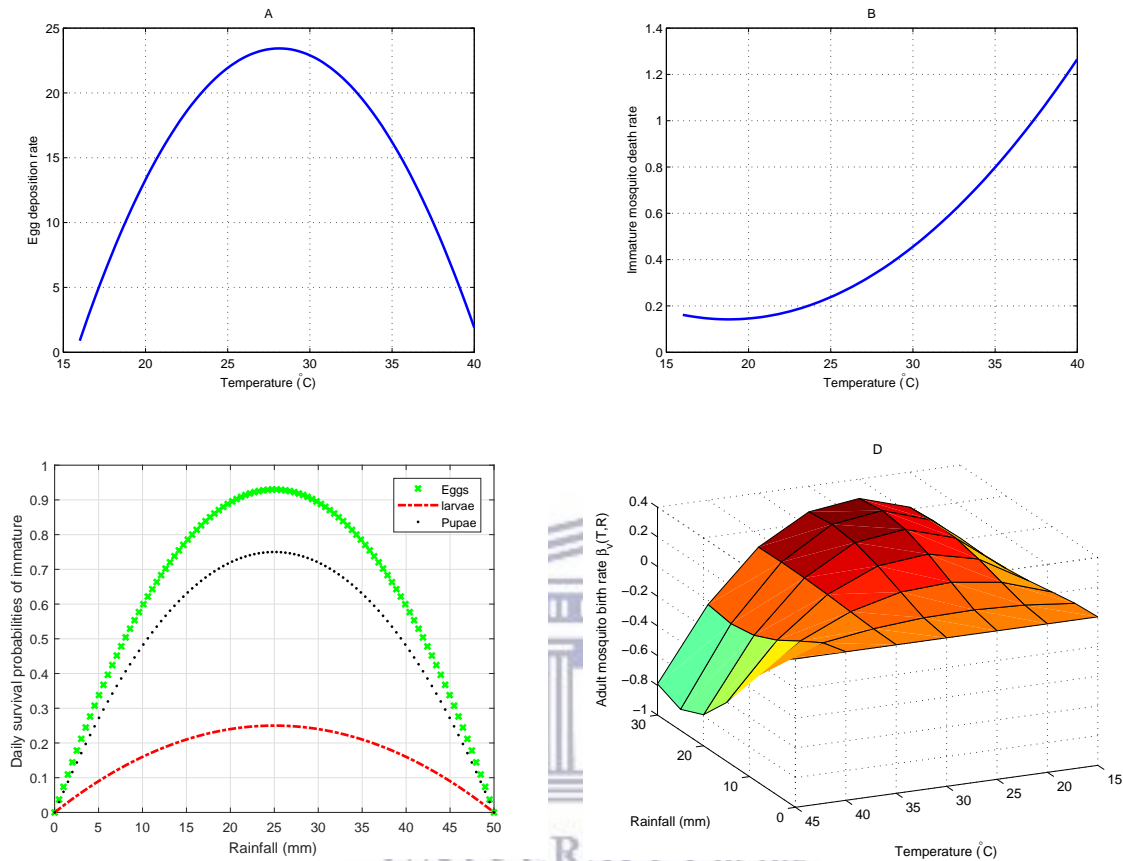


Figure 5.4: Simulation of model parameter function, showing mosquitoes cycle development against various values of mean monthly temperature in the range of 15- 40°C and rainfall in the range of 0-50 mm, using parameter functions in Table 5.1, (A) dependence of eggs deposition rate process on temperature (B) dependence of the daily survival probability of mosquito during aquatic stages on temperature (C) the per-capita death rate of mosquito during aquatic stages depend on temperature (D) the per-capita maturation rate of pupae (into adult mosquitoes) as a function of rainfall and temperature.

If the system has non-negative initial data, then the solution will remain inside \mathfrak{R} for all time $t > 0$. Thus we state the following lemma.

Lemma 5.1.

Given the model (5.3.1), suppose that $S_H(0) \geq 0, E_H(0) \geq 0, I_H(0) \geq 0, R_H(0) \geq 0, M(0) \geq 0, S_H \geq 0, E_H(0) \geq 0, I_H(0) \geq 0$ for all t . Then the solution $S_H(t); E_H(t);$

Chapter 5: Modeling the effect of climate change on malaria transmission

$I_H(t); R_H(t); M(t); S_V(t); E_V(t); I_V(t)$ of the model remain positive for all time $t > 0$.

Moreover,

$$\lim_{t \rightarrow \infty} N_H(t) \leq \frac{\Gamma}{\mu_H}$$

Furthermore, if

$$N_H(0) \leq \frac{\Gamma}{\mu_H}$$

then

$$N_H(t) \leq \frac{\Gamma}{\mu_H}$$

In particular, the region \mathfrak{R} is positively invariant. It can be seen from the result in Figure 5.8 that human mobility is sufficient to preserve malaria disease firmness in the patches with the low transmission.

Proof. Let us assume that the set X below is bounded.

$$X = \{T \geq 0 : S_H > 0, E_H > 0, I_H > 0, R_H > 0; M > 0; S_V > 0; E_V > 0; I_V > 0, \forall 0 \leq t \leq T\}.$$

Then X has a supremum T . Since $S_H(t), E_H(t), I_H(t), R_H(t), M(t), S_V(t), E_V(t)$ and $I_V(t)$ are continuous, we have $T > 0$. From the first equation of the model (5.3.1) we have

$$\frac{dS_H}{dt} = \Gamma - \Lambda_H S_H + \kappa R_H - \mu_H S_H.$$

Let $B(t) = \exp\{\mu_H t + \int_0^t \Lambda_H(s) ds\}$, and note that $B(0) = 1$.

Then we have

$$\begin{aligned} \frac{d}{dt}[S_H(t).B(t)] &= \dot{S}_H(t).B(t) + S_H(t).\dot{B}(t) \\ &= \dot{S}_H(t).B(t) + S_H(t).B(t)(\mu_H + \Lambda_H(t)) \\ &= B(t)[\dot{S}_H(t) + S_H(t).(\mu_H + \Lambda_H(t))] \\ &= (\Gamma + \kappa R_H(t))B(t). \end{aligned} \tag{5.3.3}$$

Hence

$$S_H(T).B(T) - S_H(0).B(0) = \int_0^T (\Gamma + \kappa R_H(t))B(t)dt,$$

Chapter 5: Modeling the effect of climate change on malaria transmission

so that

$$S_H(T) = B(T)^{-1} [S_H(0) + \int_0^T (\Gamma + \kappa R_H(t)) B(t)].$$

Note that $R_H(t) > 0$, $B(t) > 0$ for all t , and so $S_H(0) \geq 0$. Therefore $S_H(T) > 0$.

A similar reasoning on the remaining equations shows that E_H , I_H , R_H , M , S_V , E_V , and I_V are always positive for $t > 0$.

Further by adding the equations of the system (5.3.1) we obtain

$$\frac{dN_H}{dt} = \Gamma - \mu_H N_H(t).$$

Using a standard comparison

$$N_H(t) = \frac{\Gamma}{\mu_H} + (N_H(0) - \frac{\Gamma}{\mu_H}) e^{-\mu_H t}$$

Therefore,

$$\lim_{t \rightarrow \infty} \sup N_H(t) = \frac{\Gamma}{\mu_H}.$$

This establishes the invariance of X as claimed. \square

5.3.2 Model fitting

In this subsection, we fit our model to data in a Bayesian framework using Markov Chain Monte Carlo (MCMC) methods. The Bayesian method combines the likelihood of the data as well as the prior distribution of the parameters of the model to obtain the posterior distribution of the parameters of the model, expressed by

$$p(\theta|Data) = \frac{p(Data|\theta)p(\theta)}{p(Data)},$$

where $p(\theta|Data)$ is the posterior, $p(Data|\theta)$ is the likelihood, $p(\theta)$ is the prior, $p(Data)$ is a normalization constant. This allows one to make inference based on the posterior mean/ median of the parameters. The parameters driving the human model were jointly estimated by utilizing MCMC in fitR (version 0.1 [18]) package to clinical incidence data, weighted by a demographic change.

Chapter 5: Modeling the effect of climate change on malaria transmission

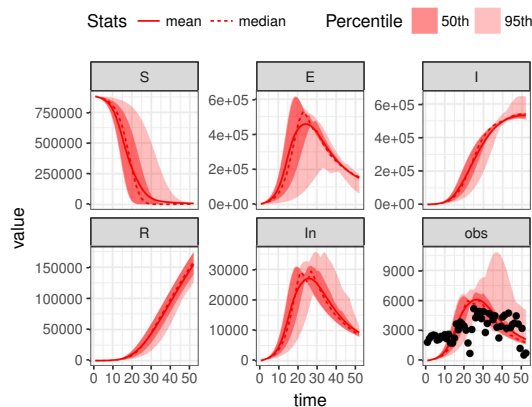


Figure 5.5: Illustration of the model fitting and the trajectory simulation, the model assessment (line) run against data (dots) of CES for 2015 attached with the parameters estimated during fitting process in Table 5.2.

The process of parameter estimation will guide to more accurate and informative model predictions of malaria disease on these specific locations. A compartmental equation was added into the human model to account for malaria incidence cases during model fitting process. The model fitting was undertaken by using weekly malaria data of 2015 for each region under investigation (for CES and WBGZ shown in Figure 5.5 and 5.6 respectively) using MCMC. The model is run from the year 2000 to reach a steady state before being fitted to data from the year 2011, then validated with data from 2011 to 2015.

We assume that weekly malaria data were reported according to a Poisson process with reporting rate ζ . Since the reporting rate is unknown we assume it to be no larger than 85%. We assume that $x_{ij}(i = 1, \dots, n; j = 1, \dots, m)$ are the observed weekly malaria incidence cases for state j during week i . We used uniform distributions to model the prior belief regarding the parameters. During this fitting process the model parameters β_{HV} , ϵ_j , γ , τ , ν , and κ were estimated and presented in Table 5.2. These parameters were assumed to be constant and were jointly estimated by utilizing fitR (version 0.1 [18]) to obtain posterior samples 10000 iterations and a burn-in of 1000 iterations used for three chains. The confidence intervals produced in Figure 5.5 and 5.6 was a 95% confidence

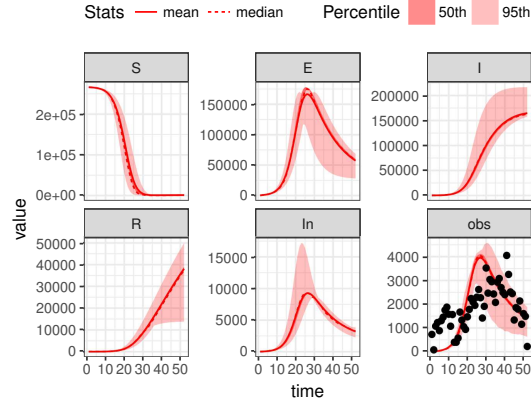


Figure 5.6: Illustration of the model fitting and the trajectory simulation, the model assessment (line) run against data (dots) of WBGZ for 2015 attached with the parameters estimated during fitting process in Table 5.2.

intervals with accepting rate of 0.22 and 0.178 for CES and WBGZ respectively.

5.4 Model analysis

The existence of a trivial equilibrium of the model (5.3.1) and (5.3.2) will be explored by setting the equations equal to zero. Consider the following disease free model:

$$\begin{aligned}
 \frac{dS_H}{dt} &= \Gamma - \mu_H S_H \\
 \frac{dM}{dt} &= \beta_{VT} \left(1 - \frac{M}{K}\right) S_V - \mu_i(T) M - \eta(T, R) M \\
 \frac{dS_V}{dt} &= \eta(T, R) M - \mu_{VT} S_V
 \end{aligned} \tag{5.4.4}$$

This system has two equilibrium points:

- i. The vector free equilibrium point $E_{00} = \left(\frac{\Gamma}{\mu_H}, 0, 0\right)$ and
- ii. The disease free equilibrium point

$$E_0 = \left(\frac{\Gamma}{\mu_H}, \frac{K\mu_{VT}(\eta(T, R) + \mu_i(T))(\Theta - 1)}{\eta(T, R)\beta_{VT}}, \frac{K\mu_{VT}(\eta(T, R) + \mu_i(T))(\Theta - 1)}{\beta_{VT}\mu_{VT}} \right)$$

Chapter 5: Modeling the effect of climate change on malaria transmission

Table 5.2: Parameters for the human transmission model

Description	Est for CES	Est for WBZ
Human natural death rate, μ_H	0.00006166	0.00006166
Population size, N	882846	266745
Mosquito biting rate, ϵ	26.065	18.895
Probability of infection from infected mosquito, β_{HV}	0.6458	0.7458
lost of immunity, κ	1/25	1/36
Rate of progression of humans from E to I , σ_H	1/16	1/13
Proportion of infected population receiving treatment π	0.84978	0.92258
All elimination half-life, ν	7	5
Treatment seeking period, τ	4	3
Natural recovery period, γ	166	152
Clinical death rate of humans due to malaria, δ	0.0027	0.0011
Probability of infection from Infected human, β_{VH}	0.48	0.48
probability of infection from recovery human, ξ	0.06	0.0028

$$\text{where } \Theta := \frac{\eta(T,R)\beta_{VT}}{\mu_{VT}(\mu_i(T)+\eta(T,R))}.$$

Note that the disease free equilibrium is positive if and only if $\Theta > 1$.

Next, we show that Θ is the basic offspring number.

Consider the submodel of (5.4.4) formed by the equations of the vector only, that is

$$\begin{aligned} \frac{dM}{dt} &= \beta_{VT} \left(1 - \frac{M}{K}\right) S_V - \mu_i(T) M - \eta(T, R) M \\ \frac{dS_V}{dt} &= \eta(T, R) M - \mu_{VT} S_V \end{aligned} \quad (5.4.5)$$

Let $\mathcal{G} = \begin{pmatrix} \beta_{VT} S_V \\ 0 \end{pmatrix}$ denote the vectors of new offspring in the disease free model (5.4.5)

and

let $\mathcal{W} = \begin{pmatrix} \beta_{VT} \frac{M}{K} S_V + \mu_i(T) M + \eta(T, R) M \\ -\eta(T, R) M + \mu_{VT} S_V \end{pmatrix}$ be the vector formed by the other

transfers.

Chapter 5: Modeling the effect of climate change on malaria transmission

The next generation matrix is given by GW^{-1} where G and W are the Jacobian matrices evaluated at $(0, 0)$ of \mathcal{G} and \mathcal{W} respectively.

Such that :

$$GW^{-1} = \begin{bmatrix} -\frac{\eta(T,R)\beta_{VT}}{(\mu_i(T)+\eta(T,R))\mu_{VT}} & \frac{\beta_{VT}}{\mu_{VT}} \\ 0 & 0 \end{bmatrix}.$$

The basic offspring number, Θ , is given by the spectral radius of GW^{-1} .

We obtain

$$\begin{aligned} \Theta = \rho(GW^{-1}) &= \max\left(0, \left|-\frac{\eta(T,R)\beta_{VT}}{(\mu_i(T)+\eta(T,R))\mu_{VT}}\right|\right) \\ &= \frac{\eta(T,R)\beta_{VT}}{(\mu_i(T)+\eta(T,R))\mu_{VT}}. \end{aligned}$$

Evaluating the Jacobian matrix at the vector free equilibrium, we obtain:

$$J_0 = \begin{bmatrix} -\mu_H & 0 & 0 \\ 0 & -\mu_i(T) - \eta(T, R) & \beta_{VT} \\ 0 & \eta(T, R) & -\mu_{VT} \end{bmatrix}$$

The characteristic polynomial of the Jacobian matrix evaluated at E_{00} , is

$$(\mu_H + z) \left(z^2 + (\eta(T, R) + \mu_i(T) + \mu_{TV})z + \mu_{TV}(\eta(T, R) + \mu_i(T))(1 - \Theta) \right)$$

Hence, E_{00} is locally asymptotically stable if and only if $\Theta < 1$.

Similarly, the Jacobian matrix at the disease free equilibrium

$$J_1 = \begin{bmatrix} -\mu_H & 0 & 0 \\ 0 & -\frac{\beta_{VT}S_{V0}}{K} - \mu_i(T) - \eta(T, R) & \beta_{VT}\left(1 - \frac{M_0}{K}\right) \\ 0 & \eta(T, R) & -\mu_{VT} \end{bmatrix}$$

The characteristic polynomial of the Jacobian matrix evaluated at E_0 , is

$$(\mu_H + z) \left[\begin{array}{c} Kz^2 + (\eta(T, R)K + \mu_i(T)K + K\mu_{VT} + \beta_{VT}S_{V0})z \\ + \beta_{VT}\eta(T, R)M_0 + S_{V0}\beta_{VT}\mu_{VT} + K(\eta(T, R)\mu_{VT} + \mu_i(T)\mu_{VT})(1 - \Theta) \end{array} \right]$$

Hence, E_0 is locally asymptotically stable if $\Theta > 1$.

Next, we calculate the basic reproduction number. The basic reproduction number, denoted by \mathcal{R}_0 , plays a vital role in the propagation of the relevant epidemic. It gives

Chapter 5: Modeling the effect of climate change on malaria transmission

conditions on when a disease free equilibrium exists or is unstable. The threshold quantity, \mathcal{R}_0 , is defined (see [131] for instance) as the average number of new infections that occur when one infective individual is introduced into a completely susceptible human population. Here, the \mathcal{R}_0 of the model (5.3.1) and (5.3.2) is established in Lemma 5.2 using the next generation matrix concomitant with disease free equilibrium.

Lemma 5.2. *The basic reproduction number of the system (5.3.1) and (5.3.2) is*

$$\mathcal{R}_0 = \sqrt{\frac{\epsilon^2 \sigma_{VT} \sigma_H \mu_H \beta_{VH} \beta_{HV} K (\xi \rho + \kappa + \mu_H) (\mu_i(T) + \eta(T, R)) (\Theta - 1)}{\Gamma \beta_{VT} (\rho + \delta + \mu_H) (\sigma_H + \mu_H) (\kappa + \mu_H) (\sigma_{VT} + \mu_{VT}) \mu_{VT}}}.$$

Proof.

Let \mathcal{F} denote the vectors of new infection in the full model and let \mathcal{F} and \mathcal{V} be the vector formed by the other transfers. We have

$$\mathcal{F} = \begin{bmatrix} \frac{\epsilon \beta_{HV} I_V S_H}{S_H + E_H + I_H + R_H} \\ 0 \\ 0 \\ \frac{\epsilon (\xi R_H + \beta_{VH} I_H) S_V}{S_H + E_H + I_H + R_H} \\ 0 \end{bmatrix}, \mathcal{V} = \begin{bmatrix} (\sigma_H + \mu_H) E_H \\ -\sigma_H E_H + (\rho + \delta + \mu_H) I_H \\ -\rho I_H + (\kappa + \mu_H) R_H \\ (\sigma_{VT} + \mu_{VT}) E_V \\ \mu_{VT} I_V - E_V \sigma_{VT} \end{bmatrix}$$

The next generation matrix is given by FV^{-1} where $F = \partial \mathcal{F}_{E_0}$ and $V = \partial \mathcal{V}_{E_0}$ denote the jacobian matrices of \mathcal{F} and \mathcal{V} evaluated at E_0 . Note that some of our model parameters are climate dependent, but during the calculation procedure of the next generation matrix are deemed as constant. We obtain:

$$FV^{-1} = \begin{bmatrix} 0 & 0 & 0 & \frac{\epsilon \beta_{HV} \sigma_{VT}}{(\sigma_{VT} + \mu_{VT}) \mu_{VT}} & \frac{\epsilon \beta_{HV}}{\mu_{VT}} \\ 0 & 0 & 0 & 0 & 0 \\ 0 & 0 & 0 & 0 & 0 \\ A & B & C & 0 & 0 \\ 0 & 0 & 0 & 0 & 0 \end{bmatrix}$$

Chapter 5: Modeling the effect of climate change on malaria transmission

where

$$\begin{aligned} A &= \frac{\beta_{HV} K \epsilon \sigma_H \mu_H (\eta(T, R) + \mu_i(T)) (\kappa + \mu_H + \xi \rho) (\Theta - 1)}{\Gamma \beta_{TV} (\sigma_H + \mu_H) (\delta + \rho + \mu_H) (\kappa + \mu_H)} \\ B &= \frac{\beta_{HV} K \epsilon \mu_H (\eta(T, R) + \mu_i(T)) (\kappa + \mu_H + \xi \rho) (\Theta - 1)}{\Gamma \beta_{TV} (\delta + \rho + \mu_H) (\kappa + \mu_H)} \\ C &= \frac{\epsilon \beta_{VH} \xi \mu_H K (\mu_i(T) + \eta(T, R)) (\Theta - 1)}{\Gamma \beta_{VT} (\kappa + \mu_H)} \end{aligned}$$

The eigenvalues of FV^{-1} are $0, -\sqrt{\frac{\epsilon \beta_{HV} \sigma_{TV} A}{\mu_{TV} (\sigma_{TV} + \mu_{TV})}}$ and $\sqrt{\frac{\epsilon \beta_{HV} \sigma_{TV} A}{\mu_{TV} (\sigma_{TV} + \mu_{TV})}}$.

Therefore the basic reproduction number for the system is as claimed. \square

According to a general result established in [131], we conclude that the disease-free equilibrium E_0 of the model (5.3.1) and (5.3.2) is locally asymptotically stable if $\mathcal{R}_0 < 1$, and unstable if $\mathcal{R}_0 > 1$.

We will now analyse the sensitivity index of \mathcal{R}_0 with respect to the parameters V , χ , T and R according to the definition below.

Definition 1. *The sensitivity index of \mathcal{R}_0 with respect to a parameter p is given by*

$$\Gamma_{\mathcal{R}_0}^p = \frac{\partial \mathcal{R}_0}{\partial p} \frac{p}{\mathcal{R}_0}.$$

The sensitivity index of \mathcal{R}_0 with respect to χ and V are illustrated in Figure 5.7 and given by

$$\mathcal{S}_V := \frac{\partial \mathcal{R}_0}{\partial V} \frac{V}{\mathcal{R}_0} = \frac{\chi V}{\chi V - 1} = \frac{\partial \mathcal{R}_0}{\partial \chi} \frac{\chi}{\mathcal{R}_0}$$

With regard to the sensitivity index of \mathcal{R}_0 to T and R , we observe from Figure 5.8 that when the rainfall is averaging 50 mm, temperatures below 33.7°C have a negative impact on \mathcal{R}_0 with the proportional decrease in \mathcal{R}_0 declining with increasing temperatures to reach zero when the temperature reaches 33.7°C. Beyond this value, the temperature starts having a positive impact on \mathcal{R}_0 in which increased disease transmission. We also observe that when the rainfall is equal to 70 or 80 mm, temperatures below 28.8 °C have a positive impact on \mathcal{R}_0 . Moreover, as temperature increases, the proportional increase in \mathcal{R}_0 declines to become equal to zero when the temperature reaches 28.80C. Above 28.8°C,

Chapter 5: Modeling the effect of climate change on malaria transmission

any increase in temperature leads to a decline in \mathcal{R}_0 with the proportional decline in \mathcal{R}_0 increasing as temperature increases.

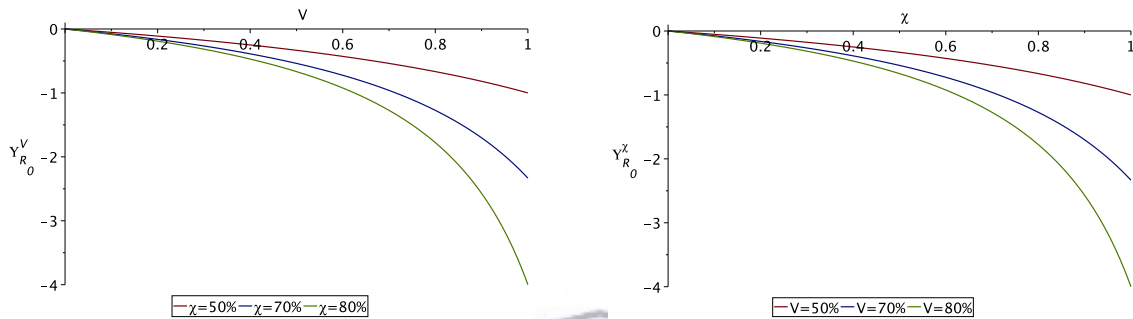


Figure 5.7: Sensitivity index of \mathcal{R}_0 with respect to χ and V .

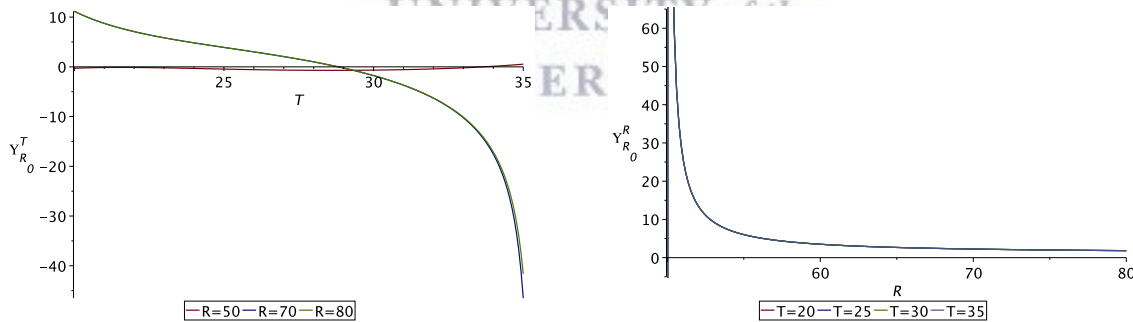


Figure 5.8: Sensitivity index of \mathcal{R}_0 with respect to R and T .

Endemic equilibrium point E^*

For simplicity, we first convert the systems (5.3.1) and (5.3.2) parameters into a constant version by setting $\eta(T, R) = \eta$, $\beta_{VT} = \beta_V$, $\sigma_{VT} = \sigma_V$, $\mu_{VT} = \mu_V$ and $\mu_m(T) = \mu_m$, then evaluate the critical points of the systems (5.3.1) and (5.3.2). The systems have the nontrivial critical point $E^* = (S_H^*, E_H^*, I_H^*, R_H^*, M^*, S_V^*, E_V^*, I_V^*)$ defined by

Chapter 5: Modeling the effect of climate change on malaria transmission

$$\left\{ \begin{array}{l} S_H^* = \frac{\Gamma(\rho+\delta+\mu_H)(\kappa+\mu_H)(\sigma_H+\mu_H)}{(\rho+\delta\mu_H)(\kappa+\mu_H)(\Lambda_H+\mu_H)(\sigma_H+\mu_H)-\Lambda_H\kappa\rho\sigma_H} \\ E_H^* = \frac{\Gamma\Lambda_H(\rho+\delta+\mu_H)(\kappa+\mu_H)}{(\rho+\delta+\mu_H)(\kappa+\mu_H)(\Lambda+\mu_H)(\sigma_H+\mu_H)-\Lambda_H\kappa\rho\sigma_H} \\ I_H^* = \frac{\Gamma\Lambda_H\sigma_H(\kappa+\mu_H)}{(\rho+\delta+\mu_H)(\kappa+\mu_H)(\Lambda+\mu_H)(\sigma_H+\mu_H)-\Lambda_H\kappa\rho\sigma_H} \\ R_H^* = \frac{\Gamma\Lambda_H\rho\sigma_H}{(\rho+\delta+\mu_H)(\kappa+\mu_H)(\Lambda+\mu_H)(\sigma_H+\mu_H)-\kappa\Lambda\rho\sigma_H} \\ M^* = \frac{\beta_V N_V K}{(\beta_V N_v + \mu_m K + \beta_V K)} \\ S_V^* = \frac{\beta_V \beta_V N_v K}{(\sigma_V + \mu_V)(\beta_V N_V + \mu_m K + \eta K)} \\ E_V^* = \frac{\Lambda_V \beta_V \eta N_V K}{(\Lambda_V + \mu_V)(\sigma_V + \mu_V)(\beta_V N_V + \mu_m K + \eta K)} \\ I_V^* = \frac{\Lambda_V \sigma_V \beta_V \eta N_V K}{\mu_V (\Lambda_V + \mu_V)(\sigma_V + \mu_V)(\beta_V N_V + \mu_m K + \eta K)}. \end{array} \right. \quad (5.4.6)$$

In this study, we consider the global stability of endemic equilibrium of our system.

Lemma 5.3 *If $\mathcal{R}_0 > 1$, then the unique endemic equilibrium of the system is globally asymptotically stable in the interior of \mathfrak{R} .*

Proof: Consider a nonlinear function

$$G = L_1(S_H, E_H, I_H, R_H) + L_2(M, S_V, E_V, I_V),$$

where

$$\begin{aligned} L_1 &= \left(S_H - S_H^* - S_H^* \ln \frac{S_H}{S_H^*} \right) + A_1 \left(E_H - E_H^* - E_H^* \ln \frac{E_H}{E_H^*} \right) \\ &\quad + A_2 \left(I_H - I_H^* - I_H^* \ln \frac{I_H}{I_H^*} \right) + A_3 \left(R_H - R_H^* - R_H^* \ln \frac{R_H}{R_H^*} \right), \\ L_2 &= \left(M - M^* - M^* \ln \frac{M}{M^*} \right) + \left(S_V - S_V^* - S_V^* \ln \frac{S_V}{S_V^*} \right) \\ &\quad + B_1 \left(E_V - E_V^* - E_V^* \ln \frac{E_V}{E_V^*} \right) + B_2 \left(I_V - I_V^* - I_V^* \ln \frac{I_V}{I_V^*} \right) \end{aligned}$$

The time derivative of G computed along solutions of system is

$$\int_0^t dG(S_H, E_H, I_H, R_H, M, S_V, E_V, I_V) = \int_0^t [\mathcal{L}L_1 + \mathcal{L}L_2] du$$

Chapter 5: Modeling the effect of climate change on malaria transmission

For the underlying deterministic model we note that at endemic steady state E^* we get,

$$\left\{ \begin{array}{l} \Gamma = \epsilon\beta_{HV}I_V S_H^* - \kappa R_H + \mu_H S_H^*, \\ \beta_V = \frac{(\eta + \mu_m)KM^*}{K - M^*}, \\ \eta = \frac{(\epsilon\beta_{VH}I_H^* + \mu_V)S_V^*}{M^*}, \\ \sigma_V = \frac{\mu_V I_V^*}{E_V^*}, \\ (\sigma_H + \mu_H) = \frac{\epsilon\beta_{HV}I_V^* S_H^*}{E_H^*}, \\ (\rho + \delta + \mu_H) = \frac{\sigma_H E_H^*}{I_H^*}, \\ (\kappa + \mu_H) = \frac{\rho I_H^*}{R_H^*}, \\ (\sigma_V + \mu_V) = \frac{\epsilon\beta_{VH}I_H^* S_H^*}{E_H^*}. \end{array} \right. \quad (5.4.7)$$

Then let us compute $\mathcal{L}L_1$ and $\mathcal{L}L_2$ in detail using the relation in (5.4.7).

$$\begin{aligned} \mathcal{L}L_1 &= \left(1 - \frac{S_H^*}{S_H}\right) \frac{dS_H}{dt} + A_1 \left(1 - \frac{E_H^*}{E_H}\right) \frac{dE_H}{dt} + A_2 \left(1 - \frac{I_H^*}{I_H}\right) \frac{dI_H}{dt} + A_3 \left(1 - \frac{R_H^*}{R_H}\right) \frac{dR_H}{dt} \\ &= \left(1 - \frac{S_H^*}{S_H}\right) (\epsilon\beta_{HV}I_V^* S_H^* + \mu_H S_H^* - \epsilon\beta_{HV}I_V S_H - \mu_H S_H - \kappa R_H^* + \kappa R_H) \\ &\quad + A_1 \left(1 - \frac{E_H^*}{E_H}\right) \left(\epsilon\beta_{HV}I_V S_H - \epsilon\beta_{HV}I_V^* S_H^* \frac{E_H}{E_H^*}\right) + A_2 \left(1 - \frac{I_H^*}{I_H}\right) \left(\sigma_H E_H - \sigma_H E_H^* \frac{I_H}{I_H^*}\right) \\ &\quad + A_3 \left(1 - \frac{R_H^*}{R_H}\right) \left(\rho I_H - \rho I_H^* \frac{R_H}{R_H^*}\right) \\ &= -\mu_H \frac{(S_H - S_H^*)^2}{S_H} - \epsilon\beta_{HV} \left(1 - \frac{S_H^*}{S_H}\right) (I_V S_H - I_V^* S_H^*) + \kappa \left(1 - \frac{S_H^*}{S_H}\right) (R_H - R_H^*) \\ &\quad + A_1 \epsilon\beta_{HV} \left(1 - \frac{E_H^*}{E_H}\right) \left(I_V S_H - I_V^* S_H^* \frac{E_H}{E_H^*}\right) + A_2 \sigma_H \left(1 - \frac{I_H^*}{I_H}\right) \left(E_H - E_H^* \frac{I_H}{I_H^*}\right) \\ &\quad + A_3 \rho \left(1 - \frac{R_H^*}{R_H}\right) \left(I_H - I_H^* \frac{R_H}{R_H^*}\right) \end{aligned}$$

and

$$\begin{aligned} \mathcal{L}L_2 &= \left(1 - \frac{M^*}{M}\right) \frac{dM}{dt} + \left(1 - \frac{S_V^*}{S_V}\right) \frac{dS_V}{dt} + B_1 \left(1 - \frac{E_V^*}{E_V}\right) \frac{dE_V}{dt} + B_2 \left(1 - \frac{I_V^*}{I_V}\right) \frac{dI_V}{dt} \\ &= \left(1 - \frac{M^*}{M}\right) \left(\frac{(\mu_m + \eta)(K - M)M^*}{(K - M)} - (\mu_m + \eta)M\right) \\ &\quad + \left(1 - \frac{S_V^*}{S_V}\right) \left(\epsilon\beta_{VH}I_H^* S_V^* \frac{M}{M^*} - \epsilon\beta_{VH}I_H S_V + \mu_V S_V^* - \mu_V S_V\right) \end{aligned}$$

Chapter 5: Modeling the effect of climate change on malaria transmission

$$\begin{aligned}
& +B_1 \left(1 - \frac{E_V^*}{E_V}\right) \left(\epsilon\beta_{VH}I_H S_V - \epsilon\beta_{VH}I_H^* S_V^* \frac{E_V}{E_V^*}\right) + B_2 \left(1 - \frac{I_V^*}{I_V}\right) \left(\sigma_V E_V - \sigma_V E_V^* \frac{I_V}{I_V^*}\right) \\
= & -\frac{(\mu_m + \eta)K}{(K - M^*)} \frac{(M - M^*)^2}{M} - \mu_V \left(1 - \frac{S_V^*}{S_V}\right) (S_V - S_V^*) - \epsilon\beta_{VH} \left(1 - \frac{S_V^*}{S_V}\right) \left(I_H S_V - I_H^* S_V^* \frac{M}{M^*}\right) \\
& +B_1 \epsilon\beta_{VH} \left(1 - \frac{E_V^*}{E_V}\right) \left(I_H S_V - I_H^* S_V^* \frac{E_V}{E_V^*}\right) + B_2 \sigma_V \left(1 - \frac{I_V^*}{I_V}\right) \left(E_V - E_V^* \frac{I_V}{I_V^*}\right).
\end{aligned}$$

Thus we have,

$$\begin{aligned}
\dot{G} = \mathcal{L}L_1 + \mathcal{L}L_2 = & -\mu_H \frac{(S_H - S_H^*)^2}{S_H} - \epsilon\beta_{HV} \left(1 - \frac{S_H^*}{S_H}\right) (I_V S_H - I_V^* S_H^*) + \kappa \left(1 - \frac{S_H^*}{S_H}\right) (R_H - R_H^*) \\
& +A_1 \epsilon\beta_{HV} \left(1 - \frac{E_H^*}{E_H}\right) \left(I_V S_H - I_V^* S_H^* \frac{E_H}{E_H^*}\right) + A_2 \sigma_H \left(1 - \frac{I_H^*}{I_H}\right) \left(E_H - E_H^* \frac{I_H}{I_H^*}\right) \\
& +A_3 \rho \left(1 - \frac{R_H^*}{R_H}\right) \left(I_H - I_H^* \frac{R_H}{R_H^*}\right) - \frac{(\mu_m + \eta)K}{(K - M^*)} \frac{(M - M^*)^2}{M} \\
& -\mu_V \left(1 - \frac{S_V^*}{S_V}\right) (S_V - S_V^*) - \epsilon\beta_{VH} \left(1 - \frac{S_V^*}{S_V}\right) \left(I_H S_H - I_H^* S_V^* \frac{M}{M^*}\right) \\
& +B_1 \epsilon\beta_{VH} \left(1 - \frac{E_V^*}{E_V}\right) \left(I_H S_V - I_H^* S_V^* \frac{E_V}{E_V^*}\right) + B_2 \sigma_V \left(1 - \frac{I_V^*}{I_V}\right) \left(E_V - E_V^* \frac{I_V}{I_V^*}\right)
\end{aligned}$$

By introducing new variables, letting $\frac{S_H}{S_H^*} = x$, $\frac{E_H}{E_H^*} = y$, $\frac{I_H}{I_H^*} = z$, $\frac{R_H}{R_H^*} = n$, $\frac{M}{M^*} = m$, $\frac{S_V}{S_V^*} = u$, $\frac{E_V}{E_V^*} = v$, $\frac{I_V}{I_V^*} = w$, it follows that

$$\begin{aligned}
\dot{G} = & -\mu_H \frac{(S_H - S_H^*)^2}{S_H} - \epsilon\beta_{HV} I_V^* S_H^* \left(1 - \frac{1}{x}\right) (xw - 1) + \kappa R_H^* \left(1 - \frac{1}{x}\right) (n - 1) \\
& +A_1 \epsilon\beta_{HV} I_V^* S_H^* \left(1 - \frac{1}{y}\right) (xw - y) + A_2 \sigma_H E_H^* \left(1 - \frac{1}{z}\right) (y - z) \\
& +A_3 \rho I_H^* \left(1 - \frac{1}{n}\right) (z - n) + \frac{(\mu_m + \eta)K}{(K - M^*)} \frac{(M - M^*)^2}{M} \\
& -\mu_V S_V^* \left(1 - \frac{1}{u}\right) (u - 1) - \epsilon\beta_{VH} I_H^* S_V^* \left(1 - \frac{1}{u}\right) (uz - m) \\
& +B_1 \epsilon\beta_{VH} I_H^* S_V^* \left(1 - \frac{1}{v}\right) (uz - v) + B_2 \sigma_V E_V^* \left(1 - \frac{1}{w}\right) (v - w)
\end{aligned}$$

The positive constant B_1, B_2, A_1, A_2 and A_3 are chosen such that the coefficient of xw , w , uz , y and n are equal to zero, that is

Chapter 5: Modeling the effect of climate change on malaria transmission

$$uz(-\epsilon\beta_{VH}I_H^*S_V^* + B_1\epsilon\beta_{VH}I_H^*S_V^*) = 0, \quad xw(-\epsilon\beta_{HV}A_1I_V^*S_H^* + \epsilon\beta_{HV}I_V^*S_H^*) = 0, \quad y(A_2\sigma_H E_H^* - \epsilon\beta_{HV}A_1I_V^*S_H^*) = 0, \quad v(B_2\sigma_V E_V^* - \epsilon\beta_{HV}B_1I_H^*S_V^*) = 0, \quad n(\kappa R_H^* - A_3\rho I_H^*) = 0,$$

Solving above equations, we get

$$A_1 = 1, \quad B_1 = 1, \quad A_2 = \frac{\epsilon\beta_{HV}I_V^*S_H^*}{\sigma_H E_H^*}, \quad B_2 = \frac{\epsilon\beta_{VH}I_H^*S_V^*}{\sigma_V E_V^*}, \quad A_3 = \frac{\kappa R_H^*}{\rho I_H^*}.$$

Then,

$$\begin{aligned} \dot{G} = & -\mu_H \frac{(S_H - S_H^*)^2}{S_H} - \frac{(\mu_m + \beta_v)K (M - M^*)^2}{(K - M^*)M} \\ & + \left(\frac{S_H^*}{S_H} - \frac{S_H^* R_H}{S_H R_H^*} - \frac{I_H R_H^*}{I_H^* R_H} \right) \kappa R_H^* \\ & + \left(3 - \frac{S_H^*}{S_H} - \frac{E_H I_H}{E_H^* I_H^*} - \frac{S_H E_H^* I_V}{S_H^* E_H I_V^*} \right) \epsilon\beta_{HV} I_V^* S_H^* \\ & + \left(3 - \frac{S_V^*}{S_V} - \frac{E_V^* I_V}{E_V I_V^*} - \frac{S_V E_V^* I_H}{S_V^* E_V I_H^*} \right) \epsilon\beta_{VH} I_H^* S_V^* \\ & + \left(2 - \frac{S_V^*}{S_V} - \frac{S_V}{S_V^*} \right) \mu_V S_V^*. \end{aligned}$$

Note that since the arithmetic mean is greater than or equal to the geometric mean, it follows that (\dot{G}) is less or equal to zero with equality only if $S_H = S_H^*$, $E_H = E_H^*$, $I_H = I_H^*$, $R_H = R_H^*$, $S_V = S_V^*$, $E_V = E_V^*$ and $I_V = I_V^*$. Thus, given E^* as endemic equilibrium, the largest compact invariant set is the singleton E^* . LaSalle's invariant principle then implies that E^* is globally asymptotically stable in the interior of \mathfrak{R} . This completes the proof. \square

5.5 Result and Discussion

In this section, we presented and analyzed a mathematical model in order to explore the impact of climatic conditions on malaria infections in two distinct regions of South Sudan. Model fitting via MCMC and the trajectory simulation of human dynamics were carried out. We derived the basic reproduction number \mathcal{R}_0 and examined the model for the existence of vector free and disease-free equilibrium points. We have discussed the stability of the diseases-free equilibrium of the model. We then performed a sensitivity analysis of \mathcal{R}_0 with respect to temperature and precipitation was performed. Temperature

Chapter 5: Modeling the effect of climate change on malaria transmission

and rainfall define the mosquito life cycle and control mosquito activity, including egg disabuse. Mosquitoes have been described as cold-blooded insects which are unable to regulate temperature on their own [29, 100]. This means that their body temperature is dependent on the atmosphere in which they live.

Yet, temperature's role in exacerbating malaria and the impact of weather and rainfall has been a controversial topic in recent years. Here Figure 5.4 (D) illustrates, the occurrence of Mosquito abundance when the mean monthly temperature and rainfall values lie in the ranges of 25 -30°C and 20 -30 mm respectively. The results demonstrate that mosquitoes are active once temperatures are consistently above 10°C, and are sedentary when temperatures reach 35°C. The results also indicate that the survivor probability of immature mosquitoes (eggs, larvae, pupae) could be reduced by low or excessive levels of rainfall (see Figure 5.4 (C)). Furthermore, the results suggest that daily rainfall in the range of 17–20 mm and temperatures in the range of 20°C to 35°C are ideal for progression of mosquitoes, and hence, for the spread of malaria. Our results also highlight the significant role of warmer temperatures in the aggravation of the disease, acting in the same direction of [1].

It can also be observed that the immature mosquitoes are more sensitive to temperatures at 25°C than the mature mosquitoes. These patterns were incorporated into a deterministic model of *Anopheles gambiae* population dynamics, in order to gain insight into the abundance of mosquitoes, thus providing an effective tool for control strategies in combating the spread of malaria. Temperatures in the range of 25°C to 30°C are more suitable for the progression of mosquitoes at all stages in their life-cycle (shown in Figure 5.9). This indicate that, mosquito dynamics are strongly shaped by warm weather ecology which appears to be consistent with other studies [12, 87, 101, 105, 112]. Accordingly, understanding the effect of climate change on malaria transmission dynamics is crucial in designing effective anti-malaria measures.

A model with a seasonal averaged climate in two study region is analyzed regarding malaria transmission. For example, investigated the sensitivity of \mathcal{R}_0 to average monthly temperature and rainfall data that are presented in Table 5.3. In numerical calculation

Chapter 5: Modeling the effect of climate change on malaria transmission

Table 5.3: Estimate of basic reproduction number \mathcal{R}_0 against Mean Rainfall (MR) and Average Temperature (AT) using parameter values from Table 2

Month	CES			WBGZ		
	AT(C)	MR(mm)	\mathcal{R}_0	AT(C)	MR(mm)	\mathcal{R}_0
Jan	38	6.1	1.11414	26.8	0	0.971627
Feb	38	27.9	3.89315	28.5	0	0.747225
Mar	38	31.4	3.58896	30.7	6	6.315132
Apr	37	72.2	4.62567	31.1	21	20.506707
May	34	132	8.62933	29.5	87	19.370367
Jun	32	146	14.27812	27.4	107	20.816907
Jul	30	304.5	20.89713	26.1	152	13.340053
Aug	31	91	17.32905	26.2	169	10.366855
Sep	32	93.1	14.27812	26.6	131	12.509831
Oct	33	111	11.70291	27.5	78	30.831914
Nov	35	28.3	7.73881	27.3	6	11.329622
Dec	36	15	5.09080	26.5	0	1.011970

of \mathcal{R}_0 , we assume 50 mm of rain will flushed out mosquitoes from their breeding site, therefore the precipitation is considered during the peak period to be less than 50 mm in \mathcal{R}_0 approximation. From April \mathcal{R}_0 is overestimated due to rainfall that increase above the average of 50 mm, we instead used a fix value of 40 mm. Our results indicate that \mathcal{R}_0 varies monotonically with the influence of rainfall and temperature. We note in the results that the reproduction number value increases during the peak period of the rainy season starting from March to October in CES. The onset of increased transmission intensity between July and September can be explained by the seasonal increase in A. Gambiae and a weakening of the clinical immunity of individuals. A similar pattern in transmission applied to WBGZ but with low disease intensity compared to CES which is most likely owing to the climate differences. Findings of this study are in agreement with other

Chapter 5: Modeling the effect of climate change on malaria transmission

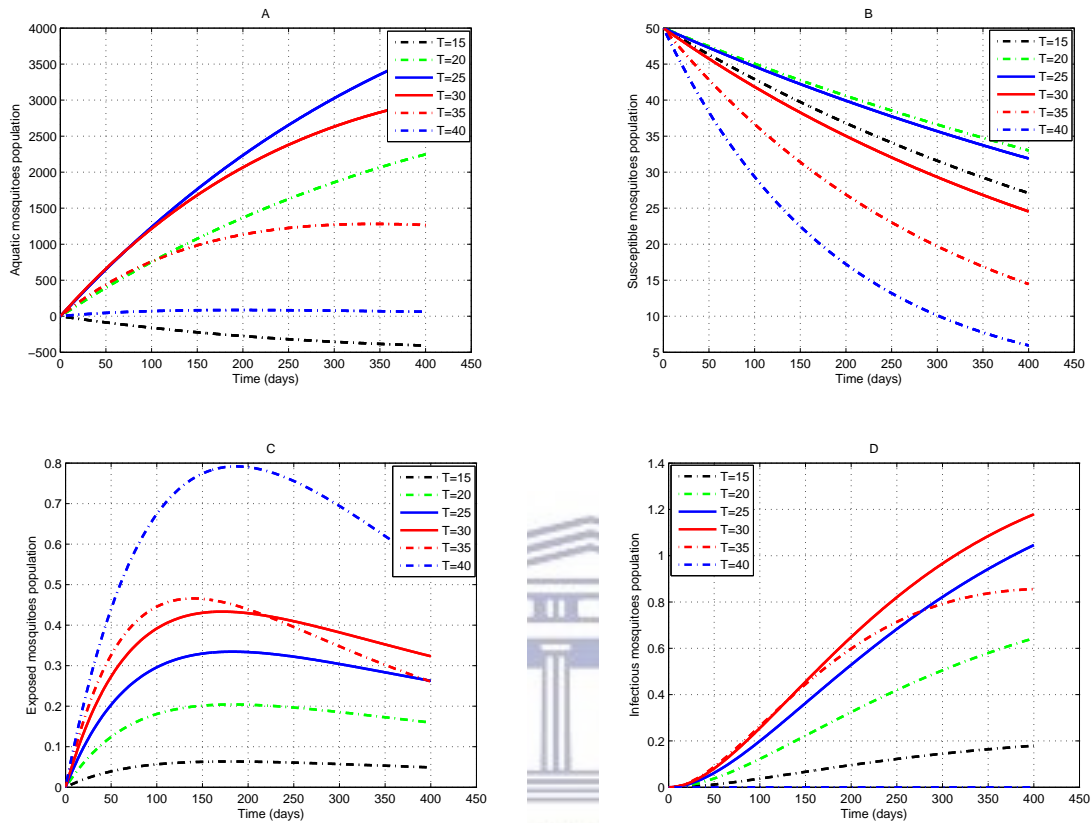


Figure 5.9: Simulation of the model, using parameter values in Table 1, assess the impact of various temperature values on the population dynamics of the mosquito

studies [1, 103] that demonstrate disease behavior changes with changes of local climate. These findings also suggest that the factor of climate can be a decisive determinant of malaria spatial distribution throughout the country.

Furthermore, in the case of WBGZ, the mosquito birth rate tends towards zero when the rainfall is minimal from November to February, hence, the reproduction number tends to zero. After February it begins to increase, reaching a peak in the months from June to October. This pattern, along with mean local rainfall and temperature shown in Figure 5.8, confirms our hypothesis that malaria transmission is influenced by weather and rainfall, since the disease is more prevalent in the favorable climate of CES than it is in WBGZ. This study, therefore, highlights the difference between the high transmission rate in tropical climates (CES) and the low transmission in hot semi-arid climates

Chapter 5: Modeling the effect of climate change on malaria transmission

(WBGZ), a difference which further coincides with the two distinct but adjacent cohorts of mesoendemic seasonal and holoendemic perennial malaria transmission [103].

These results point to the importance of incorporating detailed mosquito bionomics with climate-dependence into models for predicting the risk for malaria. These models can also be used to understand the possible changes in malaria prevalence in regions experiencing climate change: in the case of South Sudan, changes to regional climates, including changes in rainfall and temperature patterns, will alter the variability of malaria cases.

Using a realistic representation of the coupled mosquito–human model will aid to understand the dynamics of malaria over the study region. Noting that parameters such as mosquito size and mosquito bite assumption rate can influence the realization of disease behavior [72]. Hence, it was stimulating to validate our model with field data and implement parameter estimation to increase realism. Therefore, the mosquito model that provides a detailed mosquito bionomics with climate-dependence in line with several studies [12, 33, 34, 142] for predicting the risk for malaria is carried out. Moreover, our research sought to filter out the climatic factors affecting the force of infection which consist of infectious bites, and hence altered it with the effect of intervention coverage, unlike the studies [11, 63, 87, 141]. As the measurement of entomological inoculation rate (EIRs, measuring the number of infectious bites per person per year) is related to the measure of infection intensity, therefore it should be estimated during the model fitting process with the effect of intervention coverage given the disease incidence cases.

The availability of mosquito climate-based models and realistic parameter values determined through data fitting process allows researchers to predict more reliably disease transmission dynamics. We hope that this study improves understanding of the climate role as the first step in providing information that may lead to significant changes in the way that the disease is transmitted in these regions to incorporate the effective interventions.

5.6 Conclusion

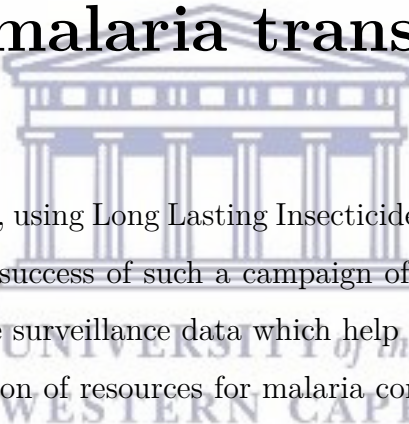
We proposed a host-mosquito model for malaria transmission in two climatic regions in South Sudan. We used MCMC to fit the model to malaria data from these two regions. The validated model is further used to calculate the basic reproductive number and assess its sensitivity to climate factors. The basic reproductive number is used to provide a numerical basis \mathcal{R}_0 is used to provide a numerical basis for further refinement and prediction of the impact of climate variability on malaria transmission intensity in two regions (i.e. CES and WBGZ).

The results in these both regions indicate that malaria trend follows the climate pattern with its epidemiological peak between February-December and between March-November when temperature and rainfall progressively increase in the CES and WBGZ respectively. The findings also demonstrated that disease is more effective and severe in tropical (CES) region than in a hot semi-arid (WBZ) region due to climate conditions. Hence, we concluded that this study which analyzes observed phenomena also seeks ways of informing decision making together with ideas for the continuation of malaria control in South Sudan. A model calibration was one of the main contributions that this study has achieved, complemented with the realistic representation of *Anopheles Gambiae* population dynamics to gain insight into the abundance of mosquitoes and hence the course of the epidemic.

However, malaria is a complex disease that can reemerge from other factors such as socioeconomic situation and population movement which need to be incorporated in studying malaria transmission. These aspects are worthy of attention in future studies.

Chapter 6

Modelling the effect of bednet coverage on malaria transmission



A campaign for malaria control, using Long Lasting Insecticide Nets (LLINs) was launched in South Sudan in 2009. The success of such a campaign often depends upon adequate available resources and reliable surveillance data which help officials understand existing infections. An optimal allocation of resources for malaria control at a sub-national scale is therefore paramount to the success of efforts to reduce malaria prevalence. In this chapter, we extend an existing SIR mathematical model to capture the effect of LLINs on malaria transmission. Available data on malaria is utilized to determine realistic parameter values of this model using a Bayesian approach via Markov Chain Monte Carlo (MCMC) methods. Then, we explore the parasite prevalence on a continued rollout of LLINs in three different settings in order to create a sub-national projection of malaria. Further, we calculate the model's basic reproductive number and study its sensitivity to LLINs' coverage and its efficacy. From the numerical simulation results, we notice a basic reproduction number, \mathcal{R}_0 , confirming a substantial increase of incidence cases if no form of intervention takes place in the community. This work indicates that an effective use of LLINs may reduce \mathcal{R}_0 and hence malaria transmission. We hope that this study will provide a basis for recommending a scaling-up of the entry point of LLINs' distribution that targets households in areas at risk of malaria.

6.1 Introduction

The Republic of South Sudan (RSS) is among the countries in sub-Saharan Africa that are most severely affected by malaria and is currently experiencing an unprecedented outbreak of malaria. Médecins Sans Frontières (MSF) have reported that, in the year 2015, malaria outbreaks in South Sudan were considered to be the most hazardous in the region [31, 93]. The country is facing a number of tremendous challenges, the most notable being the limitation of human and financial resources due to the ongoing war and civilian instability. Nonetheless, the government agencies of South Sudan, as well as many Non-Governmental Organizations (NGOs) have committed to reducing this ongoing outbreak of malaria.

Recently, the National Malaria Control Program (NMCP) reported, in its strategic plan, that LLINs have been the main health intervention deployed to reduce malaria transmission in South Sudan since it gained independence [35]. A number of LLINs nets have been distributed since 2008, when the free mass LLIN distribution campaign was piloted in the States of Warrap, Western Bahr-El-Ghazal and Western Equatoria. However, their distribution and utilization still remain relatively low [22]. Subsequently, the programme was extended to the entire country reaching a total of 2 602 021 LLINs in 2009 [21, 106]. This number declined to 1 836 401 LLINs in 2011 and then, further down to 1 592 507 LLINs in 2012 in various states [47]. Moreover, in these campaigns ownership of LLINs by community members varied by State. For instance, Eastern Equatoria has the highest (58 %) LLINs coverage, while the lowest coverage rates are found in Warap (17%), Unity (20%) and Upper Nile (22 %). Likewise, malaria infection takes a larger toll in the rural areas where the availability of LLINs is slightly lower (31 %) than in urban areas (44 %) [57].

These control measures were not sufficient to eliminate the parasite over a short time scale and failed to sustain control programs. The malaria trend increased between 2011 and 2015 in almost all of the states, as is shown in Figure 6.1. This reported case data is accumulated on a weekly-basis. The data exhibits noise and some missing data is

Chapter 6: Malaria transmission modeling with intervention scenario

observed. Nonetheless, understanding the role of insecticide-treated nets in mosquito vectors is the first and most important step in disease eradication. Here, we focus on current malaria control actions and their impact on human infection. This will help to define the specific needs for successful malaria interventions in various settings, while increasing the impact of control tools and maintaining value for money. The key to effective control is to choose policies that are appropriate to local settings. The Ministry of Health (MoH) has endeavored to scale up malaria control efforts in the country in order to lower both the morbidity and mortality rates of malaria by 80% by the year 2020. As this 80% reduction in malaria prevalence may not be achieved through a ‘more of the same’ approach, mathematical modelling may play a role in operational strategies on control.

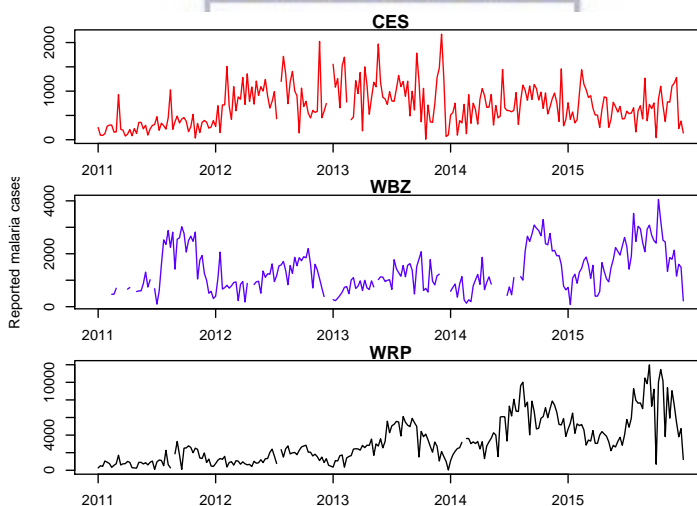


Figure 6.1: Weekly malaria reported cases from the beginning of 2011 until end of 2015 in Central Equatoria State (CES), Western Bahr El Ghazal State (WBZ) and Warrap State (WRP). The data was obtained from National Malaria Control Programme of South Sudan (NMCP).

Mathematical models usually depend on a set of parameters. In the present case, each parameter carries a biological significance such as force of infection, recovery rate or, mortality rate. It is therefore important to evaluate the numerical values of these quantities with real data in order the computational simulation to predict the reactions

Chapter 6: Malaria transmission modeling with intervention scenario

accurately, and thus to give us a better understand of the disease epidemiology. In recent years there has been an increased interest in parameters determination procedures [55, 116, 128]. Bayesian approaches and in particular, the Markov Chain Monte Carlo (MCMC) have proven to be powerful inference tools for complex systems developed in behavioral science and computational biology [48, 54, 69, 77, 107, 138].

Many mathematicians and epidemiologists (see for example, [13, 23, 26, 67, 66, 89, 90, 94, 114, 134]) have provided different mathematical models for understanding the transmission dynamics of malaria in human populations and also for consolidating various intervention tools, such as LLINs, Indoor Residual Spraying (IRS), drugs and even vaccines. For example, Ngonghala et al. [89] developed a mathematical model for malaria dynamics that incorporates Insecticide-Treated Nets (ITNs) coverage. They concluded that when the reproduction number $R_0 < 1$, the mosquito-free equilibrium is a globally asymptotically stable (GAS), whereas, when R_0 is greater than one, a locally asymptotically stable human-mosquito equilibrium exists. Their study shows that constant ITNs-efficacy may underestimate the disease transmission risk. Chitnis et al. [23] adapted a mathematical model to compare the impact of malaria vector-control Interventions consist of ITNs and IRS, implemented individually and in combination; their results showed that ITNs were more effective than IRS. Okumu et al [99] used a deterministic model of the mosquito life cycle to investigate the effect of untreated nets or LLINs with IRS combinations on the disease at the community level, they concluded that the insecticidal potential impact of LLINs and IRS is mainly due to the personal protection provided by the nets, rather than insecticidal effectiveness. Briët and Penny [16] used a stochastic simulation model based on individuals in scenarios with sustained LLIN distributions, and varying degrees of Case Management (CM) coverage. The modelling analysis indicated that under sustained vector control and scaled-up CM, transmission can rebound to higher levels than when using LLIN distribution alone. Griffin et al. [51] developed an individual-based simulation model for Plasmodium falciparum transmission in an African context incorporating the impact of the switch to Artemisinin-Combination Therapy (ACT) and scaling up the coverage of interventions from the year 2000 onwards.

Chapter 6: Malaria transmission modeling with intervention scenario

In this chapter, we propose a modification of the age structured model developed by Filipe et al. [40], in the expression of the SEIR and SEI Model formulation for host and vector respectively. Our model does not include an age structure, but accounts for LLINs' waning effect in order to forecast epidemiological aspects of malaria in South Sudan's different regions and states. Consequently, a parameter estimation of this model is carried out under a Bayesian framework via Markov Chain Monte Carlo (MCMC) methods, wherein the likelihood function is combined with the prior values of the parameters in order to calculate the posterior values for model parameters from time series data.

6.2 Study area and demography

South Sudan is a tropical landlocked country in East-Central Africa which shares borders with some of the most malaria-endemic countries in the world. Prior to 2015, the country was divided into ten states comprised of three regions.

The pre-independence national census estimated the South Sudan population at 8.2 million people in 2008, with 42% of the population aged under 15 years, 19% at the median age and only 5% aged over 60 years [120]. The population projection for 2009 may be as high as 11 million due to both growth rates and the estimated numbers of returnees, Figure 6.2. The birth rate is estimated at 40.62 per thousand people and the maternal mortality rate is estimated at 1,700 deaths per 100,000 live births [123]. The country's fertility rate of 6.7 births per woman is the highest in the Eastern Mediterranean region [123]. The census reported a life expectancy at birth of 42 years for both sexes [124]. This study is conducted in states chosen randomly in three different regions, namely:

1. Equatoria (South), we have chosen the state of Central Equatoria,
2. Bhar El Ghazal (North-west), we have chosen the state of Western Bahr El Ghazal,
3. Upper Nile (North-east), we have chosen the state of Warrap.

The map of the study area is given in Figure 6.3.

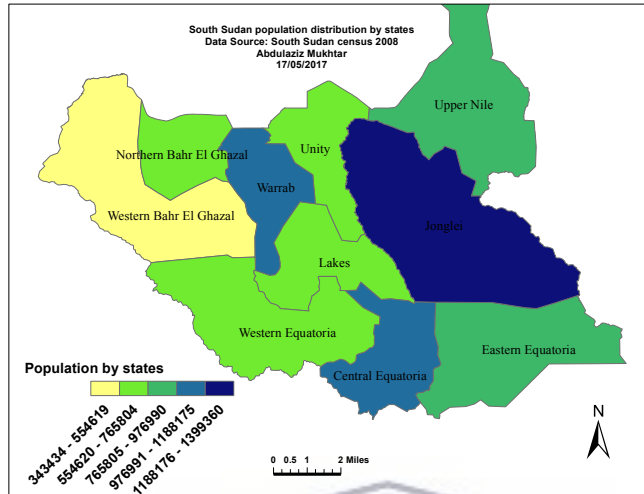


Figure 6.2: Population density of South Sudan 2009

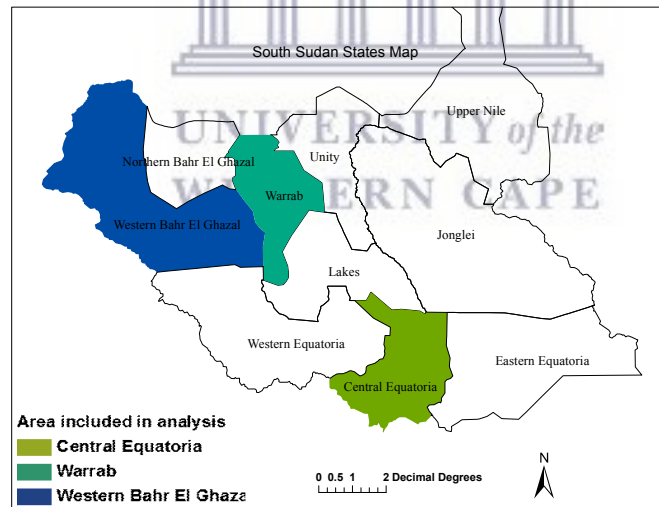


Figure 6.3: South Sudan selected state analysis map.

6.3 Method

We use a deterministic compartmental structure for the endemic malaria disease. The total human population denoted by N is subdivided into susceptible individuals S , pre-infectious with malaria parasite individuals E , clinical infectious individuals I , asymp-

Chapter 6: Malaria transmission modeling with intervention scenario

tomatic infectious individuals A and protected individuals R , Eq (6.3.1). The total mosquito population denoted by M is subdivided into susceptible mosquitoes X , mosquitoes exposed to the malaria parasite Y and infectious mosquitoes Z , Eq (6.3.2). The compartmental model is illustrated in the flow diagram in Figure 6.3, which translates to Eqs (6.3.3) and Eqs (6.3.6).

$$N(t) = S(t) + E(t) + I(t) + A(t) + R(t), \quad (6.3.1)$$

$$M(t) = X(t) + Y(t) + Z(t). \quad (6.3.2)$$

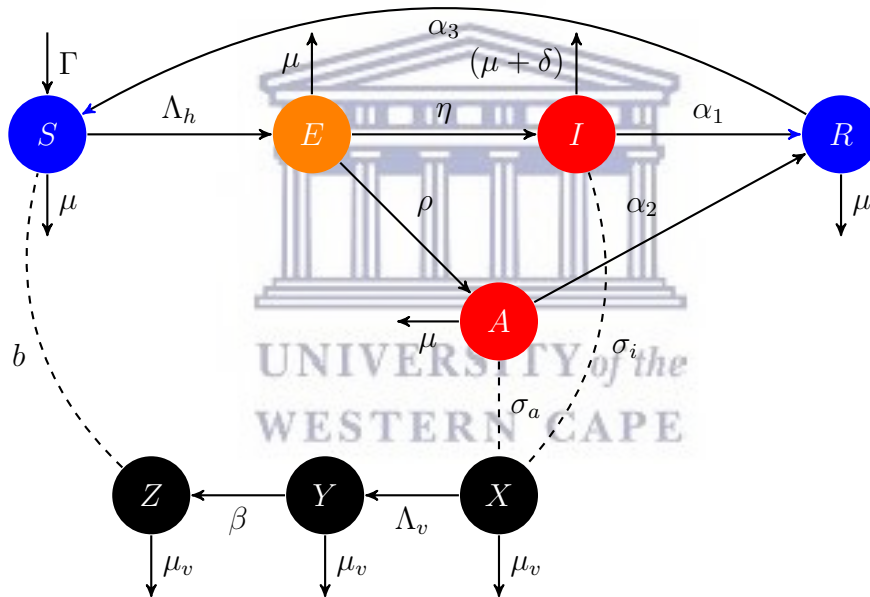


Figure 6.4: Flow diagram for Human and Mosquito infection model

The human components of the model is presented to capture the relation of effective treatment and parasite prevalence. The second components of the model represent mosquito population dynamics to capture the effects of LLINs on vector mortality and in preventing transmission. The model excludes a delay in the force of infection and includes seasonality with respect to epidemics of this disease. We examine the model and data set, by applying Bayesian approach to estimate the posterior distribution of parameters. The prior estimates of some parameters were obtained from the literature [115, 137].

6.3.1 Human model formulation

Since we are modelling the endemic malaria on a longer scale, we include birth and death rate in the model. Hence, the susceptible compartment is recruited by birth at a rate Γ . We presume susceptible individuals (S) acquire malaria and become infected at a rate Λ_h when they are bitten by infectious mosquitoes (the entomological inoculation rate, EIR). After bites from infectious mosquitoes, individuals progress to the pre-infectious compartment E and remain on average 12 days (latent period) before becoming fully infective. Upon infection, they either develop clinical infectious with probability rate η to enter compartment I or proceed with asymptomatic infection with probability rate ρ to enter compartment A . Those that develop disease (with symptoms) are successfully treated and naturally recovered with the rate α_1 and subsequently enter a compartment of recovery (or a protected compartment R) which are assumed to lose immunity and move to the susceptible compartment at a rate of α_3 . Individuals with asymptomatic infection are assumed to recover naturally with a constant per capita recovery rate α_2 and enter R compartment. All compartments are stratified by level at which people are bitten by mosquitoes and also drop individuals at a natural death rate of $\mu = \frac{1}{q \times 360} \text{ day}^{-1}$ where q is the human life expectancy in years. The deterministic model for the human dynamics is as follows

$$\begin{aligned}
 \frac{dS}{dt} &= \Gamma - \Lambda_h S + \alpha_3 R - \mu S, \\
 \frac{dE}{dt} &= \Lambda_h S - \eta E - \rho E - \mu E, \\
 \frac{dI}{dt} &= \eta E - (\alpha_1 + \delta + \mu) I, \\
 \frac{dA}{dt} &= \rho E - (\alpha_2 + \mu) A, \\
 \frac{dR}{dt} &= \alpha_1 I + \alpha_2 A - \alpha_3 R - \mu R,
 \end{aligned} \tag{6.3.3}$$

where t represents time and α_1 and α_2 symbolize human infection durations while α_3 is depend on the loss of immunity duration. The force of infection, Eq (6.3.4) is assumed to vary by degree of exposure to mosquitoes due to geographic variation and is governed by

the function

$$\Lambda_h = EIR b = \left(\frac{\epsilon Z}{N}\right)b \quad (6.3.4)$$

where EIR denotes the entomological inoculation rate, b is the probability of infection if bitten by an infectious mosquito, with $0 < b \leq 1$. The parameter ϵ is the per capita biting rate of mosquitoes to be measured for adults at study settings level.

6.3.2 Mosquitoes model formulation

We consider *Anopheles Gambiae* mosquitoes which is the main anopheles species that transmits *Plasmodium Falciparum* in South Sudan [38]. The mosquito population is divided into three classes: susceptible X , latently infected Y , infectious Z . Susceptible female mosquitoes are recruited at the birth rate Ψ . We assume reduction in this compartment at the death rate μ_v and at the force of infection (see Eq (6.3.5)). Thus, the adult susceptible mosquito acquires malaria at a rate Λ_v which depends on the infectiousness of the human population:

$$\Lambda_v = \frac{\sigma_a \epsilon A + \sigma_i \epsilon I}{N} \quad (6.3.5)$$

where σ_a is the onward infectivity from an asymptomatic infectious and σ_i is the onward infectivity from a clinical infection. The parasite (in the form of gametocytes) enters the mosquito with some probability when the mosquito bites an infectious human and the mosquito moves from the susceptible to the infectious class at a rate determined by the force of infection. Once mosquitoes are infected, they pass through a latent period. Mosquitoes then become infectious to humans and remain infectious for life (until they die). They leave the population through a per ca-pita density-dependent natural death rate. The population dynamics and infection process of *anopheles Gambiae* mosquitoes are given by the following set of ordinary differential equations.

$$\begin{aligned}\frac{dX}{dt} &= \Psi - \Lambda_v X - \mu_v X, \\ \frac{dY}{dt} &= \Lambda_v X - (\beta + \mu_v) Y, \\ \frac{dZ}{dt} &= \beta Y - \mu_v Z,\end{aligned}\tag{6.3.6}$$

where β is the probability that a mosquito survives the extrinsic incubation period (EIP) (see Equation (6.5.12) for more details), μ_v is the death rate and Λ_v is the force of infection acting on mosquitoes.

6.3.3 Model fitting

In this section, our quantitative mathematical model is fitted to data. There are a few statistical techniques that are usually used to undertake parameter estimation when building a statistical model. In particular, maximum likelihood estimation (MLE) and Bayesian estimation are the most novel statistical tools used. As with the usage of MLE, a mathematical model that confronts a data can be influenced by the exact relationship between the parameters or by the complexity of the model [53, 117]. The Bayesian method combines the likelihood of the data as well as the prior distribution of the parameters of the model to obtain the posterior distribution of the parameters of the model. This allows one to make inference based on the posterior mean/ median of the parameters.

In this study we utilise Markov Chain Monte Carlo (MCMC) to obtain the posterior samples of the parameters of the model. The model fitting was undertaken by using weekly malaria data of 2011 for each region under investigation (shown in Figures 6.5 - 6.7) using MCMC. The model is run from the year 2000 to reach a steady state before being fitted to data from the year 2011. We assume that weekly malaria data were reported according to a Poisson process with reporting rate γ . Since the reporting rate is unknown we assume it to be no larger than 85%. Assume also that x_{ij} ($i = 1, \dots, n; j = 1, \dots, 3$) are the observed weekly malaria cases for state j during week i . We used uniform distributions to model the prior belief regarding the mosquito biting rate ϵ and the clinical duration

Chapter 6: Malaria transmission modeling with intervention scenario

of infections α_1 . Specifically we assume $\epsilon \sim U(0, 200)$ and $\alpha_1 \sim U(0, 50)$ [137]. During this fitting process the model parameters described in Table 6.1, b , ϵ_j , α_1 , and α_3 were estimated and δ , α_2 , ρ and η were fixed (in agreement with previous studies) in each setting. These parameters were assumed to be constant and were jointly estimated by utilizing fitR (version 0.1 [18]) to obtain posterior samples 10000 iterations and a burn-in of 1000 iterations used for three chains. The credibility intervals produced in Figures 6.5 - 6.7 was a 95% confidence intervals with different accepting rate of each figure. It seems as if the model does not fit the weekly malaria data very well since the seasonality observed in the data has not been accounted for. Below we attempt to do so.

Table 6.1: Model Parameters: Description and value

Symbol	Description	Estimate	Ref
μ	Natural death rate of humans	0.00006614	Est
σ_a	Onward infectivity from an asymptomatic infectious	0.2	[134]
ρ	Probability of asymptomatic infectious	0.0071 (fixed)	[134]
α_2	Asymptomatic infection rate	1/200 (1/180-1/250) fixed	[52]
δ	Humans death rate due to malaria	0.0004 (0.00027-0.0005) fixed	[26]
η	Probability of acquiring clinical disease	1/12 (fixed) day ⁻¹	[52]
Γ	Birth rate of humans	Humans/Day	Est
σ_i	Onward infectivity from a clinical infectious	Derived from data	
b	Probability of infection	Derived from data	
ϵ_j	Mosquitoes biting rate for state j	Derived from data	
α_1	Clinical disease rate	Derived from data	
α_3	Human Re-susceptibility rate	Based on drug	

In the second model, we calculate the mean of posterior distribution for further validation and better fitting results, using weekly malaria data between 2011 to 2015 plotted in Figure 6.8. This includes a simple parametric model to account for seasonality, as the weekly malaria count displayed strong seasonality. We specifically assume that the

Chapter 6: Malaria transmission modeling with intervention scenario

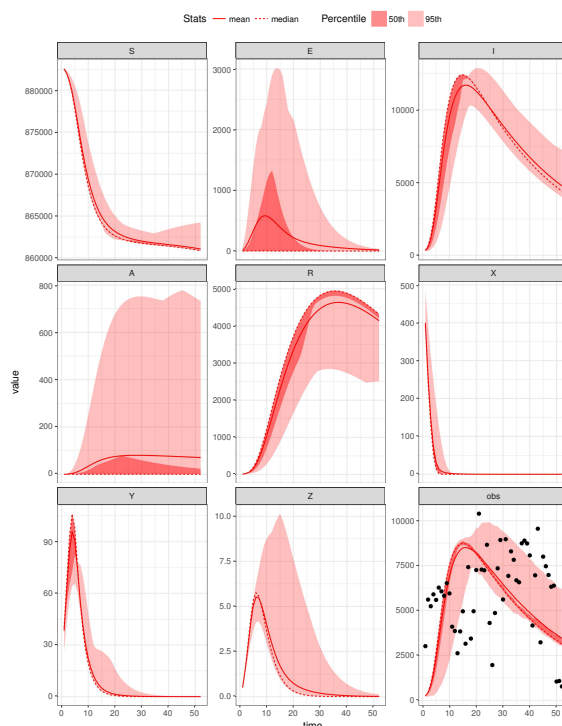


Figure 6.5: Parameters estimation by fitting model to weekly malaria cases of CES: The deterministic model (for both human and vector) trajectories and model assessment (lines) run against the CES data (points) with $\epsilon = 91.60$, $b = 0.4356804$, $\alpha_1 = 0.02169197$ (duration of infections 46.1), $\sigma_i = 0.6792$, $\alpha_3 = 0.5882$ and initial state value ($S = 882846$, $E = 0$, $I = 300$, $A = 0$, $R = 0$, $X = 600$, $Y = 0$, $Z = 0$) with the mean and the median as well as the 95th and 50th percentiles of the replicated simulations are displayed

seasonal component is modelled as

$$\beta_0(t) = \sum_{j=1}^2 a_j \cos(tw_j) + b_j \sin(tw_j), \quad (6.3.7)$$

where $w_j = 2\pi j/52$ and t represents time. We assume that the prior distribution of a_j and b_j are both Gaussian random variables with mean 0 and variance $\sigma_j = 1.67001$ [137]. For a given set of parameters, let the model-predicted malaria in site j be θ_j , the number of initial susceptible individuals at risk and number of malaria cases be E_j and x_{ij} respectively. The hierarchical model used to validate the model for the observed malaria

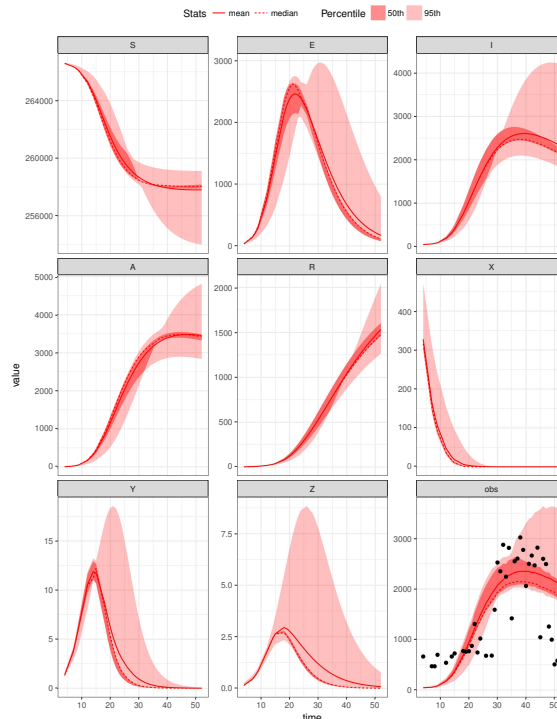


Figure 6.6: Parameters estimation by fitting model to weekly malaria cases of WBGZ: The deterministic model (for both human and vector) trajectories and model assessment (lines) run against the WBGZ data (points) for 2011, with $\epsilon = 79.50$, $b = 0.79836$, $\alpha_1 = 0.025$, $\alpha_3 = 0.01785714$, $\sigma_i = 0.06274$ and initial state value ($S = 266745$, $E = 0$, $I = 200$, $A = 0$, $R = 0$, $X = 500$, $Y = 0$, $Z = 0$); the mean and the median as well as the 95th and 50th percentiles of the replicated simulations are displayed

counts is thus:

$$x_{ij}|\theta_j, \beta_0 \sim \text{Poisson}(E_j e^{\beta_0 \theta_j}),$$

$$\theta_i \sim U(l_1, l_2),$$

where l_1 and l_2 are known constants. The E_j values were obtained using [123].

6.4 Basic reproductive number \mathcal{R}_0

To determine the stability of this model we first evaluate the critical points of the model (6.3.3 and 6.3.6) of ODEs. The trivial critical point with no infected individu-

Chapter 6: Malaria transmission modeling with intervention scenario

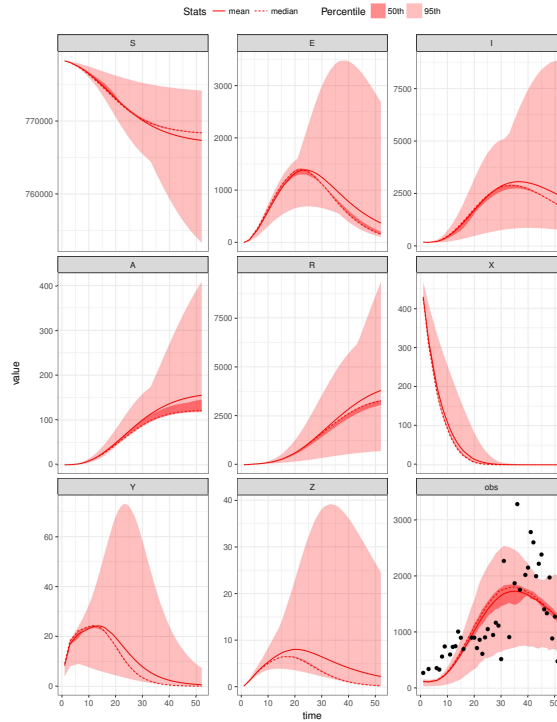


Figure 6.7: Parameters estimation by fitting model to weekly malaria cases of WRP: The deterministic model (for both human and vector) trajectories and model assessment (lines) run against the WRP data (points), with $\epsilon = 56.0$, $b = 0.63984$, $\alpha_1 = 0.0191938$, $\alpha_3 = 0.05$, $\sigma_i = 0.789852$ and initial state value ($S = 778342$, $E = 0$, $I = 200$, $A = 0$, $R = 0$, $X = 500$, $Y = 0$, $Z = 0$); the mean and the median as well as the 95th and 50th percentiles of the replicated simulations are displayed

als is the point $E_0 = (S^*, E^*, I^*, A^*, R^*, X^*, Y^*, Z^*) = (\frac{\Gamma}{\mu}, 0, 0, 0, 0, \frac{\Psi}{\mu_v}, 0, 0)$. The basic reproduction number, denoted by \mathcal{R}_0 , plays a vital role in understanding the propagation of the relevant epidemic. It is defined as the average number of secondary infections that occur when one infective individual is introduced into a completely susceptible host population [132].

For the purpose of our model, the basic reproduction number of the models can be established by using the next generation matrix as presented in [132]. In Proposition 6.1 we compute the basic reproduction number for the system.

Chapter 6: Malaria transmission modeling with intervention scenario

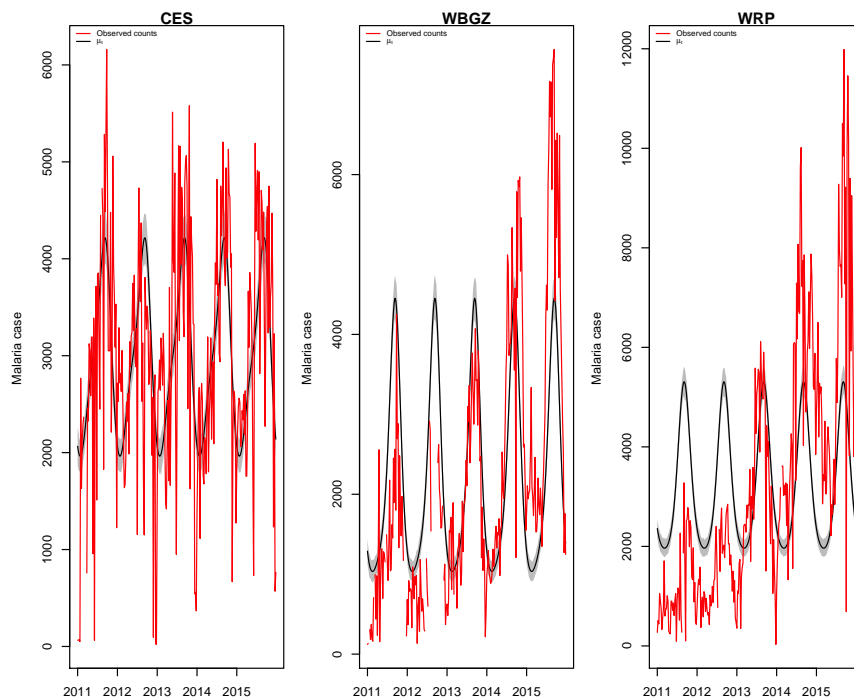


Figure 6.8: Model validation by fitting to malaria cases on weekly basis between 2011-2015: The posterior mean densities of the mosquito bite rate ϵ in CES, WBGZ and WRP with 95% credibility interval at a chosen number of 10,000 iterations.

Lemma 6.1. *The basic reproduction number of the model (6.3.3 and 6.3.6) is*

$$\mathcal{R}_0 = \sqrt{\frac{\epsilon^2 b \beta \sigma_a \rho}{\mu_v (\beta + \mu_v) (\eta + \rho + \mu) (\mu + \alpha_1)} + \frac{\epsilon^2 b \beta \sigma_i \eta}{\mu_v (\beta + \mu_v) (\eta + \rho + \mu) (\mu + \delta + \alpha_2)}} \quad (6.4.8)$$

Proof. Set $x = (I, A, E, S)^T$, with W^T being the transpose of the vector W . Then the system can be written as

$$\dot{x} = \mathcal{F}(x) - \mathcal{V}(x)$$

where

Chapter 6: Malaria transmission modeling with intervention scenario

$$\mathcal{F}(x) = \begin{pmatrix} \frac{\mu_v \epsilon b I_v S}{\psi} \\ 0 \\ 0 \\ \frac{\sigma_a \epsilon A X + \sigma_i \epsilon I X}{\Gamma} \\ 0 \end{pmatrix},$$

$$\mathcal{V}(x) = \begin{pmatrix} (\eta + \rho + \mu)E \\ (\mu + \alpha_1)A - \rho E \\ (\mu + \delta + \alpha_2)I - \eta E \\ (\beta + \mu_v)E_v \\ -\beta E_v + \mu_v I_v \end{pmatrix}.$$

According to the theory of [132], the basic reproduction number \mathcal{R}_0 of our system is the spectral radius of FV^{-1} , where F and V are the matrices

$$F = \begin{pmatrix} 0 & 0 & 0 & 0 & \frac{\mu_v \epsilon b \Gamma}{\mu \psi} \\ 0 & 0 & 0 & 0 & 0 \\ 0 & 0 & 0 & 0 & 0 \\ 0 & 0 & 0 & 0 & 0 \\ 0 & \frac{\sigma_i \epsilon \mu \psi}{\mu_v \Gamma} & \frac{\sigma_a \epsilon \mu \psi}{\mu_v \Gamma} & 0 & 0 \\ 0 & 0 & 0 & 0 & 0 \end{pmatrix}$$

and

$$V = \begin{pmatrix} (\eta + \rho + \mu) & 0 & 0 & 0 & 0 \\ -\rho & (\alpha_1 + \mu) & 0 & 0 & 0 \\ -\rho & 0 & (\alpha_2 + \delta + \mu) & 0 & 0 \\ 0 & 0 & 0 & (\beta + \mu_v) & 0 \\ 0 & 0 & 0 & -\beta & \mu_v \end{pmatrix}.$$

The matrix F is a non-negative matrix of rank one and can be written as the product of

Chapter 6: Malaria transmission modeling with intervention scenario

the vectors, where V is a non-singular M-matrix. The inverse of V is

$$V^{-1} = \begin{pmatrix} \frac{1}{\eta+\rho+\mu} & 0 & 0 & 0 & 0 \\ \frac{-\eta+}{(\eta+\rho+\mu)(\alpha_2+\delta+\mu)} & \frac{1}{\alpha_2+\delta+\mu} & 0 & 0 & 0 \\ \frac{\rho}{(\eta+\rho+\mu)(\alpha_1+\mu)} & 0 & \frac{1}{\alpha_1+\mu} & 0 & 0 \\ 0 & 0 & 0 & \frac{1}{\gamma+\mu_v} & 0 \\ 0 & 0 & 0 & \frac{-\beta}{(\beta+\mu_v)\mu_v} & \frac{1}{\mu_v} \end{pmatrix}.$$

Multiplying F and V^{-1} gives the next generation matrix

$$G := FV^{-1} = \begin{pmatrix} 0 & 0 & 0 & k_1 & k_2 \\ 0 & 0 & 0 & 0 & 0 \\ 0 & 0 & 0 & 0 & 0 \\ 0 & 0 & 0 & 0 & 0 \\ k_3 & k_4 & k_5 & 0 & 0 \\ 0 & 0 & 0 & 0 & 0 \end{pmatrix}, \quad (5.3)$$

where

$$k_1 = \frac{\beta\epsilon b\Gamma}{(\beta+\mu_v)\mu_v\psi}$$

$$k_2 = \frac{\epsilon\Gamma\sigma_i}{\mu\psi}$$

$$k_3 = \frac{\eta\sigma_i\mu\epsilon\psi}{(\eta+\rho+\mu)(\alpha_2+\delta+\mu)\mu_v\Gamma} + \frac{\rho\sigma_a\epsilon\mu\psi}{(\eta+\rho+\mu)(\alpha_1+\mu)\mu_v\Gamma}$$

$$k_4 = \frac{\sigma_i\mu\epsilon\psi}{(\alpha_2+\delta+\mu)\mu_v\Gamma}$$

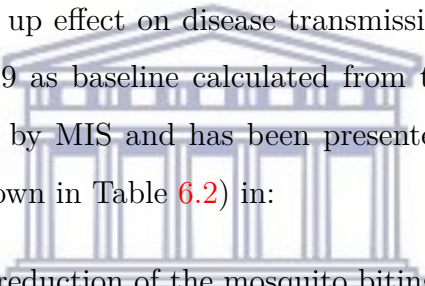
$$k_5 = \frac{\sigma_a\epsilon\mu\psi}{(\alpha_1+\mu)\mu_v\Gamma}$$

Hence we compute the eigenvalues from (5.3) to obtain the spectral radius of the matrix FV^{-1} . The spectral radius is the reproductive number R_0 . There are five eigenvalues obtained from FV^{-1} and maximum eigenvalue is $\lambda = \sqrt{k_1 k_3}$. Therefore the basic reproduction number for autonomous system (6.3.3 and 6.3.6) is as claimed. \square

6.5 Intervention with bednets (LLINs)

In this section we incorporate the impact of bednets intervention on malaria transmission with used of the threshold \mathcal{R}_0 . The LLINs is the only intervention used in the study and hence, by testing its scale up effect on disease transmission. We use data of LLINs coverage at state level for 2009 as baseline calculated from the given number of LLIN distribution which is provided by MIS and has been presented in [123]. In our model, LLINs intervention results (shown in Table 6.2) in:

1. Mosquito biting rate: A reduction of the mosquito biting rate is given by


$$(1 - \chi V)\epsilon$$

UNIVERSITY of the
WESTERN CAPE

where χ is the proportion of LLINs coverage and V is the effectiveness of LLINs. For the sake of calculating the basic reproduction number of the model with LLINs intervention, we assume that V is constant. However, in simulation practice, we consider the efficacy of LLINs wanes with time since mass distribution of LLINs campaigns were run in just one to four states in any single year. To account for this, we use in our model simulations, the following formula taken from [118].

$$V(t) = 1 - a \exp(-e^{-x(t-y)}) \quad (6.5.9)$$

where a and x are real numbers and y is a positive integer.

2. Mosquito mortality rate: LLINs intervention is also assumed to have three effects on the adult mosquito population. Firstly, increase the overall mosquito death that land on the nets. Secondly, repelling and possibly diverting mosquitoes to an

Chapter 6: Malaria transmission modeling with intervention scenario

animal blood host due to either insecticide irritation or the physical barrier of the net. Thirdly, lengthening the duration of the gonotrophic cycle leading to a reduced oviposition rate. Interested readers may also consult [52, 70] for further details.

The probability that a surviving mosquito succeeds in feeding during a single attempt is given by

$$W = 1 + \chi\phi(s - 1) \quad (6.5.10)$$

where ϕ is the proportion of people in bed when they are bitten and s is the probability of a mosquito feeding successfully on a person sleeping under a bednet.

The probability of a mosquito being repelled without feeding is thus

$$Q(\chi) = \phi\chi r. \quad (6.5.11)$$

where r is probability of a mosquito being repelled by a bednet. At χ LLIN coverage, the duration of a feeding cycle is given by $1/f(\chi) = \tau_1/(1 - Q) + \tau_2$ where τ_1 is the time spent searching for a blood meal and τ_2 is the time spent resting which is unaffected with intervention.

Thus, the probability of a mosquito surviving one feeding cycle is given by

$$\beta(\chi) = \left(\frac{\beta_1\beta_2W}{1 - Q\beta_1} \right)^{f(\chi)} \quad (6.5.12)$$

where $\beta_1 = e^{-\mu^{(0)\tau_1}$ and $\beta_2 = e^{-\mu^{(0)\tau_2}$ are the probability of a mosquito surviving the periods of feeding and resting. Note that the the probability $Q\beta_1 < 1$ sine $Q < 1$ and $\beta_1 < 1$.

The mosquitoes mortality which depend on bednets coverage is thus

$$\mu_v(\chi) = -\log \beta(\chi) \quad (6.5.13)$$

On introducing the use of LLINs, \mathcal{R}_0 becomes

$$\mathcal{R}_0(\chi) = \sqrt{\frac{(1 - V\chi)^2\epsilon^2b\beta(\chi)\sigma_a\rho}{\mu_v(\chi)(\beta(\chi) + \mu_v(\chi))(\eta + \rho + \mu)(\mu + \alpha_1)} + \frac{(1 - V\chi)^2\epsilon^2b\beta(\chi)\sigma_i\eta}{\mu_v(\chi)(\beta(\chi) + \mu_v(\chi))(\eta + \rho + \mu)(\mu + \delta + \alpha_2)}} \quad (6.5.14)$$

Chapter 6: Malaria transmission modeling with intervention scenario

We will now analyse the sensitivity index of \mathcal{R}_0 with respect to the parameters χ , V and ϵ according to the definition below.

Definition 6.1. *The sensitivity index of \mathcal{R}_0 with respect to a parameter p is given by*

$$\Gamma_{\mathcal{R}_0}^p = \frac{\partial \mathcal{R}_0}{\partial p} \frac{p}{\mathcal{R}_0}.$$

Rewriting Equation (6.5.14) as

$$\mathcal{R}_0(\chi) = C\epsilon(1 - V\chi)g(\chi), \quad (6.5.15)$$

where

$$C = \frac{b}{(\eta + \rho + \mu) \left[\frac{\sigma_a \rho}{\mu + \alpha_2} + \frac{\sigma_i \eta}{\mu + \delta + \alpha_1} \right]}$$

and

$$g(\chi) = \frac{\beta(\chi)}{\mu_v(\chi)(\beta(\chi) + \mu_v(\chi))}$$

and using the definition above, we have:

- The sensitivity index with respect to ϵ is

$$\Gamma_{\mathcal{R}_0}^\epsilon = \frac{\partial \mathcal{R}_0}{\partial \epsilon} \frac{\epsilon}{\mathcal{R}_0} = \frac{C\epsilon(1 - V\chi)g(\chi)}{\mathcal{R}_0} = 1.$$

This means that 10% increase (reductions) in ϵ would result in 10% increase (reductions) in \mathcal{R}_0 .

- The sensitivity index with respect to V is

$$\Gamma_{\mathcal{R}_0}^V = \frac{\partial \mathcal{R}_0}{\partial V} \frac{V}{\mathcal{R}_0} = -C\chi g(\chi) \frac{V}{C\epsilon(1 - V\chi)g(\chi)} = \frac{-V\chi}{C(1 - V\chi)}.$$

This means that 10% increase (reductions) in V would result in $\frac{10V\chi}{C(1 - V\chi)}$ % increase (reductions) in \mathcal{R}_0 .

Chapter 6: Malaria transmission modeling with intervention scenario

- The sensitivity index with respect to χ is

$$\begin{aligned}\Gamma_{\mathcal{R}_0}^\chi &= \frac{\partial \mathcal{R}_0}{\partial \chi} \frac{\chi}{\mathcal{R}_0} \\ &= (1 - V\chi)(g(\chi))' \frac{\chi}{C\epsilon(1 - V\chi)g(\chi)} \\ &= \frac{\chi(-Vg(\chi) + (1 - V\chi)(g(\chi))')}{C\epsilon(1 - V\chi)g(\chi)}.\end{aligned}$$

This means that 10% increase (reductions) in χ would result in $\frac{10\chi(-Vg(\chi) + (1 - V\chi)(g(\chi))')}{C\epsilon(1 - V\chi)g(\chi)}\%$ increase (reductions) in \mathcal{R}_0 .

It is to be noted that we have omitted the explicit expression of $g'(\chi)$ to avoid presenting long mathematical derivations.

Table 6.2: Intervention Parameters

Symbol	Description	Estimate	Ref
Ψ	Per ca-pita birth rate of mosquitoes	0.13	[23]
χ	LLIN coverage	Est from data	
f	Inverse of gonotrophic cycle	1/3 day ⁻¹	[51]
ϕ	Proportion of bites taken on humans when in bed	0.89	[51]
s	Probability that a mosquito feeds successfully by a bednet	0.03	[137]
r	Probability of a mosquito being repelled by a bednet	0.56	[52]
τ_1	Time spent seeking blood meal during gonotrophic cycle	0.69 days	[51]
τ_2	Time spent resting during gonotrophic cycle	2.31 days	[137]
β_1	Probability of a mosquito surviving the periods of feeding	0.91	[137]
β_2	the probability of a mosquito surviving the periods of resting	0.74	[137]
$V(t)$	The efficacy of LLIN	Equation (6.5.9)	[118]
$W(\chi)$	Probability of mosquito successfully feeding	Equation (6.5.10)	[52]
$Q(\chi)$	Probability of mosquito repeating	Equation (6.5.11)	[52]
$\beta(\chi)$	Daily survival probability	Equation (6.5.12)	[52]
$\mu_v(\chi)$	Daily mosquito mortality	Equation (6.5.13)	[52]

6.6 Results

The model fitting results are presented first before evaluating the predicted partial impact of the reduction-focused LLINs interventions. We simulate the model trajectory showing the population dynamics of humans expressed in susceptible, pre-infectious, clinical infectious, asymptomatic infectious, and in recovery compartments and vector population dynamics while simultaneously fitting the infectious class to data, using package fitR (version 0.1 [18]). The model does display some misfit due to missing values and the simplicity of the basic model. In Fig 8 model parameters estimated are b , ϵ_j , α_1 , and α_3 , again projected to five years of data after a run in order to reach a steady state, incorporating a seasonal model. We carried out a sensitivity analysis of different parameters: all parameters are fixed and one is left to hold different values (+/- 10%) so that its influence on the system behaviour can be assessed. We found that the disease transmission increases or decreases greatly with an increase or decrease in the contact rate to susceptible mosquito σ_i and the biting rate ϵ . We also observed that, a longer infection period $1/\alpha_1$ enhances disease transmission, which may lead to an increased contact rate to susceptible mosquitoes. To check the accuracy of our results, we ran the model using various sets of parameter values (independent chains) and tested whether individual distributions converge to the expected parameter value. Indeed, we found that the parameter sets converged to the posterior parameter values. Furthermore, on different occasions, the reproduction number, \mathcal{R}_0 is the parameter most sensitive to the biting rate. For instance, \mathcal{R}_0 reaches 15 when the bite rate is 117 per person per year but it is reduced to 6 when the bite rate is 34 per person per year, as obtained using Eq(6.4.8). This means that the prevalence of malaria will increase with an increase in the corresponding rate of mosquito bites and it will decrease with optimal mosquito control. The sensitivity index of \mathcal{R}_0 with respect to χ and V are simulated in Figures 6.9 and 6.10 respectively where the parameter values from Tables 6.1 and 6.2 were used.

The model's key parameters are estimated through data-fitting procedures and along with those presented in Tables 6.1 and 6.2 are used to project the disease. The model

Chapter 6: Malaria transmission modeling with intervention scenario

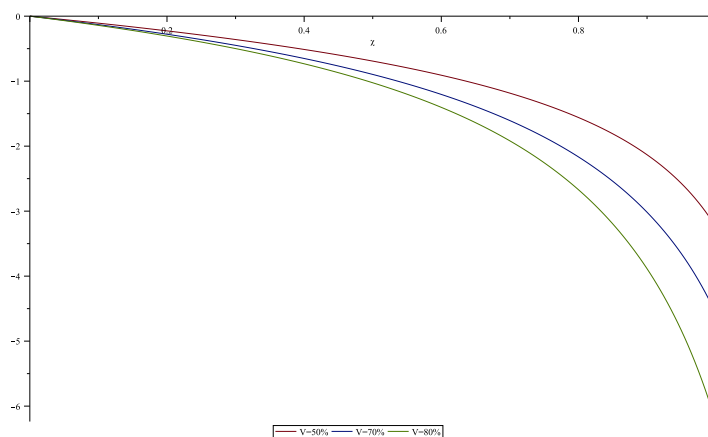


Figure 6.9: Sensitivity index of \mathcal{R}_0 with respect to χ for different values of V .

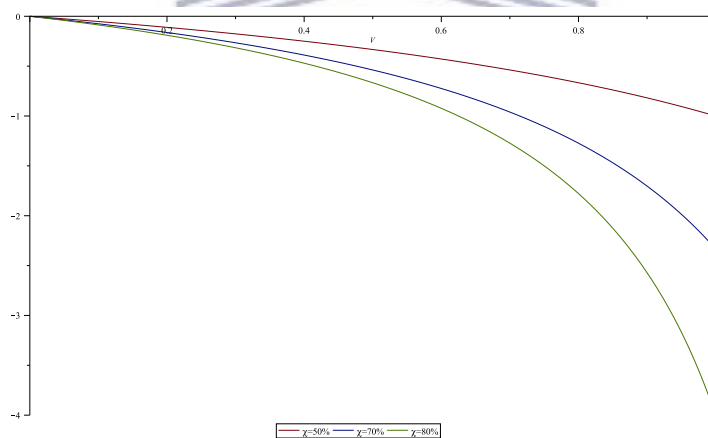


Figure 6.10: Sensitivity index of \mathcal{R}_0 with respect to V for different values of χ .

results were relatively robust to variations in the long lasting efficacy of LLINs which decrease the biting rate and increase the mosquito mortality rate. The predicted potential impact of the use of LLINs by humans as an intervention strategy for combatting malaria in the three study areas (different states in different regions) is illustrated in Figure 6.11. For instance, a slight change in LLINs coverage can drastically affect the lifespan and hence the patterns of mosquito bites.

We further derived and examined the basic reproduction number in relation to biting rate values and LLINs coverage from Eq(6.5.14) plotted in Figure 6.12. With the low transmission of a bites rate of two infectious bites per person per year, the proportion of

Chapter 6: Malaria transmission modeling with intervention scenario

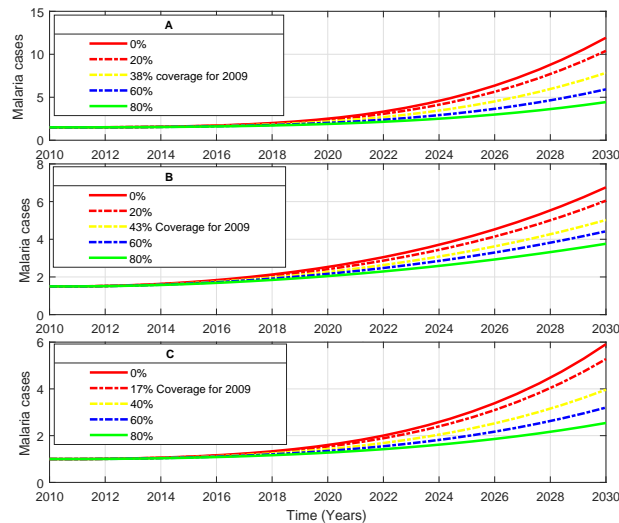


Figure 6.11: Projected cases of malaria in hundred thousands of people with: No interventions of LLINs, coverage based on 2009 LLINs distribution, and additional coverage of LLINs; (A) in Central Equatoria, (B) in Western Bahr-El-Ghazal and (C) in Warrap.

infections resulting in the reproduction number falls to less than one with the impact of intervention seemingly higher. But with more infectious bites per person per year LLINs coverage alone has less impact and may not succeed in reducing the reproduction number to less than one. Measuring the basic reproduction number can be difficult, but it can also be the most direct measurement for examining the effect of vector control interventions.

6.7 Conclusion

In this chapter, we presented a mathematical model in order to explore the impact of LLINs on malaria transmissions using a system of ordinary differential equations. The model analysis was based on a modification of a host-vector model presented by Filipe et al [40]. The Bayesian framework was incorporated to provide a posterior distribution of the parameters of the model given the malaria trial data. The threshold parameter, \mathcal{R}_0 , is the number of humans and mosquitoes expected to be infected with malaria by a single infected individual/mosquito introduced into a naive population. It was computed using the next generation matrix method. Owing to the reproduction number's sensitivity to

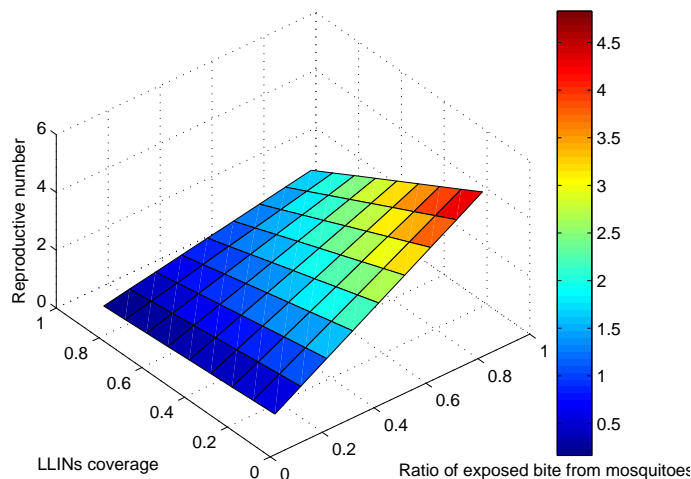


Figure 6.12: Reproduction number as a function of Mosquito bite rate and LLINs coverage, we observe that the optimum coverage window for falciparum malaria transmission is 80–90.

the mosquitoes biting rate, it is reasonable to recommend the use of LLINs as intervention strategy for malaria transmission. Therefore, we modelled the intervention to behave like a function comprised of three parameters: the proportion of LLIN coverage, the proportion of individuals exposed to mosquito bites, and the effectiveness of the bednets. Simulation results of \mathcal{R}_0 show that the use of bednets with long term effectiveness could reduce \mathcal{R}_0 to less than one in low transmission sites (at a bites rate of two infectious bites per person per year). In the absence of any intervention, we note a large number of \mathcal{R}_0 , confirming a substantial increase in incidence of malaria in the community. We cannot be sure whether the coverage of LLINs could eradicate malaria in an equivalent setting. Nevertheless, in low-transmission areas, LLINs have the ability to reduce malaria transmission to low levels, provided the interventions have high-use levels. Meanwhile, in moderate and high-transmission in these selected settings there was little change in the incidence levels. Thus, in these settings, novel tools and/or substantial social improvements might be required to achieve considerable reductions in malaria prevalence. Finally, the model is useful for further understanding future cases of malaria in South Sudan. This work shows that the

Chapter 6: Malaria transmission modeling with intervention scenario

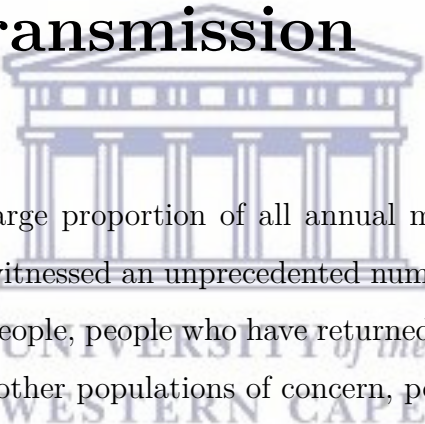
use of LLINs with long term effectiveness may reduce \mathcal{R}_0 and hence malaria transmission.



UNIVERSITY *of the*
WESTERN CAPE

Chapter 7

Assessing the role of human mobility on malaria transmission



South Sudan accounts for a large proportion of all annual malaria cases in Africa. In recent years, the country has witnessed an unprecedented number of people on the move, refugees, internally displaced people, people who have returned to their countries or areas of origin, stateless people and other populations of concern, posing challenges to malaria control. Thus, one can claim that human mobility is one of the contributing factors to the resurgence of malaria. The aim of this chapter is to assess the impact of human mobility on the burden of malaria disease in South Sudan. For this, we formulate an SIR-type model that describes the transmission dynamics of malaria disease between multiple patches. The proposed model is a system of stochastic differential equations consisting of ordinary differential equations perturbed by a stochastic Wiener process. For the deterministic part of the model, we calculate the basic reproduction number. Concerning the whole stochastic model, we use the maximum likelihood approach to fit the number of malaria cases to weekly malaria data of 2011 from Central Equatoria State, Western Bahr El Ghazal State and Warrap State. Using the parameters estimated on the fitted model, we simulate the future observation of the disease pattern. The disease was found to persist in the low transmission areas when there is human inflow in these patches and although the intervention coverage reaches 77%.

7.1 Introduction

Malaria is a vector-borne disease that causes a lot of distress to people on a global scale. In spite of recent achievements in the fight against malaria, which has led to a significant reduction in the burden, the disease still counts amongst the top ten deadly diseases in the world with an estimate of 400 000 deaths each year [140].

Malaria is transmitted more robustly and incessantly in Africa than it is elsewhere. Further constraints regarding malaria dynamics complexity, are the recurring outbreaks of conflicts on the continent which contribute to a large number of people's displacement and migration, increasing their vulnerability to infectious diseases [44, 56].

In this study we focus mainly on South Sudan, the youngest country in Africa which has just emerged from two decades of civil war and sporadic violence. This has steered to a deteriorating socioeconomic situation, collapsed health systems and disruption of disease control programs. For instance, in the rural areas, the disease exerts an enormous toll due to poor health services and lack of sufficient transport whereby people travel long hours to reach the nearest health facility. The political unrest has further led to substantial population mobility including mass population displacements [44]. There are an estimated 1.61 million Internally Displaced People (IDPs), and over 975,801 refugees in neighboring countries [120]. It was reported that in 2013 almost all states were affected directly or indirectly by conflict-induced displacement, as shown in Figure 7.1. The fluidity of displacement in the country makes it difficult for health care providers to reach all conflict-affected populations. Moreover, the displaced people are associated with poor-quality housing that makes them more vulnerable to mosquito bites and thus increases the risk factor for malaria. If displaced people are not immunized, they may move to malarious regions and acquire the infection, and if they are infectious, they may disseminate the infection to other areas. Consequently, vector-borne diseases in particular malaria, across many areas of the country have worsened. With this backdrop, it is more difficult to comprehend how the epidemic is circulating among the population.

Mathematical models for malaria transmission can help better understand the oc-

Chapter 7: Quantifying the impact of human movement on malaria transmission

currence of the disease in the community and investigate how certain factors such as migrations affect the course of the epidemic. In this regards, several mathematical models have been developed by researchers starting from the basic malaria model of Ross [110] and Macdonald [74] to more complex models considering different factors relating to malaria transmission dynamics and control [3, 33, 40, 41, 52, 56, 76, 79, 80, 86, 113, 135].

In a review article, Cosner et al.[28] explored optimal disease control in spatial environment using models that account human mobility between patches. In a recent study, Cosner et al. [27] showed, using empirical data combined with mathematical analyses, a significant effect of host and vector movement patterns on the disease burden. Kim et al. [68] pointed up the importance of border screening in the presence of human migration in Africa during an outbreak. Acevedo et al.[2] explored analytically and via numerical simulations how human mobility and spatial variation in transmission influence malaria long-term persistence determined by the basic reproduction number R_0 , and prevalence. They show that movement can reduce heterogeneity in exposure to mosquito biting. When

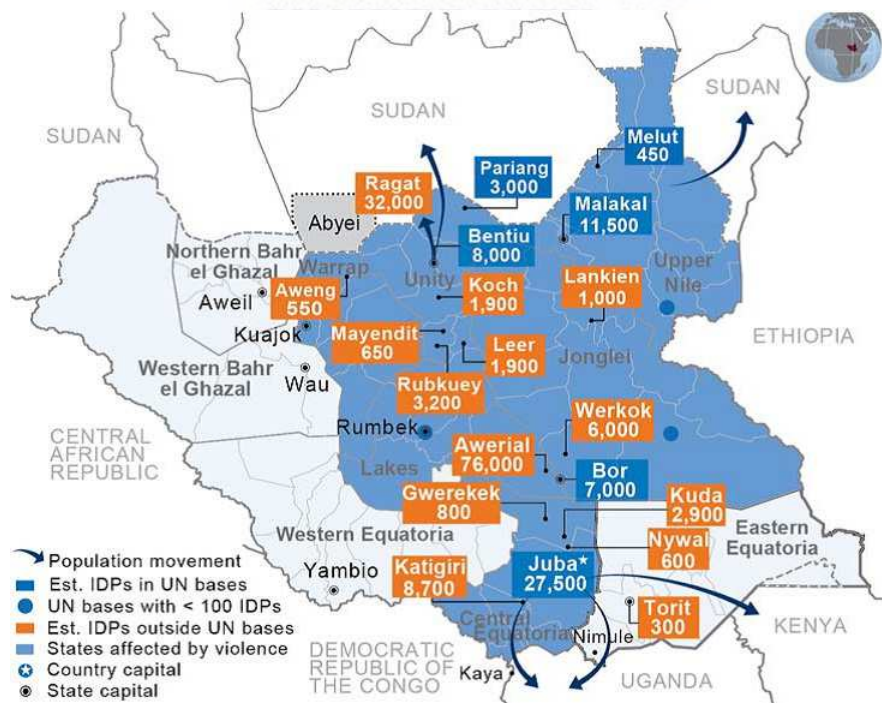


Figure 7.1: Source: [120], IDPs camp and movement patterns

Chapter 7: Quantifying the impact of human movement on malaria transmission

local transmission rates are highly heterogeneous, R_0 declines asymptotically as human mobility increases.

Using a two-patch model, Gao and Ruan [43] demonstrated that human movement can aid malaria to turn from disease-free to endemic equilibria in both patches, even though malaria could be eradicated in each patch when isolated. They concluded that decreased mobility can lead to a disease-free equilibrium point.

Malaria occurrence may be accentuated critically by factors such as environmental change, socioeconomic situation, and human mobility. For this reason, improving our perception of host-parasite interactions that attests to the seriousness of these factors is crucial. In our previous study [84], we focused on understanding the significant role that temperature and rainfall play in the dynamics of the mosquito populations in the study of malaria transmission in South Sudan. More precisely the study helps understand the course of malaria epidemic in two different climatic regions experiencing climate change, also gain insight into the abundance of mosquitoes with changes in rainfall and temperature patterns within the region that alter the volatility of malaria cases throughout the year. Consequently, the study proposed and analyzed a human-mosquito disease-based model that includes temperature and rainfall on the mosquito component. The results reflect that disease is more effective and severe in the tropical region than in a hot semi-arid region of South Sudan. Note this study focused more on mosquito population and how this is impacted by climate factor. This explain why asymptomatic infection class for human was not included in the study.

In a different study [85], the focus of the study shifted to humans where intervention variables were incorporated to contract the spread of malaria. Thus we added the asymptomatic malarial infections compartment in this case. In both of the above-mentioned works, human mobility is not taken into consideration in the transmission of malaria. Hence, this study seeks to assess whether human mobility may have an impact on the malaria epidemic in South Sudan. The model generalizes the mosquito biting rate for each patch so that it applies to wider ranges of populations. We consider that the total number of mosquito bites on humans depends only on the number of mosquitoes, similar

to that model of [85, 91].

The deterministic modeling based on ordinary differential equations (ODEs) is the most widely used approach. However, such systems are often subject to random influences (such as people's mobility) that are not fully understood or difficult to model explicitly. To accommodate such randomness, we extend a classical deterministic SIR-type epidemic model with migration flows by adding a stochastic noise term in the form of a Wiener process to the model's deterministic equations. The resulting model consists of a system of stochastic differential equations (SDEs) comprising of deterministic terms which are perturbed by a stochastic noise. To estimate the model's parameter we use maximum likelihood to fit it to weekly malaria data of 2011 from Central Equatoria State, Western Bahr El Ghazal State and Warrap State.

7.2 Model formulation

In this section, we begin with the formulation of a deterministic metapopulation malaria epidemic model which we further extend by adding a white noise perturbation. The deterministic part of the model is based on the SEIAR-SEI model of [85], in which we incorporate human migration factors similar to that considered [68]. The human components in the model are utilized to capture disease dynamics and population's movement. Conflicts force individual irrespective of their health status to flee to safer zones. For the purpose of our study, the migration factors considered in our model formulation account for movement of people between n different states. We assume that disease transmission conditions are homogeneous within each of these regions. Subsequently, we divide the human population in each patch i , N_i (with $i = 1, \dots, n$) into susceptible individuals S_i , pre-infectious individuals with malaria parasite E_i , individuals with malaria symptoms I_i , asymptomatic infectious individuals A_i and recovered individuals R_i , so that

$$N_i(t) = S_i(t) + E_i(t) + I_i(t) + A_i(t) + R_i(t).$$

Accordingly, we assume that individuals of all disease classes are subject to migration flows between patches. Although some individuals, during their travel, may change their

Chapter 7: Quantifying the impact of human movement on malaria transmission

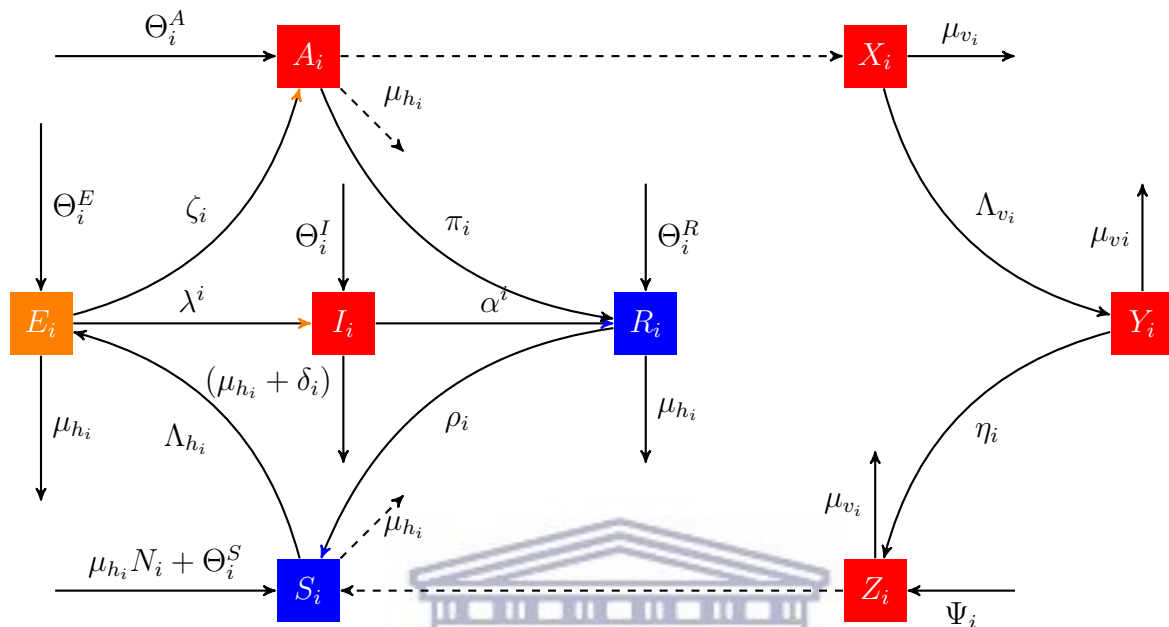


Figure 7.2: Model flow diagram for human and mosquito populations in State i , where $\Theta_i^Q = \sum_{j \neq i=1}^n \psi_{j,i}^Q Q_j - \sum_{j \neq i=1}^n \psi_{i,j}^Q Q_i$, with $Q = S, E, A, R$ and I .



disease status (for instance from susceptible to latently infected or symptomatic disease), we assume, for simplicity, that individuals keep their disease status as they move between patches. Subsequently, for each disease state $Q = S, E, I, A, R$, individuals are assumed to immigrate from patch j to patch i at rate $\psi_{i,j}^Q$ without changing their states. The disease transmission dynamics and population's migration are considered to have both deterministic and stochastic components that operate simultaneously. This provides an additional degree of realism compared to deterministic models. In order to account for stochasticity, we introduce white noise stochastic perturbations onto deterministic model, and formulate the necessary assumptions hitherto. Additionally, the mosquito components in the model are represented to capture the effects of vector control in preventing transmission. We consider *Anopheles Gambiae* mosquitoes which are the main anopheles species that transmit *Plasmodium Falciparum* in South Sudan. The total mosquito population M_i is divided into susceptible mosquitoes X_i , mosquitoes exposed to the malaria

Chapter 7: Quantifying the impact of human movement on malaria transmission

parasite Y_i , and infectious mosquitoes Z_i , that is

$$M_i(t) = X_i(t) + Y_i(t) + Z_i(t).$$

Hence we propose the following system of stochastic differential equations:

$$\left\{ \begin{array}{l} dS_i = \left[\Gamma_i - \Lambda_{h_i} S_i - \mu_{h_i} S_i + \rho_i R_i + \sum_{j \neq i=1}^n \psi_{j,i}^S S_j - \sum_{j \neq i=1}^n \psi_{i,j}^S S_i \right] dt + \sigma_1 S_i dW_1(t) \\ dE_i = \left[\Lambda_{h_i} S_i - (\lambda_i + \zeta_i + \mu_{h_i}) E_i + \sum_{j \neq i=1}^n \psi_{j,i}^E E_j - \sum_{j \neq i=1}^n \psi_{i,j}^E E_i \right] dt + \sigma_2 E_i dW_2(t) \\ dI_i = \left[\lambda_i E_i - (\alpha_i + \delta_i + \mu_{h_i}) I_i + \sum_{j \neq i=1}^n \psi_{j,i}^I I_j - \sum_{j \neq i=1}^n \psi_{i,j}^I I_i \right] dt + \sigma_3 I_i dW_3(t) \\ dA_i = \left[\zeta_i E_i - (\pi_i + \mu_{h_i}) A_i + \sum_{j \neq i=1}^n \psi_{j,i}^A A_j - \sum_{j \neq i=1}^n \psi_{i,j}^A A_i \right] dt + \sigma_4 A_i dW_4(t) \\ dR_i = \left[\alpha_i I_i + \pi_i A_i - (\rho_i + \mu_{h_i}) R_i + \sum_{j \neq i=1}^n \psi_{j,i}^R R_j - \sum_{j \neq i=1}^n \psi_{i,j}^R R_i \right] dt + \sigma_5 R_i dW_5(t) \\ dX_i = [\Psi_i - \Lambda_{v_i} X_i - \mu_{v_i} X_i] dt \\ dY_i = [\Lambda_{v_i} X_i - (\eta_i + \mu_{v_i}) Y_i] dt \\ dZ_i = [\eta_i Y_i - \mu_{v_i} Z_i] dt \end{array} \right. \quad (7.2.1)$$

where

- $\Lambda_{h_i}(Z_i, N_i) = \frac{\epsilon_i b Z_i}{N_i}$, represents the force of infection on humans defined as the product of the average number of bites given to susceptible humans by each mosquito per unit time, $\epsilon_i S_h M_i / N_i$ to be measured at study settings level i , the probability that an infected mosquito bite on a susceptible human to transmit the infection to humans, b_i , the proportion of the total number of bites that are potentially infectious to humans Z_i / M_i .
- $\Lambda_{v_i}(A_i, I_i, N_i) = \frac{\epsilon_i (\kappa_i A_i + \nu_i I_i)}{N_i}$, represents the force of infection on mosquitoes which is defined similarly as on humans, assuming that the reservoir of possible infections from humans includes ν_i and κ_i defined as the probability that a susceptible mosquitoes bite on an infected human to transfer the infection to the mosquito from

Chapter 7: Quantifying the impact of human movement on malaria transmission

Table 7.1: Model Variables

Symbols	Description
S_i	Susceptible individuals
E_i	Pre-infectious individuals with malaria parasite
I_i	Individuals with malaria symptoms
A_i	Asymptomatic infectious individuals
R_i	Recover individuals
X_i	Susceptible mosquitoes
Y_i	Mosquitoes exposed to the malaria parasite
Z_i	Infectious mosquitoes

a clinical infectious and an asymptomatic infectious human respectively, excluding a recovery stage to be releasing merozoites into the bloodstream.

The recruitment rate of susceptible s into the population in patch i is given by Γ_i . We assume that transmission occurs solely between individuals and mosquitoes from the same state; subsequently susceptible individuals (S_i) in patch i acquire malaria and become pre-infectious and move to class E_i at a rate Λ_h when they are bitten by infectious mosquitoes from the same patch i . Thereafter, individuals either develop clinical infection and progress to the infectious compartment I_i with probability λ_h or individuals turn asymptomatic at a probability ζ_i , and enter compartment A_i . Those that develop disease are successfully treated at rate α_i^i and subsequently enter a period of prophylaxis (recovery compartment R_i). The disease-induced mortality rate is denoted by δ_i . Individuals with asymptomatic infection are assumed to recover naturally with a constant per capita recovery rate π_i and enter R_i compartment. We assume that recovered individuals move to the susceptible compartment at rate ρ_i , when they are immunized. Super-infection is possible to occur from the asymptomatic infection. All compartments are stratified in patch i by level at which people are bitten by mosquitoes and also drop individuals at a

Chapter 7: Quantifying the impact of human movement on malaria transmission

natural death rate of $\mu_{h_i} = \frac{1}{q \times 360} \text{day}^{-1}$ where q is the human life expectancy in years. Susceptible female mosquitoes in patch i are recruited at the birth rate Ψ_i . We assume

Table 7.2: Model parameters

Symbols	Description
Γ	Per ca-pita birth rate of Humans. Humans/Day ⁻¹
ψ	Immigration rate of humans. Day ⁻¹
μ_h	Natural mortality rate of humans. Day ⁻¹
δ	Mortality rate of humans due to malaria. Day ⁻¹
ϵ	The average number of bites given to humans by each mosquito per unit time.
b	Probability of transmitting malaria to susceptible humans from an infectious mosquito provided that contact occurs between the two.
ν	Probability of transmitting malaria to susceptible mosquitoes from a clinical infectious human-provided that contact occurs between the two.
κ	Probability of transmitting malaria to susceptible mosquitoes from an asymptomatic infectious human-provided that contact occurs between the two.
λ	Progression rate of humans from pre-infectious state to a clinical infectious state, that is the reciprocal of the duration of the latent period. Day ⁻¹
ζ	Progression rate of humans from pre-infectious state to asymptomatic infectious state, that is the reciprocal of the duration of the patent infection. Day ⁻¹
α	Per ca-pita recovery rate for humans from clinical infectious state to the recovered state, that is the reciprocal duration of the infectious period. Day ⁻¹
π	Per ca-pita recovery rate for humans from asymptomatic infectious state to the recovered state, that is the reciprocal duration of the sub-patent infection period. Day ⁻¹
ρ	Per ca-pita rate of loss of immunity, that is the reciprocal duration of the immune (Prophylaxis following treatment) period. Day ⁻¹
η	Progression rate of mosquitoes from pre-infectious state to infectious state.
μ_v	Daily mosquito mortality.
Ψ	Per ca-pita birth rate of mosquitoes.

that reduction in the susceptible mosquitoes occurs through natural death at rate μ_{v_i} , or through infection at rate Λ_v . At this rate Λ_v susceptible mosquitoes move to the pre-infectious class Y_i (pass through a latent period of fixed length) from the same patch i . Latently infected mosquitoes move at rate η_i to infectious mosquitoes class and remain in that class until they die at rate μ_{v_i} . We note here that we made all mosquito parameters depend on the patch they live in to reflect dependency on some internal factors such as temperature and rainfall.

7.3 Model well-posedness

Since it is a population system, it is important that we do not obtain negative values. In order to find conditions of existence of unique positive global solution of the stochastic epidemic model, we use the method of Lyapunov functions. Let $(\Omega, \mathcal{F}, \{\mathcal{F}_t\}_{t \geq t_0}, P)$ be a probability space which is right continuous with a filtration $\{\mathcal{F}_t\}_{t \geq t_0}$. Let $C^{2,1}(\mathbb{R}^5 \times [0, \infty); \mathbb{R}_+)$ be the family of all nonnegative functions $V(x, t)$ defined on $\mathbb{R}^5 \times [0, \infty)$ which are continuously twice differentiable in x and once in t . Let $W(t) = (W_1(t), W_2(t), W_3(t), W_4(t), W_5(t))$ a 5-dimensional Wiener process defined on this probability space. The non-negative constants $\sigma_1, \sigma_2, \sigma_3, \sigma_4$ and σ_5 denote the intensities of the stochastic perturbations. We shall assume that the components of the 1-dimensional Wiener process W_i are mutually independent. It is important to show that the SDE model (7.2.1) has at least a unique global solution in order for the model to have meaning and also that the solution will remain positive whenever the initial conditions are positive. Thus, the following theorem:

Theorem 1. *For model (7.2.1) and any initial value in \mathbb{R}_+^{8n} , there is a unique solution $L = (S_i(t), E_i(t), I_i(t), A_i(t), R_i(t), X_i(t), Y_i(t), Z_i(t))_{i=1, \dots, n}$, of the system (7.2.1) for $t \geq 0$ which will remain in \mathbb{R}_+^{8n} with probability one.*

Proof. The total human population in system (7.2.1) verifies the equation (7.3.2), if $(S_i(s), E_i(s), I_i(s), A_i(s), R_i(s))_{i=1, \dots, n} \in \mathbb{R}_+^{5n}$ for all $0 \leq s \leq t$ almost surely (a.s)

$$dN_i(t) < [\Gamma_i - \varphi N_i] a.s \tag{7.3.2}$$

Chapter 7: Quantifying the impact of human movement on malaria transmission

where

$$\begin{cases} \Gamma_i = \sum_{j \neq i=1}^n \psi_{i,j}^Q N_j + \Gamma_i \text{ for } Q = S, R \text{ and } j = 1, \dots, n, j \neq i \\ \varphi = \mu_{h_i} + \sum_{j \neq i=1}^n \psi_{i,j}^Q. \end{cases}$$

Hence, by integration we check

$$N_i(s) < \frac{\Gamma_i}{\varphi} + (N_0 - \frac{\Gamma_i}{\varphi}) \exp(-\varphi s) \text{ for all } s \in [0, t] \text{ a.s.}$$

Then

$$N(s) < \frac{\Gamma_i}{\varphi}, \text{ so}$$

$$(S_i(s), E_i(s), I_i(s), A_i(s), R_i(s),)_{i=1, \dots, n} \in (0, \frac{\Gamma_i}{\varphi}) \text{ for all } s \in [0, t] \text{ a.s.} \quad (7.3.3)$$

Note that the coefficients of the system (7.2.1) are locally Lipschitz continuous, for any given initial value, there is a unique maximal local solution

$(S_i(t), E_i(t), I_i(t), A_i(t), R_i(t), X_i(t), Y_i(t), Z_i(t))_{i=1, \dots, n}$ on $t \in [0, \tau_e)$, where τ_e is the explosion time (see e.g., [7, 46]).

To show this solution is global, we need to show that $\tau_e = \infty$ almost surely (a.s.).

Let $m_0 > 0$ such that $(S_i(0), E_i(0), I_i(0), A_i(0), R_i(0), X_i(0), Y_i(0), Z_i(0))_{i=1, \dots, n} \in [\frac{1}{m_0}, m_0]$.

For each integer $m \geq m_0$, define a sequence of stopping times by

$$\tau_m = \inf \left\{ t \in [0, \tau_e) : S(t), E(t), I(t), A(t), R(t), X(t), Y(t) \text{ or } Z(t) \notin \left(\frac{1}{m}, m \right) \right\}$$

where we set $\inf \emptyset = \infty$. Now since τ_m is nondecreasing, the following limit exists: $\tau_\infty = \lim_{m \rightarrow \infty} \tau_m$, and $\tau_\infty \leq \tau_e$ (a.s.). We need to show that $\tau_\infty = \infty$ a.s.

If this statement is violated, then there exists $T > 0$ and $\epsilon \in (0, 1)$ such that

$$\mathbb{P}\{\tau_\infty \leq T\} > \epsilon. \quad (7.3.4)$$

Thus, there is an integer $m_1 \geq m_0$ such that

$$\mathbb{P}\{\tau_m \leq T\} \geq \epsilon, \text{ for all } m \geq m_1.$$

Define a C^2 -function $V : \mathbb{R}_+^{8n} \rightarrow \mathbb{R}_+$ by

$$\begin{aligned} V(L) = & \sum_{i=1}^n \left[(S_i - 1 - \ln S_i) + (E_i - 1 - \ln E_i) + (I_i - 1 - \ln I_i) + (A_i - 1 - \ln A_i) \right. \\ & \left. + (R_i - 1 - \ln R_i) + (X_i - 1 - \ln X_i) + (Y_i - 1 - \ln Y_i) + (Z_i - 1 - \ln Z_i) \right] \end{aligned} \quad (7.3.5)$$

Chapter 7: Quantifying the impact of human movement on malaria transmission

By applying Itô's formula we get,

$$dV(L) = \sum_{i=1}^n \left[\left(1 - \frac{1}{S_i}\right) dS_i + \frac{1}{2S_i^2} dS_i dS_i + \left(1 - \frac{1}{E_i}\right) dE_i + \frac{1}{2E_i^2} dE_i dE_i \right. \\ \left. + \left(1 - \frac{1}{I_i}\right) dI_i + \frac{1}{2I_i^2} dI_i dI_i + \left(1 - \frac{1}{A_i}\right) dA_i + \frac{1}{2A_i^2} dA_i dA_i \right. \\ \left. + \left(1 - \frac{1}{R_i}\right) dR_i + \frac{1}{2R_i^2} dR_i dR_i + \left(1 - \frac{1}{X_i}\right) dX_i + \frac{1}{2X_i^2} dX_i dX_i \right. \\ \left. + \left(1 - \frac{1}{Y_i}\right) dY_i + \frac{1}{2Y_i^2} dY_i dY_i + \left(1 - \frac{1}{Z_i}\right) dZ_i + \frac{1}{2Z_i^2} dZ_i dZ_i, \right]$$

and using (7.2.1) we obtain

$$dV(L) = \mathcal{L}V dt + \left(1 - \frac{1}{S_i}\right) \sigma_1 S_i dW_1(t) + \left(1 - \frac{1}{E_i}\right) \sigma_2 E_i dW_2(t) + \left(1 - \frac{1}{I_i}\right) \sigma_3 I_i dW_3(t) \\ + \left(1 - \frac{1}{A_i}\right) \sigma_4 A_i dW_4(t) + \left(1 - \frac{1}{R_i}\right) \sigma_5 R_i dW_5(t)$$

where

$$\mathcal{L}V = \sum_{i=1}^n \epsilon_i b_i Z_i N_i - \epsilon_i b_i S_i Z_i N_i E_i + \mu_{h_i} N_i + \zeta_i + \lambda_i + \rho_i + \alpha_i + \delta_i + \pi_i \\ + \sum_{i=1}^n \epsilon_i \kappa_i A_i N_i - \epsilon_i \kappa_i A_i X_i N_i Y_i - \frac{\rho_i R_i}{S_i} - \frac{\pi_i A_i}{R_i} - \frac{\alpha_i I_i}{R_i} - \frac{\mu_{h_i} N_i}{S_i} \\ + \sum_{i=1}^n \epsilon_i \nu_i I_i N_i - \epsilon_i \nu_i I_i X_i N_i Y_i - \frac{\Psi_i}{X_i} - \frac{\eta_i Y_i}{Z_i} - \frac{\lambda_i E_i}{I_i} - \frac{\zeta_i E_i}{A_i} \\ + \sum_{i=1}^n 5\mu_{h_i} + \Psi_i + \eta_i + 3\mu_{v_i} - \mu_{v_i} X_i - \mu_{v_i} Y_i - \mu_{v_i} Z_i \\ + \frac{1}{2} (\sigma_1^2 + \sigma_2^2 + \sigma_3^2 + \sigma_4^2 + \sigma_5^2)$$

By (7.3.3) we assert that $(S_i(s), E_i(s), I_i(s), A_i(s), R_i(s))_{i=1, \dots, n} \in (0, \frac{\Gamma_i}{\varphi})$ for all $s \in [0, t \wedge \tau_m]$ a.s. Hence $\sum_{i=1}^n \epsilon_i b Z_i N_i < \frac{\Gamma_i}{\varphi}$, $\sum_{i=1}^n \epsilon_i \kappa_i A_i N_i < \frac{\Gamma_i}{\varphi}$ and $\sum_{i=1}^n \epsilon_i \kappa_i I_i N_i < \frac{\Gamma_i}{\varphi}$, therefore

$$\mathcal{L}V \leq \mu_{h_i} N_i + \zeta_i + \lambda_i + \rho_i + \alpha_i + \delta_i + \pi_i + 5\mu_{h_i} + \Psi_i + \eta_i + 3\mu_{v_i} + \frac{1}{2} (\sigma_1^2 + \sigma_2^2 + \sigma_3^2 + \sigma_4^2 + \sigma_5^2) =: D$$

Denote by $\xi = \min(\tau_m, T)$, then

$$\int_0^\xi dV(S_i(s), E_i(s), I_i(s), R_i(s), A_i(s), X_i(s), Y_i(s)) \leq \int_0^\xi D ds + H(\xi), \quad (7.3.6)$$

where

$$H(s) = \int_0^s (S(u) - 1) \sigma_1 dW_1(u) + \int_0^s (E(u) - 1) \sigma_2 dW_2(u) + \int_0^s (I(u) - 1) \sigma_3 dW_3(u) \\ + \int_0^s (A(u) - 1) \sigma_4 dW_4(u) + \int_0^s (R(u) - 1) \sigma_5 dW_5(u). \quad (7.3.7)$$

Taking expectation, yields

$$\mathbb{E}[V(S_i(\xi), E_i(\xi), I_i(\xi), A_i(\xi), R_i(\xi), X_i(\xi), Y_i(\xi), Z_i(\xi))] \\ \leq V(S_i(0), E_i(0), I_i(0), A_i(0), R_i(0), X_i(s), Y_i(s)) + \mathbb{E} \int_0^\xi D ds \\ \leq V(S_i(0), E_i(0), I_i(0), A_i(0), R_i(0), X_i(s), Y_i(s)) + DT.$$

Chapter 7: Quantifying the impact of human movement on malaria transmission

Set $\Omega_m = \{\omega \in \Omega : \tau_m(\omega) < T\}$ for each $m \geq m_1$ and from equation set, we have $\mathbb{P}(\Omega_m) \geq \epsilon$. Note that for every $\nu \in \Omega_m$, we get

$$\{S_i(\tau_m, \nu), E_i(\tau_m, \nu), I_i(\tau_m, \nu), A_i(\tau_m, \nu), R_i(\tau_m, \nu)\} \cap [m, \frac{1}{m}] \neq \emptyset.$$

Consequently,

$$V\left((S_i(\xi), E_i(\xi), I_i(\xi), A_i(\xi), R_i(\xi))_{i=1, \dots, n}\right) \geq U_m$$

where

$$U_m = \min_{u \in \{1, a_0\}} \left\{ m - u - u \ln \frac{m}{u}, \frac{1}{m} - u - u \ln \frac{1}{um} \right\}.$$

Then we obtain

$$\begin{aligned} & V\left((S_i(0), E_i(0), I_i(0), A_i(0), R_i(0), X_i(s), Y_i(s))_{i=1, \dots, n}\right) + DT \\ & \geq \mathbb{E}(1_{\Omega_m} V\left((S_i(\xi), E_i(\xi), I_i(\xi), A_i(\xi), R_i(\xi))_{i=1, \dots, n}\right)) \geq \epsilon U_m. \end{aligned}$$

Letting $m \rightarrow \infty$ leads to the contradiction $\infty = V\left((S_i(0), E_i(0), I_i(0), A_i(0), R_i(0))_{i=1, \dots, n}\right) + DT < \infty$. Thus, as $\tau_m \geq \tau_\infty$, then $\tau_m = \tau_\infty = \infty$ a.s. This completes the proof. \square

7.4 Basic Reproductive Number

The basic reproduction number, denoted by \mathcal{R}_0 , is defined as the average number of secondary infections that occur when one infective is introduced into a completely susceptible host population (see [131] for instance).

To evaluate \mathcal{R}_0 , we need to determine the model's disease free equilibrium points which are given by the solutions of the following system

$$\begin{cases} \Gamma_i - (\mu_{h_i} + \sum_{j \neq i=1}^n \psi_{i,j}^S) S_i + \sum_{j \neq i=1}^n \psi_{j,i}^S S_j = 0, \\ -(\rho_i + \mu_{h_i}) R_i + \sum_{j \neq i=1}^n \psi_{j,i}^R R_j - \left(\sum_{j \neq i=1}^n \psi_{i,j}^R\right) R_i = 0, \\ \Psi_i - \mu_{v_i} X_i = 0, \end{cases}$$

We obtain $X_i = \frac{\Psi_i}{\mu_{v_i}}$, and

$$\begin{cases} \sum_{j=1}^n \varphi_{i,j}^S S_j = \Gamma_i \\ \sum_{j=1}^n \varphi_{i,j}^R R_j = 0, \end{cases} \quad (7.4.8)$$

Chapter 7: Quantifying the impact of human movement on malaria transmission

where

$$\begin{cases} \varphi_{i,j}^Q = -\psi_{i,j}^Q \text{ for } Q = S, R \text{ and } j = 1, \dots, n, j \neq i \\ \varphi_{i,j}^S = \mu_{h_i} + \sum_{j \neq i=1}^n \psi_{i,j}^S \text{ and } \varphi_{i,j}^R = \rho_i + \mu_{h_i} + \sum_{j \neq i=1}^n \psi_{i,j}^R \text{ for } j = i. \end{cases}$$

Using matricial form, equation (7.4.8) reads as

$$\begin{cases} \varphi^S S = \Gamma \\ \varphi^R R = 0 \end{cases} \quad (7.4.9)$$

where $\varphi^Q = (\varphi_{i,j}^Q)_{1 \leq i,j \leq 1}$, $S = (S_1, \dots, S_n)^\top$, $R = (R_1, \dots, R_n)^\top$ and $\Gamma = (\Gamma_1, \dots, \Gamma_n)^\top$.

It can be shown that the matrix φ^Q is an invertible Z-matrix whose off-diagonal entries are nonzero implying that system (7.4.9) has a unique solution $R = 0$ and $S = S^0 = (\varphi^S)^{-1} \Gamma$.

Thus, model (7.2.1) has a unique disease free equilibrium point

$$\mathcal{E}_0 = \left((S_i^0)_{i=1, \dots, n}, \mathbf{0}, \mathbf{0}, \mathbf{0}, \mathbf{0}, (X_i^0)_{i=1, \dots, n}, \mathbf{0}, \mathbf{0} \right)$$

where $\mathbf{0} = (n \times 0, \dots, 0)$, $(X_i^0)_{i=1, \dots, n} = \left(\frac{\Psi_i}{\mu_{v_i}} \right)_{i=1, \dots, n}$ and $(S_i^0)_{i=1, \dots, n} = (\varphi^S)^{-1} \Gamma$.

We are now in a position to compute \mathcal{R}_0 for the deterministic counterpart of the stochastic model (7.2.1) by following the approach of Van den Driessche and Watmough [131]. The model's diseased compartments are E_i, I_i, A_i, Y_i and Z_i .

First we rewrite the equations for the model's infected classes

$$(E_1, \dots, E_n, I_1, \dots, I_n, A_1, \dots, A_n, Y_1, \dots, Y_n, Z_1, \dots, Z_n)$$

as

$$\begin{cases} dE_i dt = \Lambda_{h_i} S_i - \sum_{j=1}^n \varphi_{i,j}^E E_j \\ dI_i dt = \lambda_i E_i - \sum_{j=1}^n \varphi_{i,j}^I I_j \\ dA_i dt = \zeta_i E_i - \sum_{j=1}^n \varphi_{i,j}^A A_j \\ dY_i dt = \lambda_{v_i} X_i - (\eta_i + \mu_{v_i}) Y_i \\ dZ_i dt = \eta_i Y_i - \mu_{v_i} Z_i \end{cases}$$

Chapter 7: Quantifying the impact of human movement on malaria transmission

where

$$\begin{cases} \varphi_{i,j}^Q = -\psi_{i,j}^Q \text{ for } Q = E, I \text{ or } A \text{ and } j = 1, \dots, n, j \neq i \\ \varphi_{i,i}^E = \lambda_i + \zeta_i + \mu_{h_i} + \sum_{j \neq i=1}^n \psi_{i,j}^E, \\ \varphi_{i,i}^I = \alpha_i + \delta_i + \mu_{h_i} + \sum_{j \neq i=1}^n \psi_{i,j}^I, \\ \varphi_{i,i}^A = \pi_i + \mu_{h_i} + \sum_{j \neq i=1}^n \psi_{i,j}^A \end{cases}$$

With these notations the vector of the rates of new infections and the vector of the rates of other transfers between disease states are respectively given by

$$\mathcal{F}(x) = \begin{bmatrix} [\epsilon_i b_i Z_i S_i S_i + E_i + I_i + A_i + R_i]_{i=1, \dots, n} \\ 0_n \\ 0_n \\ [\epsilon_i \kappa_i A_i X_i + \epsilon_i \nu_i I_i X_i S_i + E_i + I_i + A_i + R_i]_{i=1, \dots, n} \\ 0_n \end{bmatrix}$$

, and

$$\mathcal{V}(x) = \begin{bmatrix} [\sum_{j=1}^n \varphi_{i,j}^E E_j]_{i=1, \dots, n} \\ [-\lambda_i E_i + \sum_{j=1}^n \varphi_{i,j}^I I_j]_{i=1, \dots, n} \\ [-\zeta_i E_i + \sum_{j=1}^n \varphi_{i,j}^A A_j]_{i=1, \dots, n} \\ [(\eta_i + \mu_{v_i}) Y_i]_{i=1, \dots, n} \\ [-\eta_i Y_i + \mu_{v_i} Z_i]_{i=1, \dots, n} \end{bmatrix}$$

The Jacobian matrices of \mathcal{F} and \mathcal{V} with respect to infected classes (E_i, I_i, A_i, Y_i , and Z_i) evaluated at the disease free equilibrium point \mathcal{E}_0 are respectively given by

$$F = \begin{bmatrix} \mathbb{O} & \mathbb{O} & \mathbb{O} & \mathbb{O} & F_{1,5} \\ \mathbb{O} & \mathbb{O} & \mathbb{O} & \mathbb{O} & \mathbb{O} \\ \mathbb{O} & \mathbb{O} & \mathbb{O} & \mathbb{O} & \mathbb{O} \\ \mathbb{O} & F_{4,2} & F_{4,3} & \mathbb{O} & \mathbb{O} \\ \mathbb{O} & \mathbb{O} & \mathbb{O} & \mathbb{O} & \mathbb{O} \end{bmatrix} \text{ and } V = \begin{bmatrix} V_{1,1} & \mathbb{O} & \mathbb{O} & \mathbb{O} & \mathbb{O} \\ V_{2,1} & V_{2,2} & \mathbb{O} & \mathbb{O} & \mathbb{O} \\ V_{3,1} & \mathbb{O} & V_{3,3} & \mathbb{O} & \mathbb{O} \\ \mathbb{O} & \mathbb{O} & \mathbb{O} & V_{4,4} & \mathbb{O} \\ \mathbb{O} & \mathbb{O} & \mathbb{O} & V_{5,4} & V_{5,5} \end{bmatrix}$$

where

$$\begin{cases} F_{1,5} = \text{diag} \{ \epsilon_1 b_1, \epsilon_2 b_2, \dots, \epsilon_n b_n \} \\ F_{4,2} = \text{diag} \{ \epsilon_1 \nu_1 X_1^0 S_1^0, \epsilon_2 \nu_2 X_2^0 S_2^0, \dots, \epsilon_n \kappa_n X_n^0 S_n^0 \} \\ F_{4,3} = \text{diag} \{ \epsilon_1 \kappa_1 X_1^0 S_1^0, \epsilon_2 \kappa_2 X_2^0 S_2^0, \dots, \epsilon_n \kappa_n X_n^0 S_n^0 \} \end{cases}$$

Chapter 7: Quantifying the impact of human movement on malaria transmission

and

$$\left\{ \begin{array}{l} V_{1,1} = (\varphi_{i,j}^E)_{1 \leq i,j \leq n} \\ V_{2,1} = \text{diag}(-\lambda_1, \dots, -\lambda_n) \\ V_{2,2} = (\varphi_{i,j}^I)_{1 \leq i,j \leq n} \\ V_{3,1} = \text{diag}(-\zeta_1, \dots, -\zeta_n) \\ V_{3,3} = (\varphi_{i,j}^A)_{1 \leq i,j \leq n} \\ V_{4,4} = (\eta_1 + \mu_{v_1}, \dots, \eta_n + \mu_{v_n}) \\ V_{5,4} = \text{diag}(-\eta_1, \dots, -\eta_n) \\ V_{5,5} = \text{diag}(\mu_{v_1}, \dots, \mu_{v_n}) \end{array} \right.$$

and \mathbb{O} is the n by n matrix with all entries being equal to 0.

The matrix F is a non-negative matrix of rank one and can be written as the product of vectors. Matrices $V_{1,1}$, $V_{2,2}$, $V_{3,3}$, $V_{4,4}$ and $V_{5,5}$ are irreducible non-singular M-matrix and thus their inverses are

$$V^{-1} = \begin{bmatrix} V_{1,1}^{-1} & \mathbb{O} & \mathbb{O} & \mathbb{O} & \mathbb{O} \\ -V_{2,2}^{-1}V_{2,1}V_{1,1}^{-1} & V_{2,2}^{-1} & \mathbb{O} & \mathbb{O} & \mathbb{O} \\ -V_{3,3}^{-1}V_{3,1}V_{1,1}^{-1} & \mathbb{O} & V_{3,3}^{-1} & \mathbb{O} & \mathbb{O} \\ \mathbb{O} & \mathbb{O} & \mathbb{O} & V_{4,4}^{-1} & \mathbb{O} \\ \mathbb{O} & \mathbb{O} & \mathbb{O} & -V_{5,5}^{-1}V_{5,4}V_{4,4}^{-1} & V_{5,5}^{-1} \end{bmatrix}$$

The Next Generation Matrix is given by:

$$M = FV^{-1} = \begin{bmatrix} \mathbb{O} & \mathbb{O} & \mathbb{O} & M_{1,4} & M_{1,5} \\ \mathbb{O} & \mathbb{O} & \mathbb{O} & \mathbb{O} & \mathbb{O} \\ \mathbb{O} & 0_{n \times n} & \mathbb{O} & \mathbb{O} & \mathbb{O} \\ M_{4,1} & M_{4,2} & M_{4,3} & \mathbb{O} & \mathbb{O} \\ \mathbb{O} & \mathbb{O} & \mathbb{O} & \mathbb{O} & \mathbb{O} \end{bmatrix}$$

Chapter 7: Quantifying the impact of human movement on malaria transmission

where

$$\begin{cases} M_{1,4} := F_{1,5}V_{4,4}^{-1}V_{5,4}V_{5,5}^{-1}, \\ M_{1,5} := F_{1,5}V_{5,5}^{-1}, \\ M_{4,1} := F_{4,2}V_{1,1}^{-1}V_{2,1}V_{2,2}^{-1} + F_{4,3}V_{1,1}^{-1}V_{3,1}V_{3,3}^{-1} \\ M_{4,2} := F_{4,2}V_{2,2}^{-1} \\ M_{4,3} := F_{4,3}V_{3,3}^{-1}. \end{cases}$$

Hence, the basic reproductive number \mathcal{R}_0 given by the spectral radius of FV^{-1} , is

$$\mathcal{R}_0 = \rho(B)$$

where B is the $n \times n$ positive matrix given by

$$B = M_{1,4}M_{4,1} = F_{1,5}V_{4,4}^{-1}V_{5,4}V_{5,5}^{-1} \left(F_{4,2}V_{1,1}^{-1}V_{2,1}V_{2,2}^{-1} + F_{4,3}V_{1,1}^{-1}V_{3,1}V_{3,3}^{-1} \right).$$

$$F_{1,5}V_{4,4}^{-1}V_{5,4}V_{5,5}^{-1} = \text{diag} \left(\frac{-\epsilon_1 b_1 \eta_1}{\mu_{v_1}(\eta_1 + \mu_{v_1})}, \dots, \frac{-\epsilon_n b_n \eta_n}{\mu_{v_n}(\eta_n + \mu_{v_n})} \right)$$

$$F_{4,2}V_{1,1}^{-1}V_{2,1}V_{2,2}^{-1} = \text{diag} \{ \epsilon_1 \nu_1 X_1^0 S_1^0, \dots, \epsilon_n \kappa_n X_n^0 S_n^0 \} (\varphi^E)^{-1} \text{diag} (-\lambda_1, \dots, -\lambda_n) (\varphi^I)^{-1}$$

$$F_{4,3}V_{1,1}^{-1}V_{3,1}V_{3,3}^{-1} = \text{diag} \{ \epsilon_1 \kappa_1 X_1^0 S_1^0, \dots, \epsilon_n \kappa_n X_n^0 S_n^0 \} (\varphi^E)^{-1} \text{diag} (-\zeta_1, \dots, -\zeta_n) (\varphi^A)^{-1}$$

Clearly the calculation of $\rho(B)$ involves the inversion of n by n matrices which can lead to some tedious calculations when n is large. We discuss the following particular cases:

- If we ignore population movement between patches, that is $\psi_{i,j}^Q = \psi_{j,i}^Q = 0$ for $j = 1, \dots, n$ $j \neq i$ and $Q = E, I$ or A , we have

$$\begin{cases} \varphi_{i,j}^Q = 0 \text{ for } j = 1, \dots, n, j \neq i \text{ and } Q = E, I \text{ or } A \\ \varphi_{i,i}^E = \lambda_i + \zeta_i + \mu_{h_i}, \varphi_{i,i}^I = \alpha_i + \delta_i + \mu_{h_i}, \varphi_{i,i}^A = \pi_i + \mu_{h_i}. \end{cases}$$

Then

$$F_{1,5}V_{4,4}^{-1}V_{5,4}V_{5,5}^{-1} = \text{diag} \left(\frac{-\epsilon_1 b_1 \eta_1}{\mu_{v_1}(\eta_1 + \mu_{v_1})}, \dots, \frac{-\epsilon_n b_n \eta_n}{\mu_{v_n}(\eta_n + \mu_{v_n})} \right)$$

$$F_{4,2}V_{1,1}^{-1}V_{2,1}V_{2,2}^{-1} = \text{diag} \left\{ -\lambda_1 \epsilon_1 \nu_1 X_1^0 S_1^0 \varphi_{11}^E \varphi_{11}^I, \dots, -\lambda_n \epsilon_n \nu_n X_n^0 S_n^0 \varphi_{nn}^E \varphi_{nn}^I \right\}$$

$$F_{4,3}V_{1,1}^{-1}V_{3,1}V_{3,3}^{-1} = \text{diag} \left\{ -\zeta_1 \epsilon_1 \kappa_1 X_1^0 S_1^0 \varphi_{11}^E \varphi_{11}^A, \dots, -\zeta_n \epsilon_n \kappa_n X_n^0 S_n^0 \varphi_{nn}^E \varphi_{nn}^A \right\}$$

Therefore

$$B = \text{diag} \left\{ \frac{\epsilon_1^2 b_1 \eta_1 X_1^0}{\mu_{v_1}(\eta_1 + \mu_{v_1}) S_1^0 \varphi_{11}^E} \left(\lambda_1 \nu_1 \varphi_{11}^I + \zeta_1 \kappa_1 \varphi_{11}^A \right), \dots, \frac{\epsilon_n^2 b_n \eta_n X_n^0}{\mu_{v_n}(\eta_n + \mu_{v_n}) S_n^0 \varphi_{nn}^E} \times \Psi \right\}.$$

Chapter 7: Quantifying the impact of human movement on malaria transmission

Where

$$\Psi = (\lambda_n \nu_n \varphi_{nn}^I + \zeta_n \kappa_n \varphi_{nn}^A)$$

Hence

$$\mathcal{R}_0 = \max \mathcal{R}_{0i}$$

where

$$\mathcal{R}_{0i} = \frac{\epsilon_i^2 b_i \eta_i X_i^0}{\mu_{v_i} (\eta_i + \mu_{v_i}) (\lambda_i + \zeta_i + \mu_{h_i}) S_i^0} (\lambda_i \nu_i \alpha_i + \delta_i + \mu_{h_i} + \zeta_i \kappa_i \pi_i + \mu_{h_i}).$$

- In the case of nonzero rates of population's movement, we consider a situation where the whole population is divided in two (large) patches only, that is $n = 2$, then we have

$$\begin{cases} F_{1,5} = \text{diag} \{ \epsilon_1 b_1, \epsilon_2 b_2 \} \\ F_{4,2} = \text{diag} \{ \epsilon_1 \nu_1 X_1^0 S_1^0, \epsilon_2 \nu_2 X_2^0 S_2^0 \} \\ F_{4,3} = \text{diag} \{ \epsilon_1 \kappa_1 X_1^0 S_1^0, \epsilon_2 \kappa_2 X_2^0 S_2^0 \} \end{cases}$$

and

$$\begin{cases} V_{1,1} = (\varphi_{i,j}^E)_{1 \leq i,j \leq 2} \\ V_{2,1} = \text{diag} (-\lambda_1, -\lambda_2) \\ V_{2,2} = (\varphi_{i,j}^I)_{1 \leq i,j \leq 2} \\ V_{3,1} = \text{diag} (-\zeta_1, -\zeta_2) \\ V_{3,3} = (\varphi_{i,j}^A)_{1 \leq i,j \leq 2} \\ V_{4,4} = \text{diag} (\eta_1 + \mu_{v_1}, \eta_2 + \mu_{v_2}) \\ V_{5,4} = \text{diag} (-\eta_1, -\eta_2) \\ V_{5,5} = \text{diag} (\mu_{v_1}, \mu_{v_2}) \end{cases}$$

Then

$$B = F_{1,5} V_{4,4}^{-1} V_{5,4} V_{5,5}^{-1} (F_{4,2} V_{1,1}^{-1} V_{2,1} V_{2,2}^{-1} + F_{4,3} V_{1,1}^{-1} V_{3,1} V_{3,3}^{-1}) = \begin{bmatrix} B_{11} & B_{12} \\ B_{21} & B_{22} \end{bmatrix}$$

where

$$\left\{ \begin{array}{l} B_{11} = \frac{-\epsilon_1 b_1 \eta_1}{\mu_{v_1} (\eta_1 + \mu_{v_1}) ((\varphi_{12}^E)^2 + \varphi_{11}^E \varphi_{22}^E)} \left(\frac{\nu_1 \epsilon_1 (\lambda_2 \varphi_{12}^E \varphi_{12}^I - \lambda_1 \varphi_{11}^E \varphi_{11}^I)}{(\varphi_{12}^I)^2 + \varphi_{11}^I \varphi_{22}^I} + \frac{\kappa_1 \epsilon_1 (\zeta_2 \varphi_{12}^E \varphi_{12}^A - \zeta_1 \varphi_{11}^E \varphi_{11}^A)}{(\varphi_{12}^A)^2 + \varphi_{11}^A \varphi_{22}^A} \right) \\ B_{12} = \frac{\epsilon_1 b_1 \eta_1}{\mu_{v_1} (\eta_1 + \mu_{v_1}) ((\varphi_{12}^E)^2 + \varphi_{11}^E \varphi_{22}^E)} \left(\frac{\nu_1 \epsilon_1 (\lambda_1 \varphi_{11}^E \varphi_{12}^I + \lambda_2 \varphi_{12}^E \varphi_{22}^I)}{(\varphi_{12}^I)^2 + \varphi_{11}^I \varphi_{22}^I} + \frac{\kappa_1 \epsilon_1 (\zeta_1 \varphi_{11}^E \varphi_{12}^A + \zeta_2 \varphi_{12}^E \varphi_{22}^A)}{(\varphi_{12}^A)^2 + \varphi_{11}^A \varphi_{22}^A} \right) \\ B_{21} = \frac{-\epsilon_2 b_2 \eta_2}{\mu_{v_2} (\eta_2 + \mu_{v_2}) ((\varphi_{12}^E)^2 + \varphi_{11}^E \varphi_{22}^E)} \left(\frac{\nu_2 \epsilon_2 (\lambda_1 \varphi_{12}^E \varphi_{11}^I + \lambda_2 \varphi_{22}^E \varphi_{12}^I)}{(\varphi_{12}^I)^2 + \varphi_{11}^I \varphi_{22}^I} + \frac{\kappa_2 \epsilon_2 (\zeta_1 \varphi_{12}^E \varphi_{11}^A + \zeta_2 \varphi_{22}^E \varphi_{12}^A)}{(\varphi_{12}^A)^2 + \varphi_{11}^A \varphi_{22}^A} \right) \\ B_{22} = \frac{-\epsilon_2 b_2 \eta_2}{\mu_{v_2} (\eta_2 + \mu_{v_2}) ((\varphi_{12}^E)^2 + \varphi_{11}^E \varphi_{22}^E)} \left(\frac{\nu_2 \epsilon_2 (\lambda_1 \varphi_{12}^E \varphi_{12}^I - \lambda_2 \varphi_{22}^E \varphi_{22}^I)}{(\varphi_{12}^I)^2 + \varphi_{11}^I \varphi_{22}^I} + \frac{\kappa_2 \epsilon_2 (\zeta_1 \varphi_{12}^E \varphi_{12}^A - \zeta_2 \varphi_{22}^E \varphi_{22}^A)}{(\varphi_{12}^A)^2 + \varphi_{11}^A \varphi_{22}^A} \right) \end{array} \right.$$

Hence

$$R_0 = \frac{1}{2} \left(B_{11} + B_{22} + \sqrt{(B_{11} - B_{22})^2 + 4B_{12}B_{21}} \right)$$

Thus if $\mathcal{R}_{0i} > 1$ for all i , then the disease-free equilibrium (DFE) is unstable and the disease may invade the population, but if $\mathcal{R}_{0i} < 1$ for all i , then DFE is locally asymptotically stable and the disease may be eliminated. It is worth noting that the basic reproduction number of the deterministic model is closely related to that of the stochastic model which is dependent on the initial number of infectious individuals for each patch i . Thus, it is important to reduce \mathcal{R}_{0i} in every patch i for the disease to be controlled. One of the interventions that are aimed at reducing \mathcal{R}_{0i} is the Long-lasting insecticide treated nets (LLINs) which mainly reduce the contact between humans and mosquitoes. Implementing this intervention in our model can be expressed by $(1 - \chi\vartheta)\epsilon$ where χ is the proportion of LLINs coverage and ϑ is the effectiveness of vector control. These two parameters are estimated using the data fitting process.

7.5 Model fitting

We restrict our model simulations and data fitting to the three safest zones of Equatorial region: Central Equatoria State, Bahr El Ghazal region: Western Bahr El Ghazal State and Upper Nile region : Warrap State. By doing so, we are assuming that movements from and into other regions are negligible compared to those from these three main regions. Basically, this turns out to considering the three regions together as a closed

Chapter 7: Quantifying the impact of human movement on malaria transmission

system, whereby only movements within and between these three regions are considered. Our stochastic model is fitted to weekly malaria data of 2011 from these three regions (shown in Figure 7.4) using the maximum likelihood approach. The model is run from the year 2000 to reach a steady state before being fitted to data from the year 2011. We assume that weekly malaria data were reported according to a Poisson process with reporting rate γ . Since the reporting rate is unknown we assume it to be no larger than 85%.

Model parameters are estimated during this fitting process and those which are not

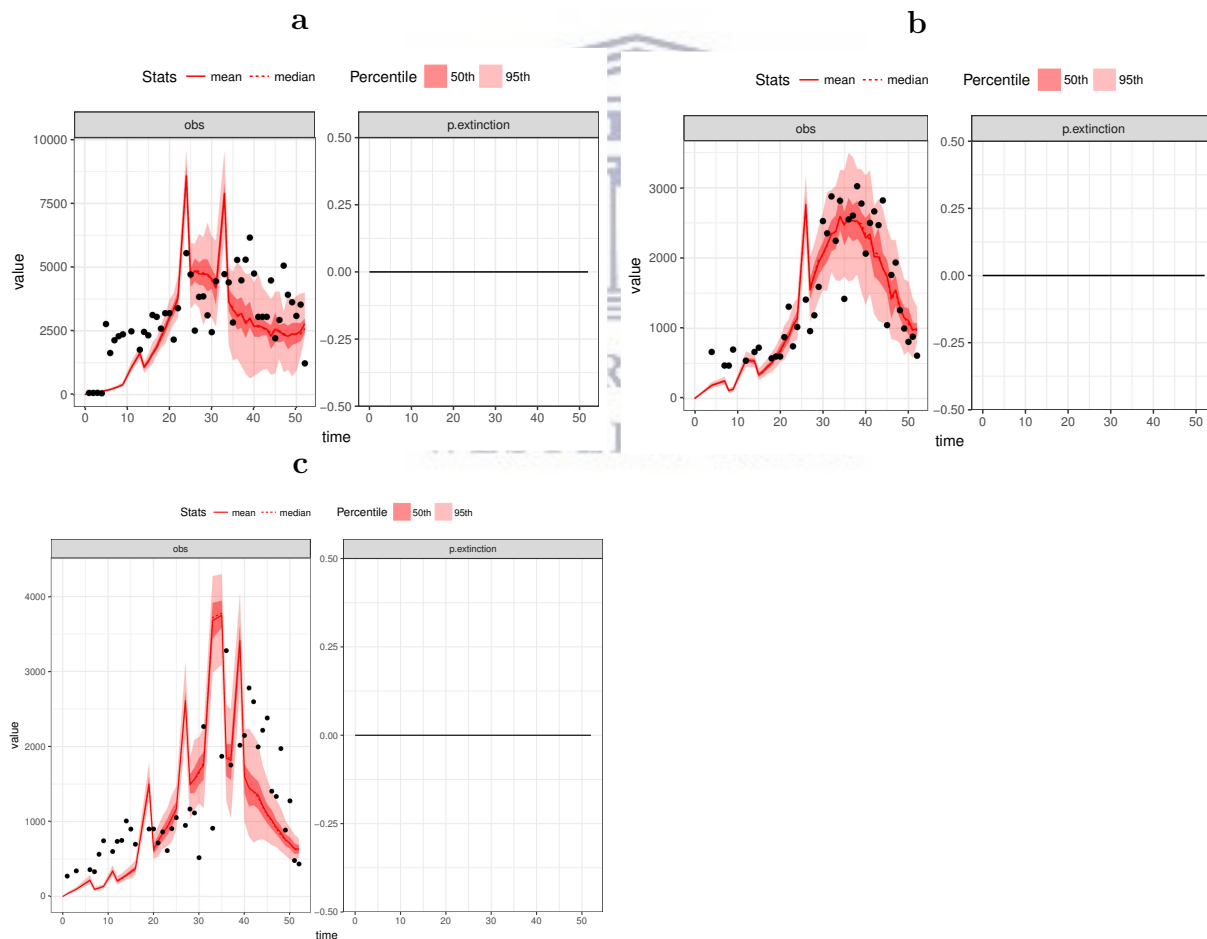


Figure 7.3: Illustration of the model fitting: the model assessment (line) run against data (dots) of CES (a), WBGZ (b) and WRP (c) for 2011, attached with the parameters estimated during fitting process in Table 7.3, along with the time-series of the extinction probability (i.e. the proportion of faded out simulations).

Chapter 7: Quantifying the impact of human movement on malaria transmission

estimated were collected from literature and are listed in Table 4.4. These parameters were assumed to be constant and were jointly estimated by utilizing fitR (version 0.1 [18]) and by plotting the mean and the median as well as the 95th and 50th percentiles of several replicated simulations. We assume an underlying Poisson distribution with a canonical vectors' parameter, θ , to be estimated. The resulting model fit of the observed measurement (the annual cases recorded) is shown in Figure 7.3.

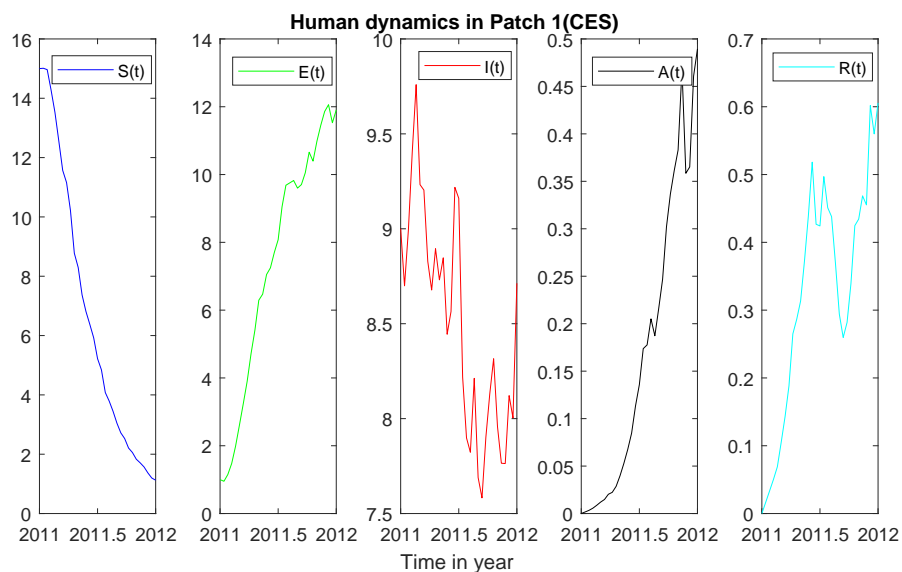


Figure 7.4: Simulation trajectory for the fitted model of human population dynamics expressed in *SEIAR* for Patch 1

We add new state variable onto the model to track the daily number of new cases, assuming that these new cases are reported when they become symptomatic or infectious. In order for the model to predicted incidence of malaria cases, we use the simulation function of the model with the initial state and given parameters calibrated with $x_{i,j}$ ($i = 1, \dots, n; j = 1, \dots, m$) as the observed weekly malaria cases for state j during week i . Calculating the likelihood of each data point $x_{i,j}$ taking its observations (cases) member and evaluating it with respect to a Poisson distribution centred around the member of the model point. We assume that the Poisson probability of observing x_i IID (Independent and Identically Distributed) counts with unknown parameter θ .

Chapter 7: Quantifying the impact of human movement on malaria transmission

$$X|\theta \sim \text{Poisson}(\theta)$$

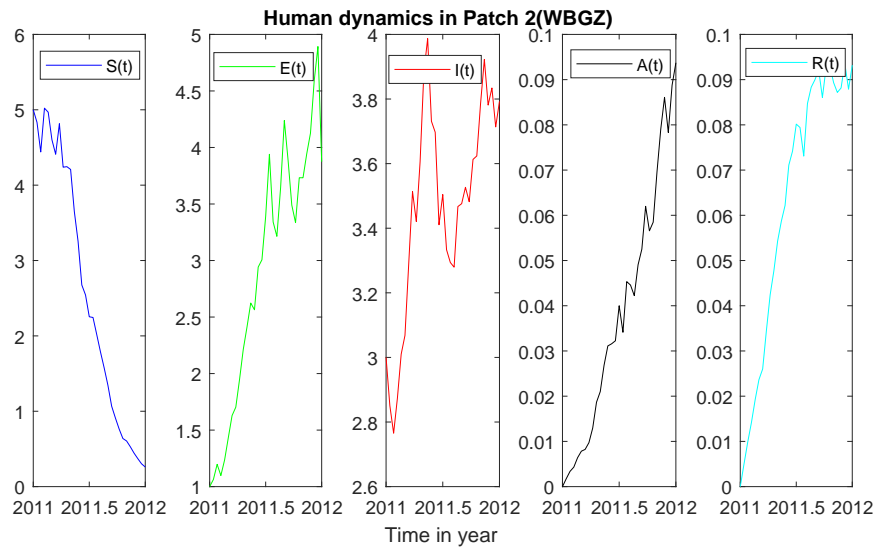


Figure 7.5: Simulation trajectory for the fitted model of human population dynamics expressed in *SEIAR* for Patch 2

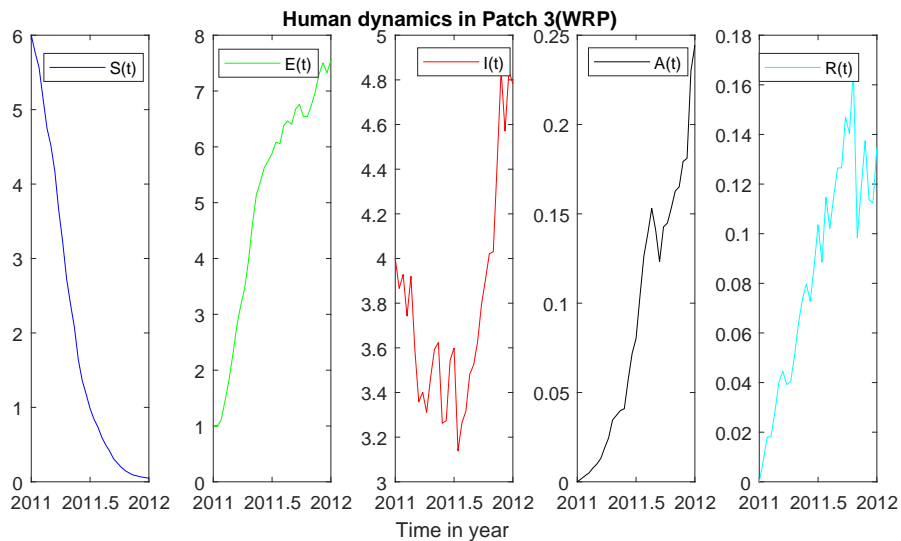


Figure 7.6: Simulation trajectory for the fitted model of human population dynamics expressed in *SEIAR* for Patch 3

Chapter 7: Quantifying the impact of human movement on malaria transmission

The likelihood function is:

$$\begin{aligned}
 L(\theta|x_1, x_2, \dots, x_n) &= p(X = x_1|\theta)p(X = x_2|\theta) \cdots p(X = x_n|\theta) \\
 &= \frac{e^{-n\theta} \theta^{x_1+x_2+\dots+x_n}}{x_1! x_2! \cdots x_n!} \\
 &= \frac{e^{-n\theta} \theta^{\sum_{i=1}^n x_i}}{\prod_{i=1}^n x_i!}
 \end{aligned}$$

and log likelihood function becomes

$$\ln(L(\theta|x_1, x_2, \dots, x_n)) = -n\theta + \left(\sum_{i=1}^n x_i \right) \ln \theta - \ln\left(\prod_{i=1}^n x_i! \right)$$

The model is fitted to three patch dataset, considering an iid sample x_{ij} for patch j from a Poisson variable the log likelihood to be maximised as

$$\ln(L(\theta_j|x_{ij})) = \sum_{i=1}^n \sum_{j=1}^3 x_i \theta_j - \theta_j$$

7.6 Concluding remarks

In this chapter we investigated the role of human mobility on malaria severity in South Sudan. We used a modified model of Mukhtar et al. [85] to carry out our investigation. The model is a metapopulation deterministic model consisting of three patches in three different regions of South Sudan. We incorporate a white noise in deterministic model to account for unpredictable population. The basic reproductive number \mathcal{R}_0 , for metapopulation deterministic model, was calculated using the next generation matrix method. The threshold parameter, \mathcal{R}_0 , is the expected number of humans and mosquitoes that would be infected with malaria by a single infected human/mosquito who had been introduced into disease-free population. A precise usage of \mathcal{R}_0 , is to advise on the disease steady state of the considered patches. Another task in this study was to perform the model calibration. To this end, model parameter value estimates are determined to provide incidence case data (weekly cases data for the patches) for 2011.

Chapter 7: Quantifying the impact of human movement on malaria transmission

We used a statistical approach, namely the maximum likelihood of Poisson distribution. Figure 7.3 illustrates the infectious class of the model fitted into data of three patches using the package fitR (version 0.1 [18]) and this include the mean, the median as well as the 95th and 50th percentiles of multiple replicated simulations.

The introduction of random motion increase realism of the model. One of the most important lessons to be learned from stochastic model is that when the noise intensity is high, the disease is susceptible to extinction in finite time (epidemic become extinct in a more direct sense) unlike the deterministic model. This provide us with some useful

Table 7.3: Model parameters estimated during the fitting process

Symbols	CES estimates	WBGZ estimates	WRP estimates	References
Γ	$0.0000514 * N_1$	$0.0000514 * N_2$	$0.0000514 * N_3$	Estimated
N_i	$N_1 = 7983420$	$N_2 = 9967450$	$N_3 = 78826740$	[120]
ψ	$\psi_{ij} = 10^{-3}, \psi_{ji} = 1/1800$	$\psi_{ij} = 1/20, \psi_{ji} = 10^{-3}$	$\psi_{ij} = 10^{-2}, \psi_{ji} = 10^{-3}$	Estimated
μ_h	0.0000514	0.0000514	0.0000514	Estimated
δ	0.00004	0.00004	0.00004	[26]
ϵ	36.6 (25.24, 50.4)	29.7 (20.2, 40.4)	32.5 (20.7, 45.31)	Estimated
b	0.84 (0.72, 0.94)	0.84 (0.72, 0.94)	0.84 (0.72, 0.94)	Estimated
ν	0.48	0.48	0.48	Estimated
κ	0.4	0.4	0.4	[134]
λ	0.2 (0.083, 0.25);	0.167 (0.083, 0.25)	0.167 (0.083, 0.25)	Estimated
ζ	0.0525	0.0525	0.0525	Estimated
α	1/16,	1/20,	1/18	Estimated
π	1/150	1/190	1/220	Estimated
ρ	1/25	1/20	1/37	Estimated
η	1/12	1/12	1/12	[26]
μ_v	0.04	0.04	0.04	[26]
Ψ	0.13	0.13	0.13	[85]

Chapter 7: Quantifying the impact of human movement on malaria transmission

control strategies to regulate disease dynamics.

We used simulation to generate an observation trajectory for the fitted model and also to demonstrate the population dynamics of humans (see Figures 7.4- 7.6). The predicted pattern of observation for a stochastic model with a variety of migration pattern was carried out, as shown in Figure 7.7. It turns out that the disease persists in the low transmission patches when there is human inflow in these patches and even though intervention coverage is as high as 77%. This implies that with an unprecedented number of people who are on the move (one out of every five people in South Sudan have been forcibly displaced) can pose challenges to malaria control and elimination. Figure 7.8 demonstrates the correlation pattern of malaria disease with intervention coverage and no intervention involving mobility. With the usage of threshold \mathcal{R}_0 , the result indicated migration of a large number of people (the case of the conflict that leads to population pressure) and their circulation can favor malaria transmission (increase of \mathcal{R}_0) compared to less or no migration (see Figure 7.8). This confirms that human movement is one of the contributing factors to the resurgence of malaria, which can be explained by when infected individual move from areas where malaria was still endemic to malaria-free areas and also could happen when susceptible people move to malarious regions, they can in-

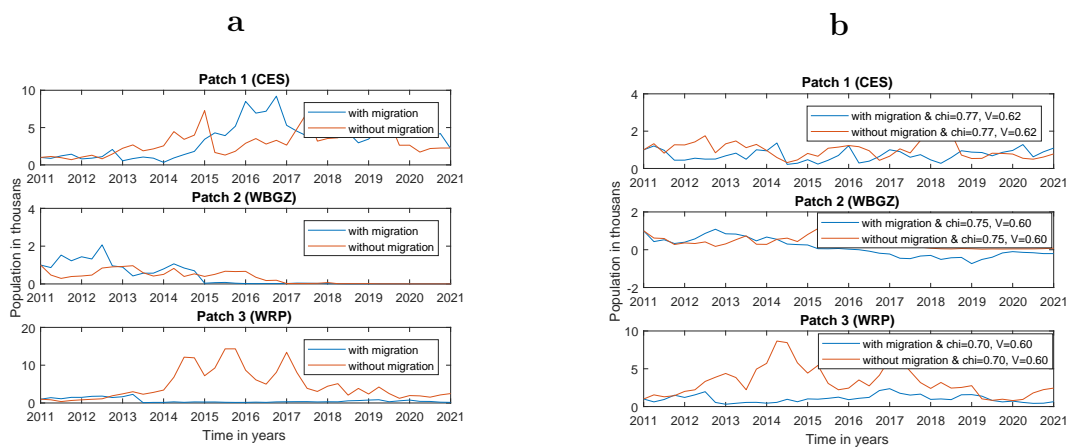


Figure 7.7: Projected cases of malaria using parameter values in Table 1, assess the impact of movement between patches with no interventions of LLINs (a), with interventions of LLINs (b)

Chapter 7: Quantifying the impact of human movement on malaria transmission

crease their risk of acquiring the disease. It can be seen from the result in Figure 7.8 that human mobility is sufficient to preserve malaria disease firmness in the patches with the low transmission. We concluded that the sensitivity of malaria to the human mobility is high that can cause the implications on malaria control in South Sudan, and efforts to ameliorate health and monitoring of migrants and collect disaggregated data on malaria and population movements must, therefore, be strengthened.

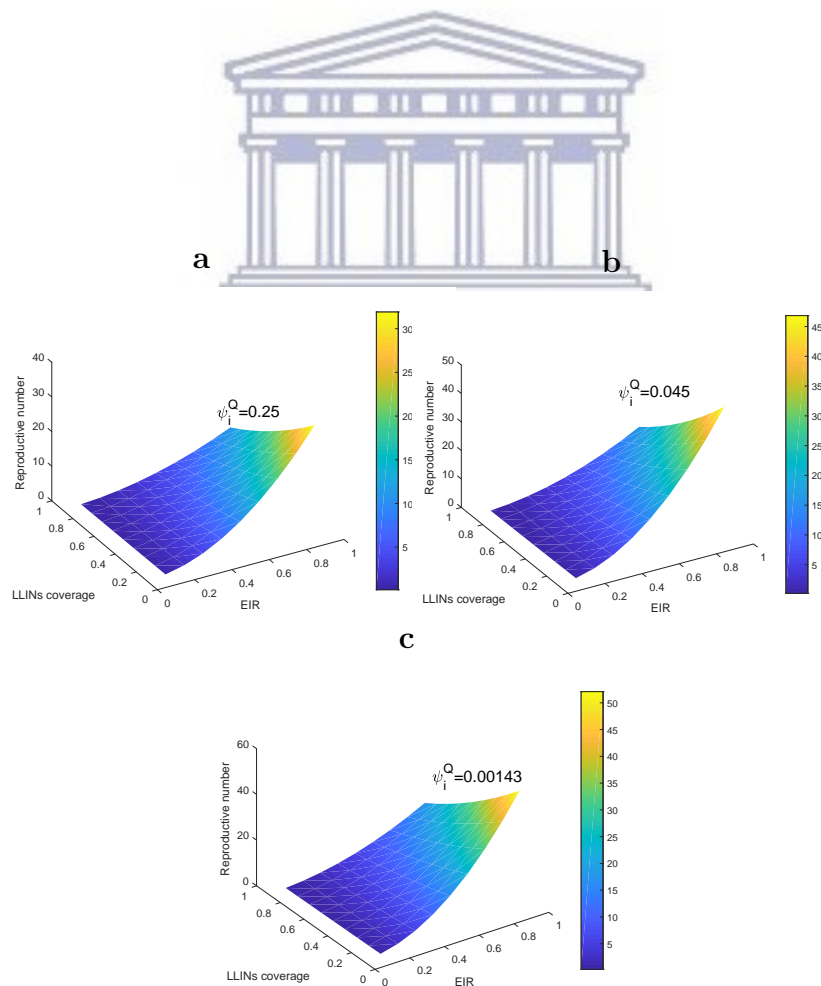
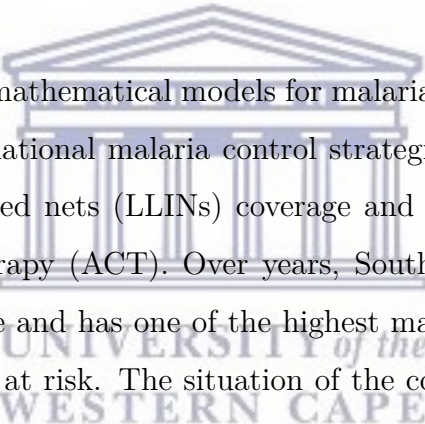


Figure 7.8: Basic reproduction number and mosquito biting rate against LLINs Coverage with various migration rate

Chapter 8

Conclusion



We constructed and analyzed mathematical models for malaria transmission in the South Sudan context incorporating national malaria control strategies plan by a scaling up of Long-Lasting Insecticide-Treated nets (LLINs) coverage and the effect of the switch to Artemisinin-Combination Therapy (ACT). Over years, South Sudan has been exposed to the brunt of chronic warfare and has one of the highest malaria burdens in the world where the entire population is at risk. The situation of the country is aggravated by an increase in number of population due to refugees, returnees, and conflict-related internal displacements which occurred in 2013. This situation has created a major stumbling block to malaria control.

Moreover, malaria dynamics complexity emerges from other factors such as agro-climatic zones, average rainfall, topography, deteriorated socio-economic situation and lack of drugs and vaccination. LLINs mass campaigns countrywide have been piloted with the target coverage of 80% and about 4.7 million LLINs have been delivered to the population who are in need [106]. Despite this, the number of infected cases and deaths increased in all age groups. Malaria Indicator Survey of 2009 indicates that the proportion of disease burden goes higher in the Southern part than in the Northern part of the country, and disease prevalence could be in some counties as higher as 75%-100% in South. This can be attributed to some factors: the climate being more impactful to the disease, the collapse of the health system caused by war or the high concentration of

Chapter 8: Conclusion

internally displaced persons (IDPs) camps in the South.

Against this background, the study answered the following research questions ideally to support metrics for pre-elimination and recommended a scaling-up entry point of LLIN distribution that targets households in areas at risk of malaria in the country.

- Could the heterogeneity on prevalence of malaria in South Sudan be explained by the varied agro-climatic conditions ?
- What is the impact of LLINs coverage used on parasite prevalence in selected settings based on the given coverage of MIS 2009 and 2013 as a baseline ?
- Could the huge burden in the aggregated distribution of malaria parasite among hosts be ascribed to population distribution changes due to displacements?

We aimed at using mathematical models to assess the effect of various factors on the severity of this disease as no mathematical study has been conducted previously in South Sudan to establish the effects of multi-intervention on the malaria epidemic. Thus, we proposed systems of deterministic and stochastic differential equations. To accommodate stochasticity, we extended a classical deterministic SIR-type epidemic model with migration flows by adding a stochastic noise term in the form of a Wiener process to the model's deterministic equations. In chapter 4, we considered different compartmental models to test how they fit to the available weekly malaria cases data. Importantly, the test guided us in determining which of the available models in the literature best fitted the data. This enabled us make an informed choice of models to consider as basis for further analysis and better understanding of the disease epidemiology by comparing their outcome and predictions.

In the subsequent chapters, the system of deterministic and stochastic are characterized by a certain set of parameters, each with a biological significance, such as the force of infection, the recovery rate, the mortality rate, and so on. We considered the importance of evaluating the numerical values of the model parameters with real data in order to allow for computational simulations of dynamics that provides accurate prediction of the

Chapter 8: Conclusion

reaction. Without accurate predictions, calculations of the basic reproduction number would be subject to a significant error. For a given set of parameters one can determine the dynamics predicted by the model and then calculate the likelihood that the observed data came from such dynamics. Available data on malaria was utilized to determine realistic parameter values of deterministic models using a Bayesian approach via Markov Chain Monte Carlo (MCMC) methods. Concerning the stochastic model, we used the maximum likelihood approach to fit the number of malaria cases to weekly malaria data.

We then explored the parasite prevalence on a continued rollout of LLINs in different settings in order to create a sub-national projection of malaria. The intervention model comprised of three parameters: the proportion of LLIN coverage, the proportion of individuals exposed to mosquito bites, and the effectiveness of the nets. Simulation results of \mathcal{R}_0 show that the use of bednets with long term effectiveness could reduce \mathcal{R}_0 to less than one in low transmission sites.

We have pressure tested different structures of models and results show that the transmission of the disease was strongly influenced by the model structure and uncertainty around the parameter's value. We observed that the SEIR model consists of an epidemic with extended peak and short tail compared to a single SIR pandemic, and it may have more than one peak due to latency. We hence considered a more realistic model by incorporating the important factors that may drive the malaria disease into a particular setting. The effect of rainfall and temperature on mosquito abundance was examined. We further derived the basic reproduction number \mathcal{R}_0 and examined the model for the existence of vector free and disease-free equilibrium points. Sensitivity analysis of \mathcal{R}_0 to temperature and rainfall indicates that when the rainfall is equal to 70 or 80 mm, temperatures below $28.8^\circ C$ will increase \mathcal{R}_0 and was shown to be thermally constrained at low and high temperatures. This study substantiated our claim that disease was more severe in tropical region than in a hot semi-arid region due to climate conditions and hence it should be treated as such whenever the intervention against malaria is applicable. The findings obtained in this study are in agreement with other studies [1, 103] that demonstrate disease behavior change with the change of local climate.

Chapter 8: Conclusion

Our model exhibits two common steady states, namely the free and the endemic equilibrium points. Key to our analysis was the definition of the basic reproduction number \mathcal{R}_0 . We computed the sensitivity indices of \mathcal{R}_0 and the endemic equilibrium. Under conditions which permit the existence of an endemic equilibrium point, we proved global stability of the endemic equilibrium for $\mathcal{R}_0 \geq 1$.

We further derived and examined the basic reproduction number in relation to biting rate values and LLINs coverage from Eq (6.5.14) plotted in Figure 6.12. Simulation results of \mathcal{R}_0 show that the use of bednets with long term effectiveness reduced \mathcal{R}_0 to less than one in low transmission sites. In the absence of any intervention, we noted a large \mathcal{R}_0 , confirming a substantial increase in the incidence of malaria in the community. The findings indicated that the disease transmission increases or decreases greatly with an increase or decrease in the contact rate to susceptible mosquito and the biting rate. We also observed that, a longer infection period enhances disease transmission, which may lead to an increased contact rate to susceptible mosquitoes.

The predicted pattern of observations for a stochastic model with a variety of migration pattern was carried out and showed to have well-behaved solutions. The result in Figure 7.8 shows that human mobility is sufficient to preserve malaria disease firmness in the patches with the low transmission. The findings indicate that the disease persists in the low transmission patches when there is human inflow and even though intervention coverage is as high as 77%. This implies that an unprecedented number of people who are on the move can pose challenges to malaria control and elimination.

We concluded that this study which analysis observed phenomena also seeks ways of informing decision making together with ideas for the continuation of malaria control in South Sudan. A model calibration was one of the main contributions that this study has achieved, complemented with the realistic representation of *Anopheles Gambiae* population dynamics to gain insight into the abundance of mosquitoes and hence the course of the epidemic. We hope that this study improves understanding of the role of these factors as the first step in providing information that may lead to significant changes in the way that the disease is transmitted in the country to incorporate the effective inter-

Chapter 8: Conclusion

ventions. The thesis concluded that malaria sensitivity to human mobility and climatic conditions are high. This has serious implications on malaria control in South Sudan. Efforts to improve health during the wet season and to monitor migrants should, therefore, be enhanced. However, malaria transmission can emerge from other factors such as lack of education, poor healthcare system and a deteriorated socioeconomic situation. These aspects are worthy of being factored in future studies of malaria transmission.



UNIVERSITY *of the*
WESTERN CAPE

Bibliography

- [1] G. J. Abiodun, R. Maharaj, P. Witbooi and K. O. Okosun. Modelling the influence of temperature and rainfall on the population dynamics of *Anopheles Arabiensis*. *Malaria Journal*, **15** (2016) DOI 10.1186/s12936-016-1411-6
- [2] M. A. Acevedo, O. Prosper, K. Lopiano, N. Ruktanonchai, T. T. Caughlin, M. Martcheva, C. W. Osenberg and D. L. Smith. Spatial Heterogeneity, Host Movement and Mosquito-Borne Disease Transmission. *PLoS ONE*, **10(6)** (2015) e0127552. doi:10.1371/journal.pone.0127552
- [3] D. Alonso, M. J. Bouma and M. Pascual. Epidemic malaria and warmer temperatures in recent decades in an East African highland. *Proceedings of the Royal Society of London B: Biological Sciences*, **278** (2011) 1661-1669.
- [4] L.J.S. Allen. *An Introduction to Mathematical Biology*, Prentice Hall, NJ, 2007.
- [5] S. Antinori, L. Galimberti, L. Milazzo, and M. Corbellino. Biology of Human Malaria Plasmodia Including *Plasmodium Knowlesi*. *Mediterranean Journal of Hematology and Infectious Diseases*, **4** (2012) DOI: 10.4084/MJHID.2012.013.
- [6] R. Aguas, L.J. White, R.W. Snow and M.G. Gomes. Prospects for malaria eradication in sub-Saharan Africa. *PLoS ONE*, **3** (2008) DOI: 10.1371/journal.pone.0001767.
- [7] L. Arnold. *Stochastic, Differential Equations: Theory and Applications*, Wiley, New York, 1972.

Bibliography

- [8] J.L. Aron. Mathematical modeling of immunity to malaria. *Mathematical Biosciences*, **90**(1988) 385-396.
- [9] N. Bacaër and R. Ouifki. Growth rate and basic reproduction number for population models with a simple periodic factor. *Mathematical Biosciences*, **210**(2007) 647-658.
- [10] J.C. Beier. Malaria parasite development in mosquitoes. *Annual Review of Entomology*, **43** (1998) 519-630.
- [11] L. M. Beck-Johnson, W. A. Nelson, K. P. Paaijmans, A. F. Read, M.B. Thomas, O. N. Björnstad. The effect of temperature on anopheles mosquito population dynamics and the potential for malaria transmission. *PLoS ONE*, **8** (2013) doi:10.1371/journal.pone.0079276.
- [12] L. M. Beck-Johnson, W. A. Nelson, K. P. Paaijmans, A. F. Read, M.B. Thomas, O. N. Björnstad. The importance of temperature fluctuations in understanding mosquito population dynamics and malaria risk. *Royal Society Open Science*, **4** (2017) DOI:10.1098/rsos.160969.
- [13] S. Bhatt, D. J. Weiss, E. Cameron, D. Bisanzio, B. Mappin, U. Dalrymple, K. E. Battle, C. L. Moyes, A. Henry, P. A. Eckhoff, E. A. Wenger, O. Brië, M. A. Penny, T. A. Smith, A. Bennett, J. Yukich, T. P. Eisele, J. T. Griffin, C. A. Fergus, M. Lynch, F. Lindgren, J. M. Cohen, C. L. J. Murray, D. L. Smith, S. I. Hay, R. E. Cibulskis and P.W. Gething. The effect of malaria control on Plasmodium Falciparum in Africa between 2000 and 2015. *Nature*, **526** (2015) 207–211.
- [14] J. I. Blanford, S. Blanford, R. G. Crane, M. E. Mann, K. P. Paaijmans, K. V. Schreiber, and M. B. Thomas. Implications of temperature variation for malaria parasite development across Africa. *Scientific Reports*, **3** (2013) doi:10.1038/srep01300.
- [15] G. Birkhoff and G. Rota. *Ordinary Differential Equations*, John Wiley and Sons, New York, 1989.

Bibliography

- [16] O. J. T. Briët and M. A. Penny. Repeated mass distributions and continuous distribution of long-lasting insecticidal nets: modelling sustainability of health benefits from mosquito nets, depending on case management. *Malaria Journal*, **12** (2013) DOI.org/10.1186/1475-2875-12-401
- [17] B. Buonomo, and C. Vargas-De-Leyn. Stability and bifurcation analysis of a vector-bias model of malaria transmission. *Mathematical Biosciences*, **242** (2013) 59-67.
- [18] Camacho A, Funk S. FitR: Tool box for fitting dynamic infectious disease models to time series. (2017) Version 0.1 Available from: <https://github.com/sbfknk/fitR>.
- [19] Centers for disease control and prevention. Global Health, Division of Parasitic Diseases and Malaria (2018). <https://www.cdc.gov/malaria/about/biology/index.html>
- [20] F. Chamchod, N. F. Britton. Analysis of a vector-bias model on malaria transmission. *Bulletin of Mathematical Biology*, **73** (2011) 639-657.
- [21] E. Chanda, C.D Remijo, H. Pasquale, S.P. Babab and R.L. Lako. Scale-up of a programme for malaria vector control using long-lasting insecticide-treated nets: lessons from South Sudan. *Bulletin World Health Organization*, **92** (2014) 290-296.
- [22] E. Chanda, C. Doggale, H. Pasquale, R. Azairwe, S. Baba and A. Mnzava. Addressing malaria vector control challenges in South Sudan: proposed recommendations. *Malaria Journal*, **12** (2013) 12-59.
- [23] N. Chitnis, J. M. Hyman, J.M. Cushing. Determining important parameters in the spread of malaria through the sensitivity analysis of a mathematical model. *Bulletin of Mathematical Biology*, **70** (2008) 1272-1296.
- [24] N. Chitnis, T. Smith, R. Steketee. A mathematical model for the dynamics of malaria in mosquitoes feeding on a heterogeneous host population. *Journal of Biological Dynamics*, **2** (2008) 259–285.

Bibliography

- [25] C. Chiyaka, W. Garira and S. Dube. Effects of treatment and drug resistance on the transmission dynamics of malaria in endemic areas. *Theoretical Population Biology*, **75** (2009) 14-29.
- [26] C. Chiyaka, J. M. Tchuente, W. Garira, and S. Dube. A mathematical analysis of the effects of control strategies on the transmission dynamics of malaria. *Applied Mathematics and Computation*, **195** (2008) 641–662.
- [27] C. Cosner. Models for the effects of host movement in vector-borne disease systems. *Mathematical Biosciences*, **270** (2015) 192-197.
- [28] C. Cosner, J. C. Beier, R. S. Cantrell, D. Impoinvi, L. Kapitanski, M. D. Potts, A. Troyee, and S. Ruan. The effects of human movement on the persistence of vector-borne diseases. *Journal of Theoretical Biology*, **258** (2009) 550–560.
- [29] C. Christiansen-Jucht, K. Erguler, C. Y. Shek, M. G. Basáñez and P. E. Parham. Modelling *Anopheles gambiae* s.s. Population Dynamics with Temperature- and Age-Dependent Survival. *International Journal of Environmental Research and Public Health*, **12** (2015) 5975-6005.
- [30] J. M. Cohen, D. L. Smith, C. Cotter, A. Ward, G. Yamey, O. J. Sabot and B. Moonen. Malaria resurgence: a systematic review and assessment of its causes. *Malaria Journal*, **11** (2012) doi.org/10.1186/1475-2875-11-122.
- [31] C. O. Cornelio and O. F. Seriano. Malaria in South Sudan 1: introduction and pathophysiology. *Southern Sudan Medical Journal*, **4** (2011) 7-9.
- [32] F. E. G. Cox. History of the discovery of the malaria parasites and their vectors. *Parasites & vectors*, **3** (2010) doi.org/10.1186/1756-3305-3-5.
- [33] M. Craig, D. Le Sueur and B. Snow. A climate-based distribution model of malaria transmission in sub-Saharan Africa. *Parasitology Today*, **15** (1999) 105–111.

Bibliography

- [34] D. A. Ewing, C. A. Cobbold, B. V. Purse, M. A. Nunn and S. M. White. Modelling the effect of temperature on the seasonal population dynamics of temperate mosquitoes. *Journal of Theoretical Biology*, **400** (2016) 65–79.
- [35] M.B. Eyobo, A.C. Awur, G. Wani, A. Julla, C.D. Remijo, B. Sebit, R. Azairwe, O. Thabo, E. Bepo, R.L. Lako, L. Riek and E. Chanda. Malaria indicator survey 2009, South Sudan: baseline results at household level. *Malaria Journal*, **13** (2014) 13-45.
- [36] K. Dietz, L. Molineaux and A. Thomas. A malaria model tested in the African savannah. *Bulletin World Health Organization*, **50** (1974) 347-357.
- [37] M.J. Dobson, M. Malowany and R.W. Snow. Malaria control in East Africa: the Kampala Conference and the Pare-Taveta Scheme: a meeting of common and high ground. *Parassitologia*, **42** (2000) 149-166.
- [38] T. Draebel, B.G. Kueil and D.W. Meyrowitsch. Prevalence of malaria and use of malaria risk reduction measures among resettled pregnant women in South Sudan. *International Health*, **5** (2013) 211-216.
- [39] L. Esteva, A. B. Gumel, C.V. De Léon. Qualitative study of transmission dynamics of drug-resistant malaria. *Mathematical and Computer Modelling*, **50** (2009) 611-630.
- [40] J. A. N. Filipe, E.M. Riley, C. J. Drakeley, C. J. Sutherland and A. C. Ghani. Determination of the processes driving the acquisition of immunity to malaria using a mathematical transmission model. *PLOS Computational Biology*, **3** (2007) 2569-2579.
- [41] F. Forouzannia and A.B. Gume. Mathematical analysis of an age-structured model for malaria transmission dynamics. *Mathematical Biosciences*, **247** (2014) 80-94.
- [42] <https://en.climate-data.org/>.
- [43] D. Gao and S. Ruan. A multipatch malaria model with logistic growth populations. *SIAM Journal of Applied Mathematics*, **72(3)** (2012) 819–841.

Bibliography

- [44] M. Gayer, D. Legros, P. Formenty and M. A. Connolly. Conflict and emerging infectious diseases. *Emerging Infectious Diseases*, **13** (2007) 1625–1631.
- [45] P. W. Gething, D. L. Smith, A. P. Patil, A. J. Tatem, R. W. Snow and S. I. Hay. Climate change and the global malaria recession. *Nature*, **465** (2010) 342-346.
- [46] G. Gonzalez Parra, A. J. Arenas and M. R. Cogollo. Positivity and boundedness of solutions for a stochastic seasonal epidemiological model for Respiratory Syncytial Virus (RSV). *IngenierĀ-a y Ciencia*, **13** (2017) 95-121.
- [47] GoSS: Malaria control strategic plan 2006-2011. Juba: Government of Southern Sudan. Ministry of Health (2006).
- [48] O. Ghasemi, M. L Lindsey, T. Yang, N. Nguyen, Y. Huang and Y. Jin. Bayesian parameter estimation for nonlinear modelling of biological pathways. *BMC Systems Biology*, **5** (2011) DOI: 10.1186/1752-0509-5-S3-S9.
- [49] Global Technical Strategy for Malaria, Action and Investment to defeat Malaria, Achieving the Malaria MDG target: reversing the incidence of malaria 2000-2015.
- [50] S. Gray and J. Roos. Pride, conflict and complexity: Applying dynamical systems theory to understand local conflicts in South Sudan. *The African Center For Constructive Resolution Of Disputes*, **4** (2012) 1-14.
- [51] J. T. Griffin, T. D. Hollingsworth, L. C. Okell, T. S. Churcher, M. White, W. Hinsley, T. Bousema, C. J. Drakeley, N. M. Ferguson, M-G. Basanez and A. C. Ghani. Reducing Plasmodium falciparum Malaria Transmission in Africa: A Model-Based Evaluation of Intervention Strategies. *PLoS Medicine*, **8** (2010) DOI: 10.1371/journal.pmed.1000324
- [52] J. T. Griffin, N. M. Ferguson and A. C. Ghani . Estimates of the changing age-burden of Plasmodium falciparum malaria disease in sub-Saharan Africa. *Nature Communications*. (2014) DOI: 10.1038/ncomms4136.

Bibliography

- [53] G. Hamra, R. MacLehose and D. Richardson. Markov Chain Monte Carlo: an introduction for epidemiologists. *International Journal of Epidemiology*, **42** (2013) 627–634.
- [54] Y. Huang, D. Liu, H. Wu. Hierarchical Bayesian methods for estimation of parameters in a longitudinal HIV dynamic system. *Biometrics*, **62** (2006) 413–423.
- [55] A. Huppert, and G. Katriel. Mathematical modelling and prediction in infectious disease epidemiology. *Clinical microbiology and infection* **19** (2013)999–1005.
- [56] G. R. Hosack, P. A. Rossignol, P. van den Driessche, The control of vector-borne disease epidemics. *Journal of Theoretical Biology* , **255** (2008) 16-25.
- [57] Health sector development plan 2011-2015. Government of South Sudan Minster of health.
- [58] M. B. Hoshen, A.P. Morse. A weather-driven model of malaria transmission. *Malaria Journal*, (2004) DOI:10.1186/1475-2875-3-32.
- [59] S. S. Imbahale, K. P. Paaijmans, W. R. Mukabana, R. van Lammeren, A. K. Githeko and W. Takken. A longitudinal study on Anopheles mosquito larval abundance in distinct geographical and environmental settings in western Kenya. *Malaria Journal*, **10** (2011) DOI.10.1186/1475-2875-10-81.
- [60] L. Jia. A malaria model with partial immunity in humans. *Mathematical Biosciences and Engineering* **5**(2008) 789-801.
- [61] N. Jitthai. Migration and malaria. *Southeast Asian J Trop Med Public Health*, **44** (2013) 166-200.
- [62] D.W. Jordan, P. Smith. *Nonlinear Ordinary Differential Equations (Second edition)*, Clarendon Press, Oxford, 1987.
- [63] F. M. M. Kakmeni, R. Y. Guimapi, F. T. Ndjomatchoua, S. A. Pedro, J. Mutunga and H. E. Tonnang. Spatial panorama of malaria prevalence in Africa under climate

Bibliography

- change and interventions scenarios. *International journal of health geographics* **17** (2018) DOI.org/10.1186/s12942-018-0122-3.
- [64] O. Kamaldeen, A. Abdelrazec and A. B. Gumel. Mathematical analysis of a weather-driven model for the population ecology mosquitoes. *Mathematical Biosciences Engineering*, **15** (2018) 57-93.
- [65] P. Kloeden and E. Platen. *Numerical Solution of Stochastic Differential Equations*. Springer, Berlin, 1995.
- [66] J. C. Koella. On the use of mathematical models of malaria transmission. *Acta Tropica*, **49** (1991) 1-25.
- [67] G. F. Killeen, T. A. Smith, H. M. Ferguson, H. Mshinda, S. Abdulla, et al. Preventing childhood malaria in Africa by protecting adults from mosquitoes with insecticide-treated nets. *PLoS Med* **4** (2007) doi:10.1371/journal.pmed.0040229.
- [68] S. Kim, A. Tridane and D. E. Chang (2016) Human migrations and mosquito-borne diseases in Africa. *Mathematical Population Studies*, **23** (2016) 123-146.
- [69] G. P. S. Kwong, R. Deardon. Linearized forms of individual-level models for large-scale spatial infectious disease systems. *Bulletin of Mathematical Biology*, **74** (2012) 1912–1937.
- [70] A. Le Menach, S. Takala, F. E. McKenzie, A. Perisse, A. Harris, A. Flahault and D. L. Smith. An elaborated feeding cycle model for reductions in vectorial capacity of night-biting mosquitoes by insecticide-treated nets. *Malaria Journal* **10** (2007) DOI:10.1186/1475-2875-6-10
- [71] S.W. Lindsay, M.H. Birley. Climate change and malaria transmission. *Annals of Tropical Medicine and Parasitology*, **90** (1996) 573-588.
- [72] T. M. Lunde, D. Korecha, E. Loha, A. Sorteberg and B. Lindtjørn. A dynamic model of some malaria-transmitting anopheline mosquitoes of the Afrotropical re-

Bibliography

- gion. I. Model description and sensitivity analysis. *Malaria Journal* **12** (2013) DOI.org/10.1186/1475-2875-12-28.
- [73] Y. Lou and X.Q. Zhao. A climate-based malaria transmission model with structured vector population. *SIAM Journal on Applied Mathematics*, **70** (2010) 20-23.
- [74] G. Macdonald. The analysis of infection rates in diseases in which super infection occurs. *Tropical Disease Bulletin*, **47** (1950) 907-915.
- [75] P. M. Macharia, P. O. Ouma, E. G Gogo, R. W. Snow and A. M. Noor. Spatial accessibility to basic public health services in South Sudan. *Geospatial health*, **12**, (2017) DOI: 10.4081/gh.2017.510.
- [76] S. Mandal, R. R. Sarkar, S. Sinha. Mathematical models of malaria-a review. *Malaria Journal*, **10** (2011) DOI.org/10.1186/1475-2875-10-202.
- [77] R. Malik, R. Deardon, G. P. S. Kwong. Parameterizing Spatial Models of Infectious Disease Transmission that Incorporate Infection Time Uncertainty Using Sampling-Based Likelihood Approximations. *PLoS ONE*, **11** (2016): e0146253. DOI.org/10.1371/journal.pone.0146253
- [78] E. M. Malik and O. Khalafalla. Malaria in Sudan: past, present and the future. *Gezira Journal of Health Sciences*, **1** (2004) 47.
- [79] W.J.M. Martens, L.W. Niessen, J. Rotmans, A.J. McMichael. Potential impacts of global climate change on malaria risk. *Environmental Health Perspectives*, **103** (1995) 458-464.
- [80] P. Martens and L. Hall. Malaria on the move: Human population movement and malaria transmission. *Emerging Infectious Diseases*, **6** (2000) 103-109.
- [81] R. J. Maude, W. Pontavornpinyo, S. Saralamba, A.M. Dondorp, N.P. Day, N.J. White and L.J. White. The role of mathematical modelling in malaria elimination

Bibliography

- and eradication (Comment on: Can malaria be eliminated?). *Transactions of the Royal Society of Tropical Medicine and Hygiene*, **103** (2009) 643-644.
- [82] E. A. Mordecai. Optimal temperature for malaria transmission is dramatically lower than previously predicted. *Ecology Letters*, **16** (2013) 22–30 .
- [83] G. G. Mwanga, H. Haario, V. Capasso. Optimal control problems of epidemic systems with parameter uncertainties: Application to a malaria two-age-classes transmission model with asymptomatic carriers. *Mathematical Biosciences*, **261** (2015) 1-12.
- [84] A. Y. A. Mukhtar, H. B. Munyakazi, R. Ouifki. Assessing the role of climate factors on malaria transmission dynamics in South Sudan. *Mathematical Bioscience*, **310** (2019); 13-23.
- [85] A. Y. A. Mukhtar, J. B. Munyakazi, R. Ouifki, A. E. Clark. Modelling the effect of bednet coverage on malaria transmission in South Sudan. *PLoS ONE*, **13(6)** (2018): e0198280. <https://doi.org/10.1371/journal.pone.0198280>
- [86] J. Nedelman. Introductory review: Some new thoughts about some old malaria models. *Mathematical Biosciences*, **73** (1985) 159-182.
- [87] E. T. Ngarakana-Gwasira, C. P. Bhunu, M. Masocha, and E. Mashonjowa. Assessing the role of climate change in malaria transmission in Africa. *Malaria Research and Treatment* (2016) DOI:10.1155/2016/7104291.
- [88] R.P. Napoleona, A.S. Anyangub, J. Omolocanc and J. R. Ongusd. Preventing malaria during pregnancy: factors determining the use of insecticide-treated bednets and intermittent preventive therapy in Juba. *Southern Sudan Medical Journal*, **4** (2011) 33-35.
- [89] C. N. Ngonghala, J. M. Awel, R. Zhao, O. Prosper. Interplay between insecticide-treated bed-nets and mosquito demography: implications for malaria control. *Journal of Theoretical Biology*, **397** (2016) 179 –192.

Bibliography

- [90] C. N. Ngonghala, S. Y. DelValle, R. Zhao, J. M. Awel. Quantifying the impact of decay in bed-net efficacy on malaria transmission. *Journal of Theoretical Biology*, **363** (2014) 247-261.
- [91] G. A. Ngwa W. S. Shu. A mathematical model for endemic malaria with variable human and mosquito populations. *Mathematical and Computer Modelling*, **32** (2000); 747-763.
- [92] J. A. Nájera, M. González-Silva and P.L. Alonso. Some lessons for the future from the Global Malaria Eradication Programme (1955–1969). *PLoS medicine*, **8** (2011) DOI: 10.1371/journal.pmed.1000412.
- [93] C, Nguyen (2016) Malaria Ravages South Sudan. Available: <http://www.healthmap.org/site/diseasedaily/article/malaria-ravages-south-sudan-11016>. Accessed 10 January 2016.
- [94] L. C. Okell, C. J. Drakeley, T. Bousema. Modelling the impact of artemisinin combination therapy and long-acting treatments on malaria transmission intensity. *PLoS Medicine*, **5** (2008) 1617-1628.
- [95] B. Øksendal. *Stochastic Differential Equations: An introduction with applications*, 4th Edition. Springer, Berlin, 1995.
- [96] K.O. Okosun, R. Ouifki, N. Marcus. Optimal control analysis of a malaria disease transmission model that includes treatment and vaccination with waning immunity. *BioSystems*, **106** (2011) 136-145.
- [97] K.O. Okosun and O.D. Makinde. Modelling the impact of drug resistance in malaria transmission and its optimal control analysis. *International Journal of the Physical Sciences*, **6** (2011) 6479-6487.
- [98] B. Øksendal. *Stochastic Differential Equations*. Springer-Verlag, 2000.

Bibliography

- [99] F. O. Okumu, S. S. Kiware, S. J. Moore and G. F. Killeen. Mathematical evaluation of community level impact of combining bed nets and indoor residual spraying upon malaria transmission in areas where the main vectors are *Anopheles arabiensis* mosquitoes. *Parasites & Vectors*, **6** (2013) DOI:10.1186/1756-3305-6-17.
- [100] K. Okuneye , A. B. Gumel. Analysis of a temperature- and rainfall-dependent model for malaria transmission dynamics. *Mathematical Biosciences*, **287** (2017) 72-92.
- [101] K. O. Okuneye, A. Abdelrazecy and A. B. Gumel. Mathematical analysis of a weather driven model for the population ecology of mosquitoes. *Mathematical Biosciences and Engineering* **15** (2017) 57-93.
- [102] V. M. Ouma, S. M. Mwalili, A. W. Kiberia. Poisson Inverse Gaussian (PIG) Model for Infectious Disease Count Data. *American Journal of Theoretical and Applied Statistics*, **5** (2016) 326-333.
- [103] K.P. Paaijmans, S. Blanford, A.S. Bell, J.I. Blanford, A. F. Read, and M.B. Thomas. Influence of climate on malaria transmission depends on daily temperature variation. *Proceedings of the National Academy of Sciences*, **107** (2010) 15135-15139.
- [104] P.E. Parham, E. Michael. Modeling the effects of weather and climate change on malaria transmission. *Environ Health Perspect*, **118** (2010) 620-626.
- [105] P.E Parham and E. Michael. Modeling climate change and malaria transmission. *Advance in Expermental Medicine and Biology*, **673** (2010) 184-199.
- [106] H. Pasquale, M. Jarvese, A. Julla, C. Doggale, B. Sebit, M.Y. Lual, S.B. Baba and E. Chanda. Malaria control in South Sudan, 2006-2013: Strategies progress and challenges. *Malaria Journal*, **12** (2013) 1475-2875.
- [107] H. Putter, S. H. Heisterkamp, J. M. A. Lange, F. de Wolf F. A Bayesian approach to parameter estimation in HIV dynamical models. *Stat. Med*, **21** (2002) 2199-2214.

Bibliography

- [108] M. Rafikov, L. Bevilacqua and A.P.P. Wyse. Optimal control strategy of malaria vector using genetically modified mosquitoes. *Journal of Theoretical Biology*, **258** (2009) 418-425.
- [109] Rivers in South Sudan - Fortune of Africa South Sudan. <https://fortuneofafrica.com/southsudan/rivers-in-south-sudan/>
- [110] R. Ross. *The Prevention of Malaria*. John Murray, London, (1911).
- [111] B. Roberts, E. Damundu, O. Lomoro and E. Sondorp. Post-conflict mental health needs: a cross-sectional survey of trauma, depression and associated factors in Juba, Southern Sudan. *BMC psychiatry*, **9** (2009) DOI.org/10.1186/1471-244X-9-7.
- [112] L. L. M. Shapiro, S. A. Whitehead, and M. B. Thomas. Quantifying the effects of temperature on mosquito and parasite traits that determine the transmission potential of human malaria. *PLoS Biology*, **15** (2017) DOI:10.1371/journal.pbio.2003489.
- [113] S. P. Silal, F. Little, K. I Barnes, L. J. White. Hitting a moving target: a model for malaria elimination in the presence of population movement. *PLoS ONE*, **10(12)** (2015): e0144990. Doi.org/10.1371/journal.pone.0144990.
- [114] D. L. Smith, K. E. Battle, S. I. Hay, C. M. Barker, T. W. Scott and F. Ellis McKenzie. Ross, Macdonald, and a Theory for the Dynamics and Control of Mosquito-Transmitted Pathogens. *PLoS Pathogens*, **8** (2012) DOI: 10.1371/journal.ppat.1002588.
- [115] D. L. Smith, S. I. Hay, A. M. Noor and R. W. Snow. Predicting changing malaria risk after expanded insecticide-treated net coverage in Africa. *Trends Parasitol*, **25** (2009) 511-516.
- [116] S. P. Silal, F. Little, K. I. Barnes, L. J. White. Towards malaria elimination in Mpumalanga, South Africa: a population-level mathematical modelling approach. *Malaria Journal*, **13** (2014) DOI: 10.1186/1475-2875-13-297.

Bibliography

- [117] K. Soetaert and T. Petzoldt. Inverse Modelling, Sensitivity and Monte Carlo Analysis in R Using Package FME. *Journal of Statistical Software*, **33** (2010) 1-28.
- [118] A. Sovi, R. Azondékon, R. Y Aíkpon, R. Govoétchan, F. Tokponnon, F. Agossa, A. S. Salako, F. Oké-Agbo, B. Aholouké, M. Oké, D. Gbénou, A. Massougbodji and M. Akogbéto. Impact of operational effectiveness of long-lasting insecticidal nets (llins) on malaria transmission in pyrethroid-resistant areas. *Parasit Vectors*, **6** (2013) 3-19.
- [119] R. W. Snow. Global malaria eradication and the importance of Plasmodium falciparum epidemiology in Africa. *BMC Medicine*, **13**(2015) DOI 10.1186/s12916-014-0254-7.
- [120] SSCCSE: South Sudan counts: Tables from the 5th Sudan population and housing census, 2008. Juba: Government of Southern Sudan: Southern Sudan Centre for Census: Statistics and Evaluation (2010).
- [121] South Sudan displacement trends analysis. Report April (2015).
- [122] South Sudan Statistical Yearbook 2011 , National Bureau of Statistics (NBS).
- [123] South Sudan malaria programme review report (2013).
- [124] South Sudan Malaria Strategic Plan 2014/15-2020/21.
- [125] E. Stivanello, P. Cavaller, F. Cassano, S.A, Omar3, D. Kariuki, J. Mwangi, P. Piola and J.Guthmann. Efficacy of chloroquine, sulphadoxine-pyrimethamine and amodiaquine for treatment of uncomplicated Plasmodium falciparum malaria in Kajo Keji county, Sudan. *Tropical Medicine and International Health*, **9** (2004) 975-980.
- [126] E. M. Stuckey, J. Stevenson, K. Galactionova, A. Y. Baidjoe, T. B. W. Odongo, S. Kariuki, C. Drakeley, T. A. Smith, J. Cox and N. Chitnis. Modeling the cost effectiveness of malaria control interventions in the highlands of western Kenya. *PLoS One*, **9** (2014) DOI: 10.1371/journal.pone.0107700.

Bibliography

- [127] A.O. Talisuna, A.M. Noor, A.P. Okui and R.W. Snow. The past, present and future use of epidemiological intelligence to plan malaria vector control and parasite prevention in Uganda. *Malaria journal*, **14** (2015) DOI: 10.1186/s12936-015-0677-4.
- [128] T. Toni, D. Welch, N. Strelkowa, A. Ipsen, M. P. Strumpf. Approximate Bayesian computation scheme for parameter inference and model selection in dynamical systems. *Journal of the Royal Society Interface*, **6** (2009) 187–202.
- [129] A. Tran, G. L’Ambert, G. Lacour, R. Benoît, M. Demarchi, M. Cros, P. Cailly, M. Aubry-Kientz, T. Balenghien and P. Ezanno. A rainfall-and temperature-driven abundance model for *Aedes albopictus* populations. *International Journal of Environmental Research and Public Health*, **10** (2013) 1698-1719.
- [130] UNHCR South Sudan Situation (2017).
- [131] P. Van den Driessche, J. Watmough, Reproduction numbers and sub threshold endemic equilibria for compartmental models of disease transmission. *Mathematical Biosciences*, **180** (2002) 29-48.
- [132] I.V. Van den Broek, T. Gatkoi, B. Lowoko, A. Nzila, E. Ochong, K. Keus. Chloroquine, sulfadoxine-pyrimethamine and amodiaquine efficacy for the treatment of uncomplicated *Plasmodium falciparum* malaria in Upper Nile, south Sudan. *Transactions of the Royal Society of Tropical Medicine and Hygiene*, **97** (2003) 229-235.
- [133] F. Vogt, P. Heudtlass and D. Guha-Sapir. Health data in civil conflicts: South Sudan under scrutiny (No. UCL-Université Catholique de Louvain). *Centre for Research on the Epidemiology of Disasters*, (2011).
- [134] D. I. Wallace, B. S. Southworth, X. Shi, J. W. Chipman, and A. K. Githeko. A comparison of five malaria transmission models: benchmark tests and implications for disease control. *Malaria J*, **13** (2014) DOI: 10.1186/1475-2875-13-268.

Bibliography

- [135] A. Wesolowski, N. Eagle, A. J. Tatem, D. L. Smith, A. M. Noor, R. W. Snow, and C. O. Buckee. Quantifying the impact of human mobility on malaria. *Science*, **338** (2012) 267–270. doi:10.1126/science.1223467.
- [136] M. T White, L. Conteh, R. Cibulskis and A. C Ghani. Costs and cost-effectiveness of malaria control interventions-a systematic review. *Malaria Journal*, **10** (2011) 10:337. <http://www.malariajournal.com/content/10/1/337>.
- [137] S M.T. White, J. T. Griffin, T. S. Churcher, N. M. Ferguson, M. G. Basanez, A. C. Ghani. Modelling the impact of vector control interventions on *Anopheles gambiae* population dynamics. *Parasit Vectors*, **4** (2011) DOI.org/10.1186/1756-3305-4-153.
- [138] M. T White, L. Conteh, R. Cibulskis and A. C Ghani. Costs and cost-effectiveness of malaria control interventions - a systematic review. *Malaria Journal*, **10** (2011) DOI 10.1186/s12936-015-0722-3.
- [139] WHO Global Malaria control and elimination: report of a technical review, 17-18 January, 2008. Geneva, Switzerland.
- [140] WHO Global Malaria Programme: World malaria report 2016.
- [141] T. K. Yamana and E. A. B. Eltahir. Projected impacts of climate change on environmental suitability for malaria transmission in West Africa. *Environ. Health Perspect* **121** (2013) 1179-1186.
- [142] T. K. Yamana, A. Bomblies and E. A. Eltahir. Climate change unlikely to increase malaria burden in West Africa. *Nature Climate Change*, **6** (2016) 1009-1013.
- [143] H. M Yang. Malaria transmission model for different levels of acquired immunity and temperature dependent parameters vector. *Journal of Public Health*, **34** (2000) 223- 231.
- [144] F. Yang, Y. H. Liu, X. P Yang ,J. Xu, A. Kapke and OA. Carretero. Myocardial infarction and cardiac remodelling in mice. *Experimental Physiology*, **87** (2002) 547-555.